Supplementary Material

Biocatalytic Asymmetric Ring-Opening of *meso*-Epoxides to Enantiopure Cyclic *trans*-β-Amino Alcohols Involving a Key Amine Transaminase

Jingqi Zhang [a][b] +, Hang Gao [a] +, Lili Gao,[b]* Mengyi Chen,[a] Shuangping Huang,[a] Jiandong Zhang [a]*

[a]*Department of Biological and Pharmaceutical Engineering, College of Biomedical Engineering, Taiyuan University of Technology, Taiyuan, Shanxi 030024, P. R. China*

[b]*College of Environmental Science and Engineering, Taiyuan University of Technology, Taiyuan, Shanxi 030024, China*

**Corresponding author:*

Phone: +86-0351-6018534; Fax: +86-0351-6018534

E-mail: zhangjiandong@tyut.edu.cn; gaolili@tyut.edu.cn

[+] These authors contributed equally to this work

Table of contents

1. Chemicals

Cyclopentene oxide **4**'j, cyclohexene oxide **4**'k, *trans*-cyclopentane-1,2-diol **3**'j, *trans*-1,2-cyclohexanediol **3**'k, (±)-1,2,3,4-tetrahydro-1-naphthylamine **1**a, (±)-1-phenylethylamine **1**b, (±)-4-(1-aminoethyl)phenol **1**c, (±)-4-(1-aminoethyl)-2-fluorophenol **1**d, (±)-4-(1-aminoethyl)-2-chlorophenol **1**e, (±)-4-(1-aminoethyl)-2-bromophenol **1**f, (±)-2-octanamine **1**g, (±)-2-amino-1-butanol **1**'h, (±)-valinol **1**'i, (±)-*trans*-2-aminocyclopentanol **1**'j, (±)-*trans*-2-aminocyclohexanol **1**'k, (±)-*trans*-1-amino-2-indanol **1**'l, (±)-*cis*-1-amino-2-indanol **1**'m, (±)-phenylglycinol **1**'n were from Energy Chemical (Shanghai, China). (±)-2-Amino-2-(4-fluorophenyl)ethanol **1**'o, (±)-2-amino-2-(4-chlorophenyl)ethanol **1**'p, (±)-2-amino-2-(4-bromophenyl)ethanol **1**'q, (±)-2-amino-2-[4-(trifluoromethyl)phenyl]ethanol **1**'r, (±)-2-amino-2-(4-methoxyphenyl)ethanol **1**'s, (±)-2-amino-2-(3-fluorophenyl)ethanol **1**'t, (±)-2-amino-2-(3-chlorophenyl)ethanol **1**'u, (±)-2-amino-2-(3-bromophenyl)ethanol **1**'v, (±)-2-amino-2-(3-methylphenyl)ethanol **1**'w, and all the enantiomers of amines and β-amino alcohols and all ketones and α-hydroxy ketones were from Amatek Scientific (Suzhou, China). All other chemicals were commercially available and analytical grade.

(*R*)-α-hydroxycyclopentan-1-one **2**'j and (*R*)-α-hydroxycyclohexan-1-one **2**'k were prepared as previous described. [1]

2. Bacterial strains, vectors and culture conditions

E. coli BL21 (DE3) super-competent cells were obtained from Tiangen (Shanghai, China). They were routinely grown in Luria-Bertani (LB) medium at 37°C unless stated otherwise. Ampicillin (100 μg/mL) and kanamycin (50 μg/mL) were used for the selection of recombinant strains in *E. coli*. The plasmids pET28a (+), pETduet-1 pRSFduet-1 and pCDFduet-1 for the heterogeneous expression studies were obtained from Novagen (Shanghai, China). Recombinant plasmids pETduet-SpEH,[2] pET28a-AnDDH[3] and pCDFduet-BsLDH [4] were constructed as our previously described, and preserved in our lab.

3. Engineering of recombinant *E. coli* strains

E. coli (SpEH), [2] *E. coli* (AnDDH),[3] and *E. coli* (BsLDH) [4] were constructed as previously described.

For *E. coli* (CepTA), the gene of CepTA (accession number: AXP_007730450.1) from *Capronia*

epimyces was synthesized by Tsingke (Beijing, China). The gene of CepTA was PCR-amplified with the following primers: forward primer CepTA-F: GGGAATTCCATATGGCTTCGATGGACAAGGTGTTTG, reverse primer CepTA-R: CCC*AAGCTT*TCACTTGTGCACGCCATTGACAC. The PCR amplification was performed with pfu DNA polymerase (Sangon Biotech, Shanghai, China), with initial denaturation at 95°C for 5 min followed by 30 cycles of denaturation at 94°C for 45 s, annealing at 65°C for 40 s, extension at 72°C for 1.5 min and followed by a final extension at 72°C for 10 min. The amplified gene was digested with *Nde*I and *Hind*III and ligated into pET28a (+) vector. After the correct clone was confirmed by DNA sequencing, the corresponding plasmid was transformed into chemo-competent *E. coli* BL21 (DE3) cells for protein expression. The transformed strain was abbreviated as *E. coli* (CepTA).

Amino acid sequence of CepTA:

MASMDKVFAGYQSRLRVLEASTNPLAQGVAWIEGELVPLSQARIPLMDQGFLHSDLTYDVPAV
WDGRFFRLDDHISRLEKSCSKLRLKLPLPRDEVKRVLVDMVARSGIRDAFVELIVTRGLTGVRG
AGRPEDLVNNLYMFLQPYLWVMPPETQLVGGSAVITRTVRRTPPGSMDPTVKNLQWGDLTRA
LLEASDRGASYPFLTDGDANITEGSGYNIVLIKDGAIHTPDRGVLEGVTRKTVFDIAKANGFEV
RLEVVPVELAYRADEIFMCTTAGGIMPITSLDGQPVNGGQIGPITKKIWDDYWALHYDPAFSFEI
KYDEAGASTNGVNGVHK

For *E. coli* (SpEH-AnDDH-BsLDH), the constructed recombinant plasmids pETduet-SpEH, pET28-AnDDH and pCDFduet-BsLDH with the same origin of replication and different antibiotic selection were transformed into *E. coli* BL21 competent cells simultaneously and plated on LB plates containing kanamycin (50 μg mL^{-1}), streptomycin (100 μg mL^{-1}) and ampicillin (100 μg mL^{-1}). The transformed strain co-expressing SpEH, AnDDH and BsLDH was abbreviated as *E. coli* (SpEH-AnDDH-BsLDH).

4. Protein expression and purification

In a 250 mL shake flask, 50 mL of Terrific Broth (TB) medium containing 50 μg mL^{-1} kanamycin was inoculated with 2% (V/V) of an overnight culture of a microbial colony of *E. coli* (CepTA). The *E. coli* (CepTA) was incubated at 37°C with shaking at 180 rpm for 2 to 3 h (OD600: 0.6−0.8), 0.5 mM isopropyl β-D-1-thiogalactopyranoside (IPTG) was added to induce expression of enzyme. Cell growth was continued at 25°C and 200 rpm for 12 h. Cells were collected by centrifugation at 8000 *g* for 10 min at 4°C and the supernatant was discarded. The cell pellet was washed twice with pre-cooled (4ºC) sodium phosphate buffer (100 mM, pH 7.0) and resuspended in the same buffer. The cell suspension was put on ice and sonicated for 90 times at 400 W for 4 s with 4 s of interval to yield cell-free extracts, after

centrifugation (12,000 × *g* and 4°C), the supernatant of cell lysate was stored at −20°C for further use. Protein purification was performed using metal affinity chromatography. The crude lysate was loaded onto a nickel sepharose column (Sangon Biotech, Shanghai, China) after equilibration with loading buffer (50 mM sodium phosphate and 300 mM NaCl, pH 7.0). Non-specifically bound proteins were removed after prewashing with two column volumes of sodium phosphate buffer (pH 7.0) with 50 mM and 100 mM imidazole, the CepTA was eluted from the column with two column volumes of sodium phosphate buffer (pH 7.0) with 250 mM imidazole and dialyzed against sodium phosphate buffer (100 mM, pH 7.0) for 24 h at 4ºC. Finally, the purified enzyme solutions were stored at 4 °C for further use.

5. Enzyme activity assay

The amine transaminase (ATA) activity toward amines was assayed by the method of Schätzle.[5] The reaction mixture (0.5 mL) consisted of 100 mM glycine-NaOH buffer (pH 9.0), 2.5 mM (*R*)- or (*S*)-amines, 2.5 mM sodium pyurvate, 0.1 mM pyridoxal 5'-phosphate (PLP) and an appropriate amount of enzyme. One unit of enzyme is defined as the amount of enzyme that catalyses the production of 1 μmol of ketone in 1 min. For the substrate β-amino alcohols, the ATA activity was assayed by 2,3,5-triphenyltetrazolium chloride (TTC) method as our previously described.[6] Briefly, the reaction mixture (0.5 mL) contained 100 mM glycine-NaOH buffer (pH 9.0), 2.5 mM (*S*)- or (*R*)-β-amino alcohols, 2.5 mM sodium pyurvate, 0.1 mM PLP and an appropriate amount of enzyme. After the enzyme solution was added, the reaction mixtures were immediately incubated at 35°C for 5 min, 200 μL of reaction mixtures was added to a 96-well plate, 40 μL TTC-solution was quickly added, then, the color formation commenced at room temperature within 10 min due to the reaction with the α-hydroxy ketones. The activity measurements were performed on a Multiskan Spectrum Microplate Reader (Thermo Scientific Fisher Inc.) at 510 nm. All activity measurements were performed in triplicate. One unit of enzyme is defined as the amount of enzyme that catalyses the production of 1 μmol of α-hydroxy ketone in 1 min. The Bradford method [7] was used to determine the protein concentration of the enzyme solution, bovine serum albumin (BSA) was used as standard.

6. Effect of pH and temperature on enzyme activity

The effect of pH and temperature on enzyme activity was analyzed with the (1*R*,2*R*)-*trans*-2-aminocyclohexanol **1**'k. Two buffer systems were used to determine the optimum pH of purified CepTA,

one system with sodium phosphate buffer (100 mM, pH 7.0–8.0), another system with glycine-NaOH buffer (100 mM, pH 8.0–10.0). To measure the optimum temperature of purified CepTA, the enzyme activity was assayed at the temperature from 20ºC to 60ºC in glycine-NaOH buffer (100 mM) under the optimized pH. The pH stability of the enzyme was examined by incubating the enzyme in 1 mL sodium phosphate buffer (pH 6.0–8.0) and glycine-NaOH buffer (100 mM, pH 9–10). To examine the thermal stability of CepTA, the enzyme was incubated in 1 mL glycine-NaOH buffer (100 mM, pH 9.0) at the temperature from 4°C to 50°C. Samples were taken at certain time intervals, and the residual transaminase activity assays were carried out under standard assay conditions.

7. Determination of kinetic parameters of purified CepTA

The kinetic parameters (K_M and V_{max}) of CepTA were determined in glycine-NaOH buffer (100 mM, pH 9.0) and six concentrations (1-10 mM) of substrates at a constant co-substrate (sodium pyruvate) concentration (30 mM).[8] Kinetic analysis with initial rate data obtained at the conversion lower than 10%. Nonlinear regression fitting of the Michaelis–Menten equation was used to determine the Michaelis constant (K_M) and the maximum velocity (V_{max}). All assays were performed in triplicate.

8. Kinetic resolution of racemic amines and β-amino alcohols with the resting cells of *E. coli* (CepTA)

In a 50 mL reaction vessel, 5 mL reaction mixture contained 100 mM glycine-NaOH buffer (pH 9.0, 0.2 mM PLP), 10-500 mM racemic amines or β-amino alcohols, 10-500 mM sodium pyruvate, and 10 g CDW L^{-1} *E. coli* (CepTA). The reaction was started by addition of substrate and shaken at 35ºC (200 rpm). After the reaction mixture was incubated for 24 h, 0.3 mL samples were taken and saturated with NaCl, followed by extraction with 0.3 mL ethyl acetate (EtOAc) containing 20 mM of n-dodecane as an internal standard. The organic phase was dried (anhydrous Na_2SO_4) and the concentration of ketones or α-hydroxy ketone was measured by GC. To extract the amines or β-amino alcohols, 0.3 mL sample was basified by adding NaOH (0.1 mL, 10 N), saturated with NaCl. Then the amines or β-amino alcohols were extracted with EtOAc (0.3 mL). The organic phase was dried over anhydrous Na_2SO_4 and measured by GC. To analysis the *ee* of *trans*-1-amino-2-indanol, 0.5 mL sample was taken, saturated with NaCl, *trans*-1-amino-2-indanol was extracted with 500 μL dichloromethane, after shaking and centrifugation (12000 rpm) for 5 min, the organic phase (dichloromethane) portion was transferred into a clean tube and dried by evaporation, 300 μL of isopropyl alcohol was added to dissolve the residues in the tube,

after centrifugation, the solvents were used for chiral HPLC analysis.

9. Asymmetric reduction amination of ketones and α-hydroxy ketones with the resting cells of *E. coli* (CepTA)

Asymmetric reductive amination of ketones and α-hydroxy ketones was performed at 35ºC in 3 mL 100 mM glycine-NaOH buffer (pH 9.0) containing PLP (0.2 mM), ketones or α-hydroxy ketones (10 mM), DMSO (5%, V/V), amine donors (200 mM D-Ala or 10 mM R-MBA) and *E. coli* (CepTA) (20 g CDW L^{-1}). When using D-alanine as an amine donor, NADH (0.5 mM), lactate dehydrogenase from *Bacillus subtilis* (20 U), glucose (50 mM) and glucose dehydrogenase (10 U) from *Bacillus subtilis* were also added. When using R-MBA as an amine donor, the same amount of R-MBA was added. After the reaction mixture was incubated for 24 h, 0.3 mL sample was basified by adding NaOH (0.1 mL, 10 N), saturated with NaCl. Then the amines and β-amino alcohols were extracted with EtOAc (0.3 mL). The organic phase was dried over anhydrous Na_2SO_4 and measured by GC. To analysis the *ee* of *trans*-1-amino-2-indanol, 0.5 mL sample was taken, saturated with NaCl, *trans*-1-amino-2-indanol was extracted with 500 μL dichloromethane, after shaking and centrifugation (12000 rpm) for 5 min, the organic phase (dichloromethane) portion was transferred into a clean tube and dried by evaporation, 300 μL of isopropyl alcohol was added to dissolve the residues in the tube, after centrifugation, the solvents were used for chiral HPLC analysis.

10. Homology modelling, molecular Docking and molecular dynamics simulations

The homology homo-dimer model of *Mv*TA[9] and *Cep*TA were built in SWISS-MODEL using the structure of (*R*)-selective amine transaminase from *Exophiala xenobiotica* (PDB ID: 6FTE, 74% identity) and *Rb*TA (PDB ID: 7DBE, 46% identity) as the template, respectively.[10] PyMOL (version 2.5) was used to perform the visual inspection and evaluation of the active site. The *Mv*TA/*Cep*TA, together with pyridoxamine-5'-phosphate (PMP) and substrate, were assigned ionization states corresponding to a pH of 7.4 in **PROPKA3**.[11] The cofactor PMP and the substrate (*R*)-α-hydroxycyclohexan-1-one **2**'k were initially optimized using the HF/6-31G (d, p) method, and atomic point charges were obtained using the RESP algorithm.[12-13] Molecular docking was performed using the AutoDock Vina suit with standard free energy scoring function.[14] To simulate the transamination process of *Mv*TA and *Cep*TA, the PMP and substrate (*R*)-α-hydroxycyclohexan-1-one **2**'k were docked into the active site of the enzymes,

respectively. The obtained *Cep*TA/*Mv*TA-PMP-substrate complexes with top-ranked conformation and lowest energy were chosen and subsequently subjected to further analysis in PyMOL. Following this detailed examination, the selected complexes were then submitted to molecular dynamics (MD) simulations for a comprehensive study.

In MD studies, each system was solvated using TIP3P (cubic, 10 Å padding, periodic boundary conditions applied) water model, and a physiological concentration of 0.15 M NaCl ions were added with an appropriate excess of either Na^+ or Cl^- to neutralize the system. The system was primarily optimized using steepest descent algorithm to meet the maximum force less than 10 Kj mol^{-1}, then followed by 5000 cycles of conjugated gradient. After the minimization, each system was gradually heated in the NVT ensemble form 0 to 298.15 K within 200 ps, followed by a 500 ps position restrain NPT ensemble at a pressure of 1 atm. For the docked complexes, several MD simulations on 100 ns with a time step of 2.0 fs were performed under a constant temperature of 298.15 K, the entire coordinate file was saved each 10 ps. The simulation temperature and pressure were controlled by a V-rescale thermostat and Parrinello-Rahman barostat, respectively.[15] The Particle-mesh Ewald (PME) method was applied to calculate the electrostatic interactions, and hydrogen bonds constraints were applied with LINCS algorithm. All simulations were performed in Gromacs 2022 using AMBER14 force filed.[16]

11. One-pot conversion of cyclic *meso*-epoxide 4'j-k to cyclic (1*R*,2*R*)-*trans*-β-amino alcohols 1'j-k with the mixtures of resting cells of *E. coli* (SpEH-AnDDH-BsLDH) and *E. coli* (CepTA)

The standard reactions were carried out in 5 mL glycine-NaOH buffer (100 mM, pH 9.0) containing 10-50 mM **4**'j-k, 10 g CDW L^{-1} *E. coli* (SpEH-AnDDH-BsLDH), 20-30 g CDW L^{-1} *E. coli* (CepTA), 10% DMSO, 200-1000 mM D-Ala was also added as the amino donor. The reactions were carried out at 30°C and 200 rpm in capped 50 mL conical flask. To quantitate the formation of **1**'j-k, 300 µL aliquots were taken out at different time points, basified by adding NaOH (0.1 mL, 10 N), saturated with NaCl and extracted with 0.3 mL ethyl acetate (EtOAc) containing 20 mM of *n*-dodecane as an internal standard. The organic phase was dried over anhydrous sodium sulfate and subjected to GC analysis. All experiments were performed in duplicate.

12. Preparative experiments

In a 250 mL reaction vessel, a 100 mL mixture containing 100 mM of glycine-NaOH buffer (pH 9.0), 15

mM (147.0 mg) of **4**'k, 5% methanol, 300 mM D-Ala, 0.2 mM PLP, 10 g CDW L^{-1} *E. coli* (SpEH-AnDDH-BsLDH) and 30 g CDW L^{-1} *E. coli* (CepTA). The reaction was conducted at 30°C and 200 rpm for 24 hours. The cells were removed by centrifuging (4500×g, 4°C for 10 minutes), the supernatant was basified (pH>10, 10 M NaOH) and saturated with NaCl, extracted three times with ethyl acetate (50 mL) by centrifugation (16000×g, 4°C for 10 minutes). The combined ethyl acetate phase was dried over anhydrous Na_2SO_4. The solvent was removed by rotary evaporation under reduced pressure, the crude products were purified through flash chromatography using a column packed with silica gel. This process yielded (1*R*,2*R*)-*trans*-**1**'k as white solid in 55.8% yield (82.0 mg). ^{1}H NMR (600 MHz, $CDCl_3$) δ 1.04–1.18 (m, 1H), 1.18–1.37 (m, 3H), 1.58–1.79 (m, 2H), 1.80–1.90 (m, 1H), 1.92–2.01 (m, 1H), 2.37–2.59 (m, 4H), 3.08–3.19 (m, 1H); ^{13}C NMR (75 MHz, $CDCl_3$) δ 24.8, 25.0, 33.9, 34.3, 56.9, 75.6.

13. Analytical methods

The concentrations of amines and β-amino alcohols were measured by gas chromatograph. Gas chromatography analysis was carried out with a GC-14C gas chromatography (Shimadzu, Japan) equipped with a flame ionization detector (FID). The analytical conditions were as follows:

Method A: Column: Agilent J&W HP-5 (30 m, 0.32 mm, 0.25 μm).

Parameter: injector temperature, 250°C; detector temperature, 275°C; temperature program: column temperature, 120°C, hold 30 min.

Method B: Column: Agilent J&W DB-WAX (30 m, 0.32 mm, 0.30 μm).

Parameter: injector temperature, 250°C; detector temperature, 300°C; temperature program: column temperature, 90°C, hold 5 min; gradient 10°C min^{-1} up to 230°C, hold 60 min.

Method C: Column: Agilent J&W DB-1701 (30 m, 0.25 mm, 0.25 μm).

Parameter: injector temperature, 250°C; detector temperature, 300°C; temperature program: column temperature, 90°C; gradient 10°C min^{-1} up to 160°C, hold 2 min; gradient 20°C min^{-1} up to 240°C, hold 30 min.

Method D: Column: Agilent J&W HP-5 (30 m, 0.32 mm, 0.25 μm).

Parameter: injector temperature, 250°C; detector temperature, 275°C; temperature program: column temperature, 90°C, gradient 2°C min^{-1} up to 100°C, hold 10 min.

Method E: Column: Agilent J&W HP-5 (30 m, 0.32 mm, 0.25 μm).

Parameter: injector temperature, 250°C; detector temperature, 275°C; temperature program: column

temperature, 130°C, hold 20 min.

Method F: Column: Agilent J&W HP-5 (30 m, 0.32 mm, 0.25 μm).

Parameter: injector temperature, 250°C; detector temperature, 275°C; temperature program: column temperature, 140°C, hold 20 min.

Method G: Column: Agilent J&W HP-5 (30 m, 0.32 mm, 0.25 μm).

Parameter: injector temperature, 250°C; detector temperature, 275°C; temperature program: column temperature, 150°C, hold 20 min.

Table S1 Retention times [min] for the product **1** and **1**' analysed by achiral GC.

Compound	[min]	Method	Compound	[min]	Method
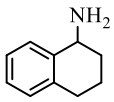 **1**a	7.28	A	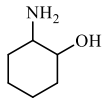 **1**'k	8.28	C
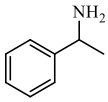 **1**b	2.53	A	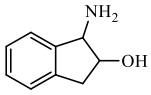 **1**'m	7.38	E
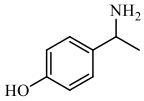 **1**c	22.72	B	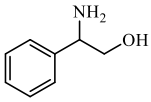 **1**'n	5.69	A
 **1**g	5.95	C	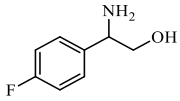 **1**'o	6.13	A
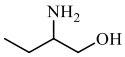 **1**'h	1.97	D	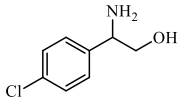 **1**'p	7.69	F
 **1**'j	7.12	C	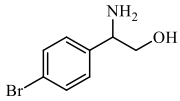 **1**'q	8.23	G

The enantiomeric excesss of amines and β-amino alcohols were determined by GC using a method described by Mutti.[17] Briefly, the samples were analyzed with a chiral column (CP-Chirasil-Dex CB, 25 m x 0.32 mm x 0.25 μm; Agilent Technologies, lnc.) after derivatization with 4-dimethylamino pyridine (DMAP) and acetic anhydride. The acetylation was performed at 40 °C in an Eppendorf orbital shaker (700 rpm) for 4 h. The reactions were quenched with a saturated NH_4Cl solution (500 μL) and the supernatant dried by anhydrous Na_2SO_4 and analyzed *via* chiral GC measurement. The enantiomeric

excesss of *trans*- or *cis*-1-amino-2-indanol **1**'l-m was determined by using a Shimadzu HPLC on a Chiralcel OJ-H column (4.6×250 mm, 5 μm). The chiral GC and HPLC analysis conditions were as follows:

Method H (chiral GC): Column: Agilent J&W CP-Chirasil-Dex CB, (25 m, 0.32 mm, 0.25 μm).

Parameter: injector temperature, 250°C; detector temperature, 275°C; temperature program: column temperature, 120°C; gradient 5°C min^{-1} up to 160°C, hold 20 min.

Method I (chiral GC): Column: Agilent J&W CP-Chirasil-Dex CB, (25 m, 0.32 mm, 0.25 μm).

Parameter: injector temperature, 250 ºC; detector temperature, 275 °C; temperature program: column temperature, 100 °C, hold 10 min; gradient 5 °C min^{-1} up to 180 °C, hold 60 min.

Method J (chiral GC): Column: Agilent J&W CP-Chirasil-Dex CB, (25 m, 0.32 mm, 0.25 μm).

Parameter: injector temperature, 250°C; detector temperature, 275°C; temperature program: column temperature, 120°C; gradient 2°C min^{-1} up to 160°C, hold 50 min.

Method K (chiral GC): Column: Agilent J&W CP-Chirasil-Dex CB, (25 m, 0.32 mm, 0.25 μm).

Parameter: injector temperature, 250°C; detector temperature, 275°C; temperature program: column temperature, 100°C; gradient 2°C min^{-1} up to 120°C, hold 3 min; gradient 5°C min^{-1} up to 160°C, hold 5 min.

Method L (chiral GC): Column: Agilent J&W CP-Chirasil-Dex CB, (25 m, 0.32 mm, 0.25 μm).

Parameter: injector temperature, 250°C; detector temperature, 275°C; temperature program: column temperature, 140°C, hold 30 min.

Method M (chiral HPLC): Column: Chiral Technologies, Chiralcel OJ-H (4.6×250 mm, 5 μm).

Parameter: mobile phase: n-hexane: isopropanol=9:1, measured at 254 nm at a flow rate of 0.5 mL/min.

Method N (chiral GC): Column: Agilent J&W CP-Chirasil-Dex CB, (25 m, 0.32 mm, 0.25 μm).

Parameter: injector temperature, 250°C; detector temperature, 275°C; temperature program: column temperature, 100°C, gradient 2°C min^{-1} up to 150°C, hold 50 min.

Method O (chiral GC): Column: Agilent J&W CP-Chirasil-Dex CB, (25 m, 0.32 mm, 0.25 μm).

Parameter: injector temperature, 250°C; detector temperature, 275°C; temperature program: column temperature, 140°C, gradient 2°C min^{-1} up to 160°C, hold 50 min.

Method P (chiral GC): Column: Agilent J&W CP-Chirasil-Dex CB, (25 m, 0.32 mm, 0.25 μm).

Parameter: injector temperature, 250°C; detector temperature, 275°C; temperature program: column temperature, 140°C, gradient 2 °C min^{-1} up to 165°C, hold 70 min.

Method Q (chiral GC): Column: Agilent J&W CP-Chirasil-Dex CB, (25 m, 0.32 mm, 0.25 μm). Parameter: injector temperature, 250°C; detector temperature, 275°C; temperature program: column temperature, 140°C, gradient 2°C min^{-1} up to 150°C, hold 120 min.

Method R (chiral GC): Column: Agilent J&W CP-Chirasil-Dex CB, (25 m, 0.32 mm, 0.25 μm). Parameter: injector temperature, 250°C; detector temperature, 275°C; temperature program: column temperature, 140°C, gradient 2°C min^{-1} up to 170°C, hold 45 min.

Method S (chiral GC): Column: Agilent J&W CP-Chirasil-Dex CB, (25 m, 0.32 mm, 0.25 μm). Parameter: injector temperature, 250°C; detector temperature, 275°C; temperature program: column temperature, 140°C, gradient 2°C min^{-1} up to 175 °C, hold 50 min.

Table S2 Retention times [min] for the product **1** and **1**' analyzed by chiral GC and HPLC.

Compound	[min]	Method	Compound	[min]	Method
 (*S*)-**1**a	21.73	H	 (*R*)-**1**a	23.79	H
 (*S*)-**1**b	8.79	H	 (*R*)-**1**b	9.10	H
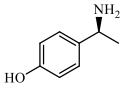 (*S*)-**1**c	34.30	I	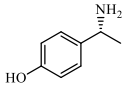 (*R*)-**1**c	34.69	I
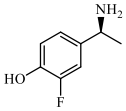 (*S*)-**1**d	32.60	I	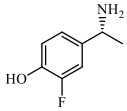 (*R*)-**1**d	33.04	I
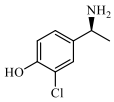 (*S*)-**1**e	41.66	I	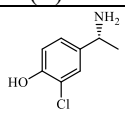 (*R*)-**1**e	42.35	I
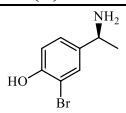 (*S*)-**1**f	49.98	I	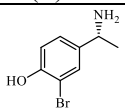 (*R*)-**1**f	50.91	I
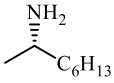 (*S*)-**1**g	6.49	H	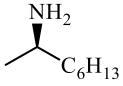 (*R*)-**1**g	6.74	H

Continued Table S2

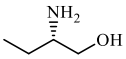 (*S*)-**1**'h	8.30	J	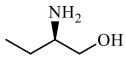 (*R*)-**1**'h	8.63	J
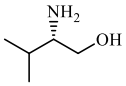 (*S*)-**1**'i	16.56	K	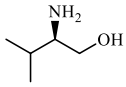 (*R*)-**1**'i	16.80	K
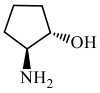 (1*S*,2*S*) -**1**'j	10.64	L	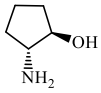 (1*R*,2*R*)-**1**'j	11.33	L
 (1*S*,2*S*)-**1**'k	13.33	L	 (1*R*,2*R*)-**1**'k	13.96	L
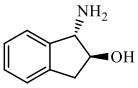 (1*S*,2*S*)-*trans*-**1**'l	14.02	M	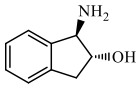 (1*R*,2*R*)-*trans*-**1**'l	10.02	M
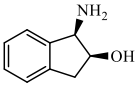 (1*R*,2*S*)-*cis*-**1**'m	12.14	M	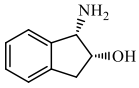 (1*S*,2*R*)-*cis*-**1**'m	15.26	M
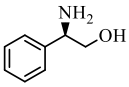 (*R*)-**1**'n	43.77	N	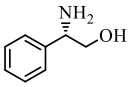 (*S*)-**1**'n	44.49	N
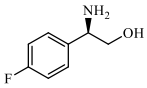 (*R*)-**1**'o	47.71	N	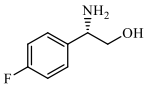 (*S*)-**1**'o	48.38	N
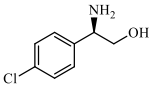 (*R*)-**1**'p	51.02	O	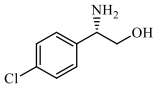 (*S*)-**1**'p	51.94	O
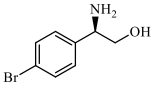 (*R*)-**1**'q	62.56	P	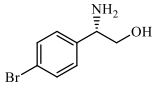 (*S*)-**1**'q	63.59	P
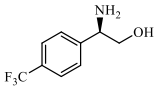 (*R*)-**1**'r	23.35	O	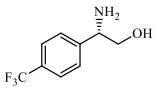 (*S*)-**1**'r	23.87	O
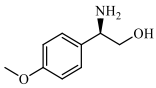 (*R*)-**1**'s	105.64	Q	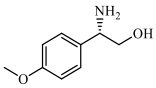 (*S*)-**1**'s	107.70	Q

Continued Table S2

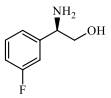 (*R*)-**1**'t	21.01	O	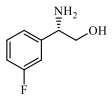 (*S*)-**1**'t	21.40	O
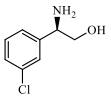 (*R*)-**1**'u	30.79	R	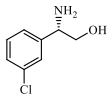 (*S*)-**1**'u	31.31	R
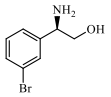 (*R*)-**1**'v	36.75	S	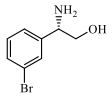 (*S*)-**1**'v	37.28	S
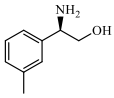 (*R*)-**1**'w	26.31	O	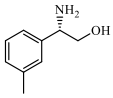 (*S*)-**1**'w	26.85	O

Table S3 Screening of ATAs for conversion of (*R*)-α-hydroxycyclohexan-1-one **2**'k to chiral 2-aminocyclohexanol **1**'k.

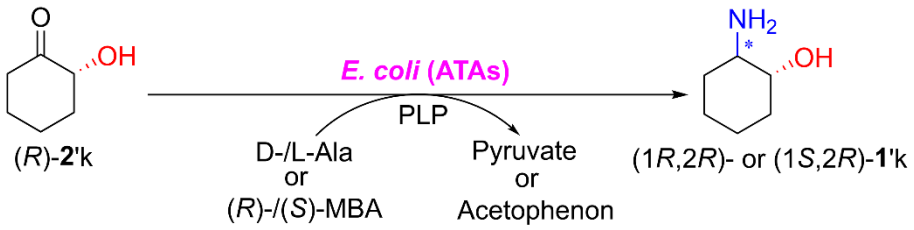

Enzymes	Selectivity	Sources	Time (h)	Conversion (%)		*ee* (%)
				D-/L-Ala	(*R*)-/(*S*)-MBA	
ArTA[18]	*R*	*Arthrobacter sp.* KNK168	24	<1.0	<1.0	-
RbTA[19]	*R*	*Rhodobacter* sp. 140A	24	<1.0	<1.0	-
MVTA[9]	*R*	*Mycobacterium vanbaalenii*	24	<1.0	<1.0	-
CepTA	*R*	*Capronia epimyces*	24	70.0	72.0	>99(1*R*,2*R*)
CV2025[20]	*S*	*Chromobacterium violaceum*	24	<1.0	<1.0	-
BMTA[21]	*S*	*Bacillus megaterium*	24	<1.0	<1.0	-
Pp21050[22]	*S*	*Pseudomonas putida* NBRC14164	24	<1.0	<1.0	-
PpbauA[22]	*S*	*Pseudomonas putida* NBRC14164	24	<1.0	<1.0	-
Pp36420[22]	*S*	*Pseudomonas putida* NBRC14164	24	<1.0	<1.0	-
PpspuC[22]	*S*	*Pseudomonas putida* NBRC14164	24	<1.0	<1.0	-
Gene393	ND	*Arthrobacter* sp. TYUT010-15[23]	24	<1.0	<1.0	-
Gene461	ND	*Arthrobacter* sp. TYUT010-15[23]	24	<1.0	<1.0	-
Gene674	ND	*Arthrobacter* sp. TYUT010-15[23]	24	<1.0	<1.0	-
Gene844	ND	*Arthrobacter* sp. TYUT010-15[23]	24	<1.0	<1.0	-
Gene1266	ND	*Arthrobacter* sp. TYUT010-15[23]	24	<1.0	<1.0	-
Gene1926	ND	*Arthrobacter* sp. TYUT010-15[23]	24	<1.0	<1.0	-
Gene2981	ND	*Arthrobacter* sp. TYUT010-15[23]	24	<1.0	<1.0	-
Gene3807	ND	*Arthrobacter* sp. TYUT010-15[23]	24	<1.0	<1.0	-
Gene3848	ND	*Arthrobacter* sp. TYUT010-15[23]	24	<1.0	<1.0	-
Gene3917	ND	*Arthrobacter* sp. TYUT010-15[23]	24	<1.0	<1.0	-
Gene1827	ND	*Arthrobacter* sp. TYUT010-15[23]	24	<1.0	<1.0	-
Gene3010	ND	*Arthrobacter* sp. TYUT010-15[23]	24	<1.0	<1.0	-
Gene892	ND	*Arthrobacter* sp. TYUT010-15[23]	24	<1.0	<1.0	-
Gene2218	ND	*Arthrobacter* sp. TYUT010-15[23]	24	<1.0	<1.0	-
Gene4053	ND	*Arthrobacter* sp. TYUT010-15[23]	24	<1.0	<1.0	-
Gene4219	ND	*Arthrobacter* sp. TYUT010-15[23]	24	<1.0	<1.0	-
Gene2577	ND	*Arthrobacter* sp. TYUT010-15[23]	24	<1.0	<1.0	-
Gene3950	ND	*Arthrobacter* sp. TYUT010-15[23]	24	<1.0	<1.0	-
Gene3879	ND	*Arthrobacter* sp. TYUT010-15[23]	24	<1.0	<1.0	-
Gene300	ND	*Arthrobacter* sp. TYUT010-15[23]	24	<1.0	<1.0	-
Gene3192	ND	*Arthrobacter* sp. TYUT010-15[23]	24	<1.0	<1.0	-
Gene869	ND	*Arthrobacter* sp. TYUT010-15[23]	24	<1.0	<1.0	-
Gene558	ND	*Arthrobacter* sp. TYUT010-15[23]	24	<1.0	<1.0	-
Gene3684	ND	*Arthrobacter* sp. TYUT010-15[23]	24	<1.0	<1.0	-

Reaction condition: 1 mL sodium phosphate buffer (100 mM, pH 8.0) containing 10 mM (*R*)-α-hydroxycyclohexan-1-one **2**'k, 10 g cdw/L *E. coli* (ATA), 0.2 mM PLP, 10% DMSO, 200 mM D-/L-Ala or 15 mM (*R*)-/(*S*)-MBA as amine donor, 30°C and 200 rpm for 24 h. ND: not determined.

Table S4 Kinetic parameters for the CepTA toward selected substrates.

Substrate	k_{cat} **(s^{-1})**	K_M **(mM)**	k_{cat}/K_M **(S^{-1}mM^{-1})**
(*R*)-**1**b	1.27	4.20	0.30
(*R*)-**1**g	0.54	4.30	0.13
(1*R*, 2*R*)-**1**'j	0.78	5.88	0.13
(1*R*, 2*R*)-**1**'k	0.10	2.14	0.05
(1*S*, 2*S*)-**1**'l	0.20	0.52	0.38
(*S*)-**1**'n	3.13	14.20	0.22

[a] Kinetic parameters represent the apparent rate constants determined at a fixed concentration of sodium pyruvate (30 mM). Standard conditions: 500 μL glycine-NaOH buffer (100 mM, pH 9.0) with 1-10 mM amine donor, 30 mM sodium pyruvate, 0.1 mM PLP, and 10 μL purified CepTA (4 mg mL^{-1}), 30°C for 5-15 min. All assays were performed in triplicate. The kinetic data presented represent averages of measurements.

Table S5 Protein sequence identity of CepTA towards other amine transaminases.

Enzymes	Sources	Protein Mw (Da)	Protein pI	Identity (%)	Reference
CepTA	*Capronia epimyces*	36966.31	5.50	100	This study
ArTA	*Arthrobacter* sp. KNK168	35927.51	4.74	47	[18]
RbTA	*Rhodobacter* sp. 140A	36688.95	5.11	46	[19]
MVTA	*Mycobacterium vanbaalenii*	36639.37	5.02	47	[9]

Table S6. Comparison residues around the pocket of CepTA with the reported *R*-TAs.

Enzyme	PDB ID	Residues around the pocket										
		O-pocket					P-pocket					
		Conserved			Non-conserved residues		Conserved					Non-conserved residues
*Cep*TA	-	H53	W183	G215	R126	V148	Y58	V60	T273	T274	A275	F113
*Mv*TA	-	H69	W199	G231	K142	A164	Y74	V76	T289	T290	A291	F129
*Ex*TA	**6FTE**	H53	W183	G215	R126	V148	Y58	V60	T273	T274	A275	F113
*Rb*TA	**7DBE**	H65	W195	G227	P138	V160	Y70	V72	T285	T286	A287	Y125

Table S7. Conversion **4**'j-k to **2**'j-k with the resting cells of *E. coli* (SpEH-AnDDH-BsLDH).

Sub.	**Sub. (mM)**	***E. coli* (SpEH-AnDDH-BsLDH) (g CDW L^{-1})**	**Time (h)**	**Conv. to 2' (%)[a]**	***ee* of 2' (%)[b]**
4'j	10	10	4	90	>99(*R*)
4'j	20	10	6	90	>99(*R*)
4'j	50	10	12	88	>99(*R*)
4'k	10	10	4	90	>99(*R*)
4'k	20	10	6	90	>99(*R*)
4'k	50	10	12	86	>99(*R*)

[a]Reaction conditions: 5 mL glycine-NaOH buffer (100 mM, pH 9.0) containing 10-50 mM **4**'j-k, 10% (V/V) DMSO, 50 mM pyruvate, 10 g CDW L^{-1} *E. coli* (SpEH-AnDDH-LDH) at 30°C and 200 rpm. Conversion was determined by achiral GC, error limit: <2%; *ee* was determined by chiral GC,

Table S8. E-factor calculation.[a]

This work[b]			**Literature reported**[24][c]		
	Waste	E-Factor ($g\ g^{-1}$)		Waste	E-Factor ($g\ g^{-1}$)
Reaction	Cyclohexanediol	0.21	Reaction (Step 1)	Cyclohexene oxide	0.63
	Lactic acid	1.31		Catalyst	0.05
	D-Ala	30.94		MeCN	1.51
	PLP	0.03		Phenyl carbamate	0.10
	Cells	48.78		Phenol	1.02
	Methanol	48.17		Si-Triamine	0.27
				CH_2Cl_2	15.28
			Reaction (Step 2)	Ethanol	36.44
				KOH	8.78
				HCOOK	0.73
Extraction	Ethyl acetate (95% recycle)	82.5	Extraction and recrystallization	CH_2Cl_2	137.54
				Ether	82.35
				Toluene	7.23
Total		211.9	Total		291.9

[a]E-factor = (amount of total waste) [g] / (amount of product) [g]; [b]E-factors were calculated including solvents used and excluding water. [c]E-factors were calculated using the values in the respective literature, including solvents used and excluding water.

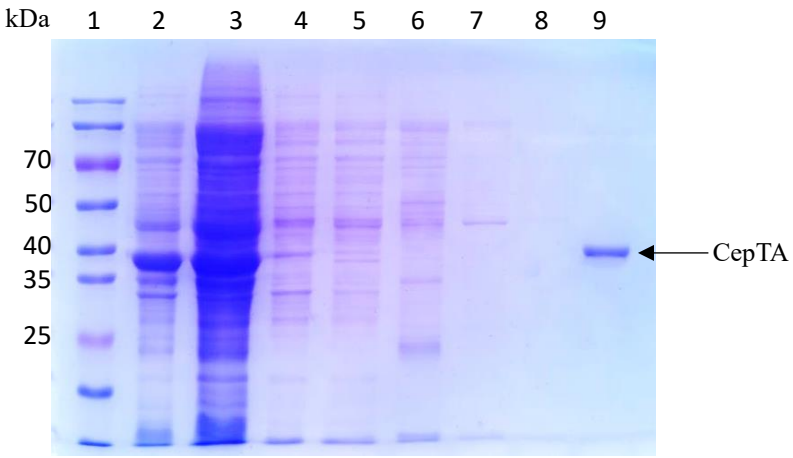

Fig. S1. SDS-PAGE analysis of CepTA. Lane 1: Marker; Lane 2: the resting cell of the *E. coli* (CepTA); Lane 3: cell free extract of *E. coli* (CepTA); Lane 4: wash fraction with 20 mM imidazole; Lane 5: wash fraction with 50 mM imidazole; Lane 6-8: wash fraction with 100 mM imidazole, lane 9: wash fraction with 250 mM imidazole (the purified CepTA) (about 37 kDa).

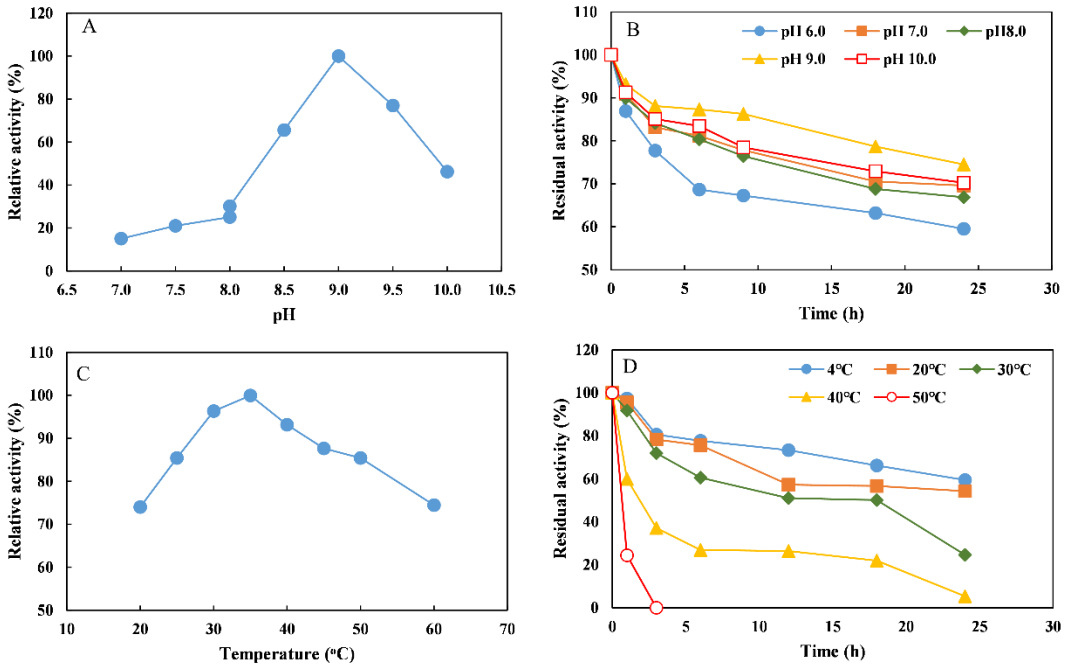

Fig. S2. The effect of pH and temperature on the activity and stability of CepTA.

```
CepTA       ----------------MASMDKVFAGYQSRLRVLEASTNPLAQGVAWIEGELVPLSQARI     44
ArTA        -------------MTSEIVYTHDTGLDYITYSDYELDPANPLAGGAAWIEGAFVPPSEARI     48
RbTA        ----MNQLTILEAGLDEIICETVPGEAIQYSRYSLDRTSPLAGGCAWIEGAFVPAAAARI     56
MVTA        MGIDTGTSNLVAVEPGAIREDTPAGSVIQYSDYEIDYSSPFAGGVAWIEGEYLPAEDAKI     60
                                 .                 :.*:* * *****  :*   *:*

CepTA       PLMDQGFLHSDLTYDVPAVWDGRFFRLDDHISRLEKSCSKLRLKLPLPRDEVKRVLVDMV    104
ArTA        SIFDQGYLHSDVTYTVFHVWNGNAFRLDDHIERLFSNAESMRIIPPLTQDEVKEIALELV    108
RbTA        SIFDAGFGHSDVTYTVAHVWHGNFFRLEDHVERFLAGAEKMRIPMPATKAEIMDLMRGCV    116
MVTA        SIFDTGFGHSDLTYTVAHVWHGNIFRLGDHLDRLLDGARKLRLDSGYTKDELADITKKCV    120
             ::* *: ***:** *  **.*. *** **:.*:  .. .:*:     : *:  :    *

CepTA       ARSGIRDAFVELIVTRGLTGVRGAGRPEDLVNNLYMFLQPYLWVMPPETQLVGGSAVITR    164
ArTA        AKTELREAFVSVSITRGYSSTPGERDITKHRPQVYMYAVPYQWIVPFDRIRDGVHAMVAQ    168
RbTA        SKSGLREAYVNVCVTRGYGRKPGEKTLEALESQLYVYAIPYLWVFSPIRQIEGIDAVIAQ    176
MVTA        SLSQLRESFVNLTITRGYGKRKGEKDLSKLTHQVYIYAIPYLWAFPPAEQIFGTTAVVPR    180
            : : :*:::*.: :***     *         ::*::  ** * .       *  *:: :

CepTA       TVRRTPPGSMDPTVKNLQWGDLTRALLEASDRGASYPFLTDGDANITEGSGYNIVLIKDG    224
ArTA        SVRRTPRSSIDPQVKNFQWGDLIRAVQETHDRGFEAPLLLDGDGLLAEGSGFNVVVIKDG    228
RbTA        SVRRSPANVMDPWIKNYQWGDLVRATFEAQERGARTAFLLDSDGFVTEGPGFNVLMVKDG    236
MVTA        HVRRAGRNTVDPTIKNYQWGDLTAASFEAKDRGARTAILMDADNCVAEGPGFNVCIVKDG    240
             ***:  . :** :** *****  *  *: :**    :* *.*  ::** *:*: ::***

CepTA       AIHTPDRGVLEGVTRKTVFDIAKANGFEVRLEVVPVELAYRADEIFMCTTAGGIMPITSL    284
ArTA        VVRSPGRAALPGITRKTVLEIAESLGHEAILADITLAELLDADEVLGCTTAGGVWPFVSV    288
RbTA        TVFTAARNVLPGITRRTALEIARDFGLQTVIGDVTPEMLRGADEIFAATTAGGVTPVVAL    296
MVTA        KLASPSRNALPGITRKTVFEIAGAMGIEAALRDVTSHELYDADEIMAVTTAGGVTPINTL    300
             : :  * .* *:**:*.::**   * :. :  :       ***::  *****: *. ::

CepTA       DGQPVNGGQIGPITKKIWDDYWALHYDPAFSFE-IKYDEAGASTNGVNGVHK   335
ArTA        DGNPISDGVPGPITQSIIRRYWELNVESSSLLTPVQY---------------   325
RbTA        DGAPVGAGVPGDWTRKIRTRYWQMMDEPSDLIEPVSYI--------------   334
MVTA        DGVPIGDGEPGPVTVAIRDRFWALMDEPGPLIEAIQY---------------   337
            ** *:. *  *  *  *   :* :  : .  :  :.*
```

Fig. S3. Amino acid sequence alignment of CepTA from *Capronia epimyces* with ArTA from *Arthrobacter* (47% identity, Accession number: 3WWH_A), RbTA from *Rhodobacter* sp. 140A (46% identity, Accession number: 7DBE_A) and MVTA from *Mycobacterium vanbaalenii* (47% identity, Accession number: WP_011781668.1). The multiple sequences alignment by the Clustal W2. Yellow: PLP binding sites. Red: putative active-site lysine. Green: putative (*R*)-selective ATA motif. "*": the identical amino acids; ".": similar amino acids; ":": highly similar amino acids.

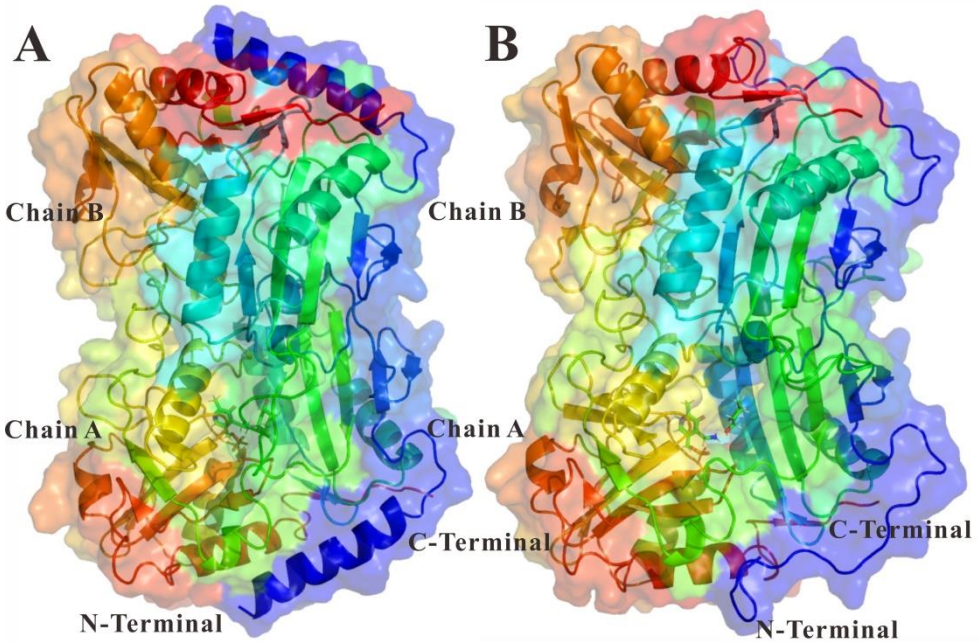

Fig. S4. Homology modeling and molecular docking. A): CepTA-PMP-(*R*)-2-hydroxycyclohexan-1-one complex. B): MvTA-PMP-(*R*)-2-hydroxycyclohexan-1-one complex.

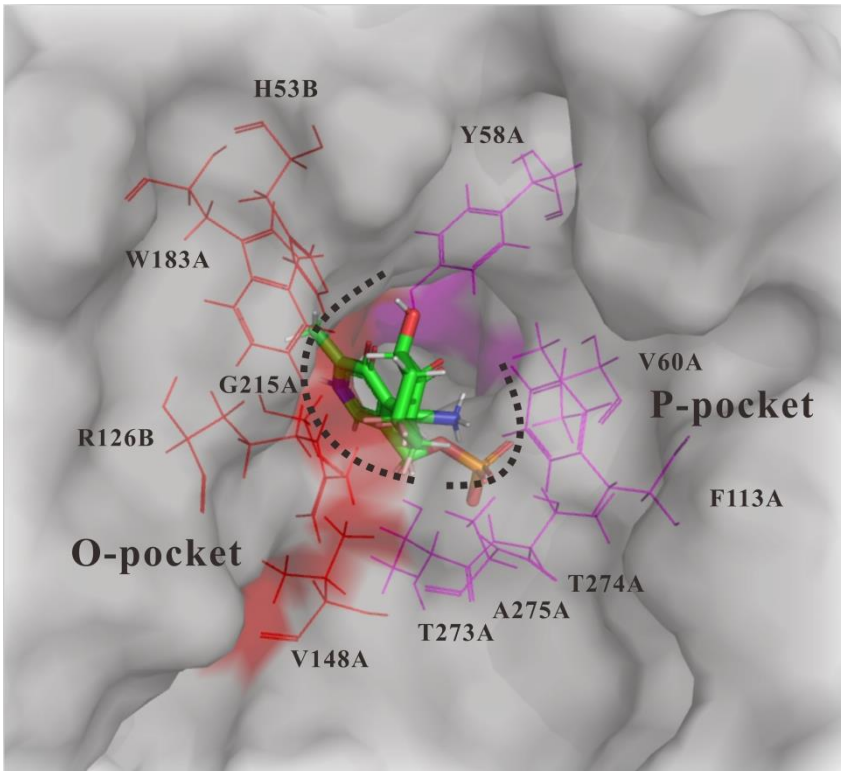

Fig. S5. The substrate binding pocket of *Cep*TA and the residues around the pocket.

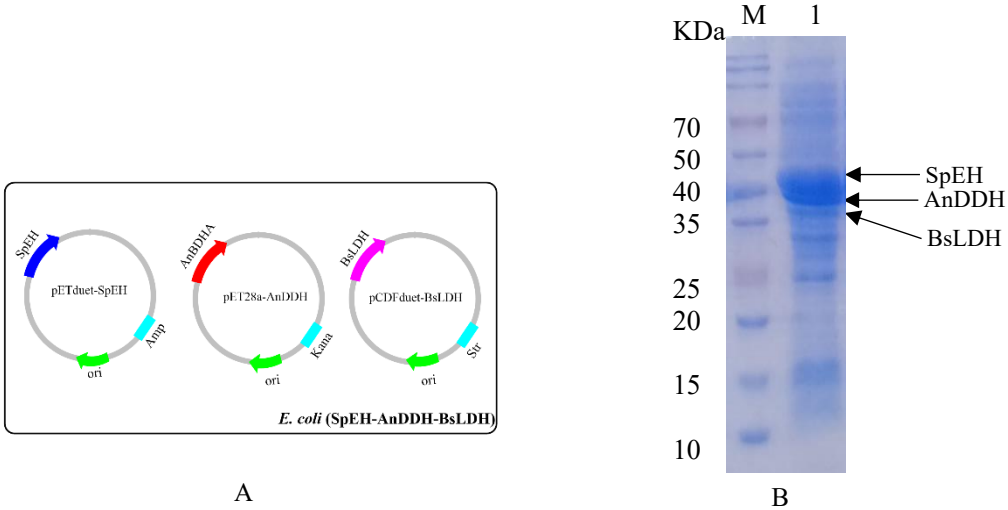

Fig. S6. Recombinant *E. coli* (SpEH-AnDDH-BsLDH) cells co-expression of multiple enzymes. A: Construction of recombinant *E. coli* (SpEH-AnDDH-BsLDH) cells; B: SDS-PAGE of the cell-free extracts of recombinant *E. coli* (SpEH-AnDDH-BsLDH) cells. Lane M: protein marker, lane 1: cell free extract of *E. coli* (SpEH-AnDDH-BsLDH).

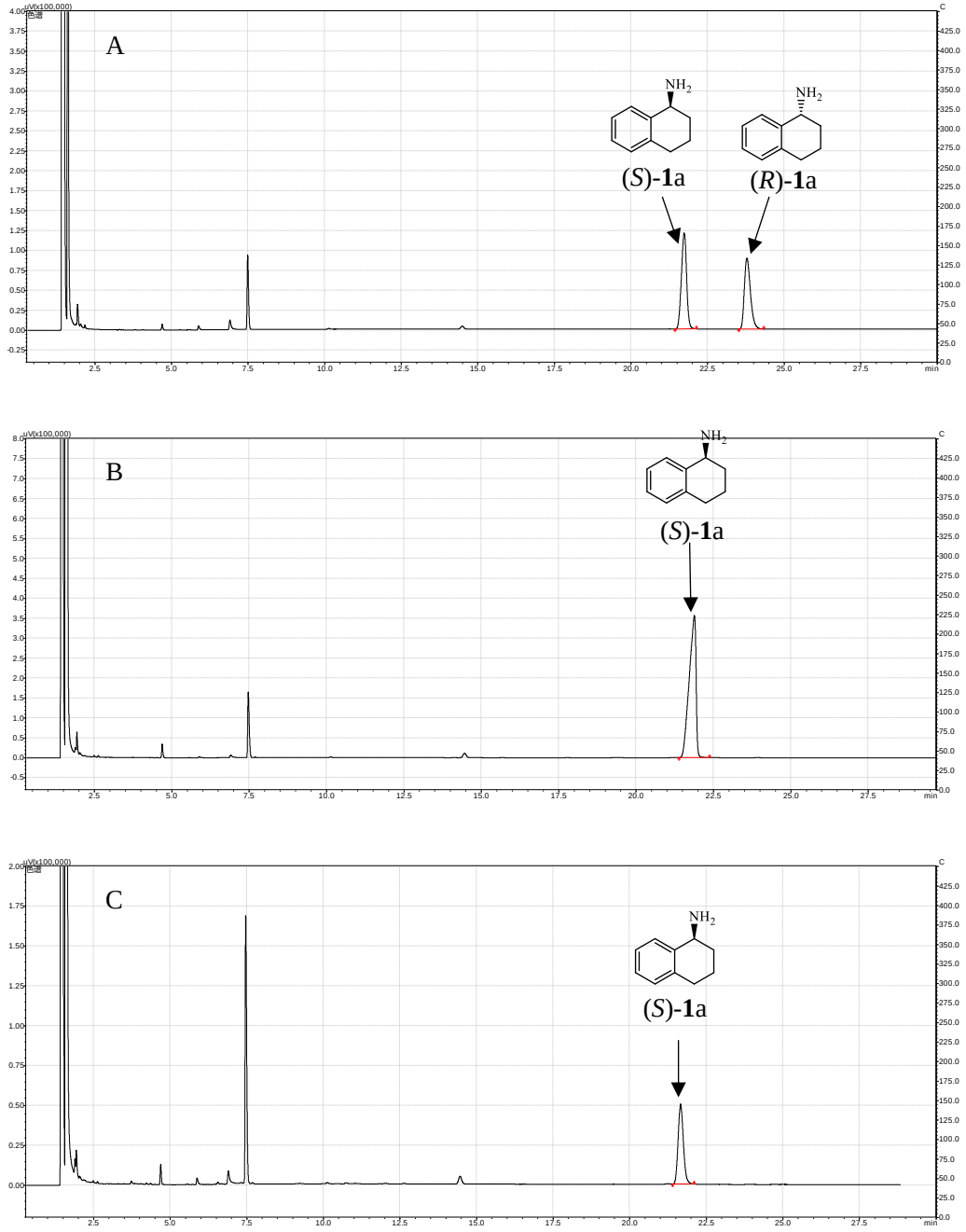

Fig. S7. Chiral GC analysis of 1,2,3,4-tetrahydro-1-naphthylamine **1**a. **A**: racemic 1,2,3,4-tetrahydro-1-naphthylamine (**1**a) standard; **B**: (*S*)-1,2,3,4-tetrahydro-1-naphthylamine (**1**a) standard; **C**: (*S*)-1,2,3,4-tetrahydro-1-naphthylamine (**1**a) (>99% *ee*) produced from kinetic resolution of racemic 1,2,3,4-tetrahydro-1-naphthylamine **1**a (10 mM) with the resting cells of *E. coli* (CepTA).

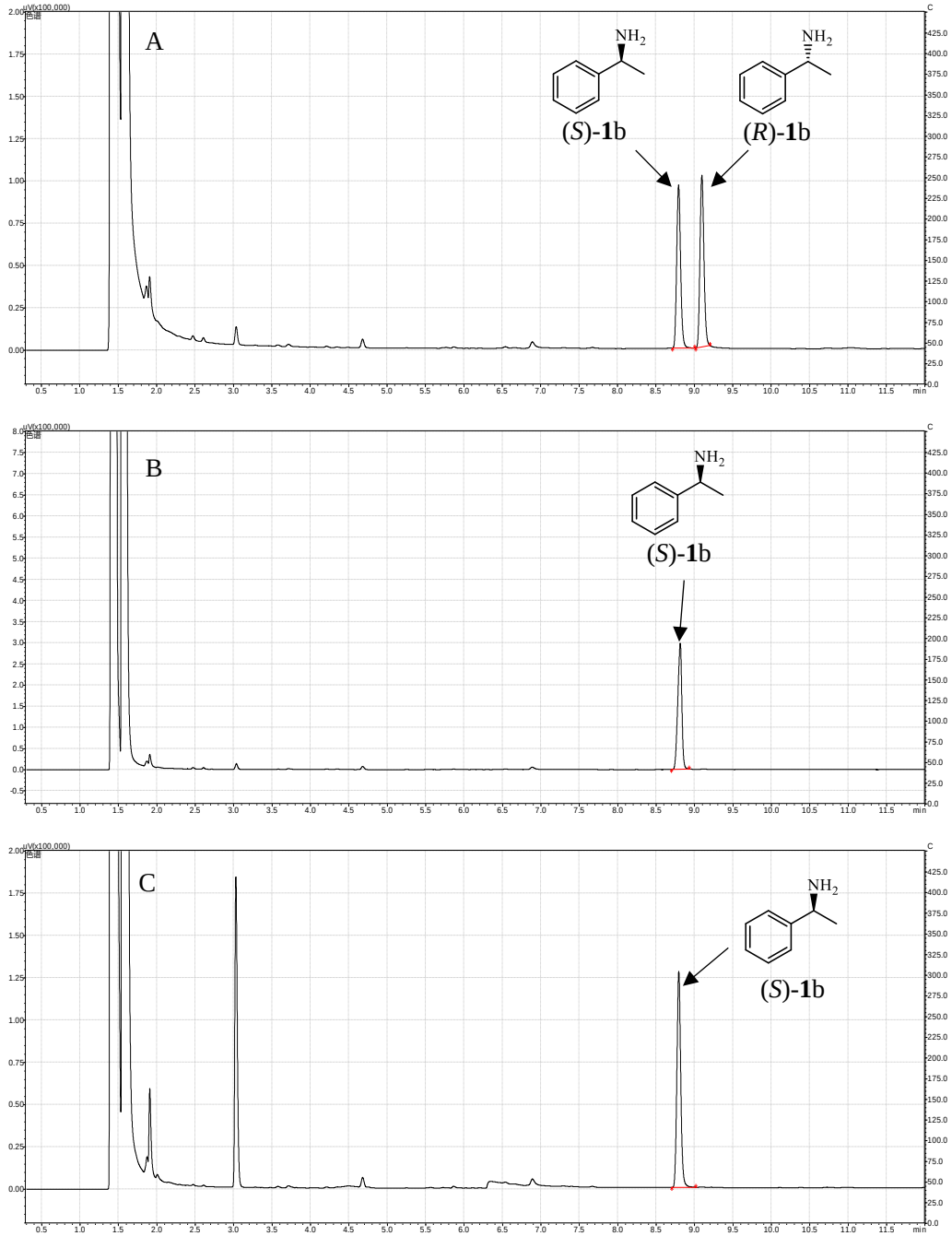

Fig. S8. Chiral GC analysis of 1-phenylethylamine **1**b. **A**: racemic 1-phenylethylamine (**1**b) standard; **B**: (*S*)-1-phenylethylamine (**1**b) standard; **C**: (*S*)-1-phenylethylamine (**1**b) (>99% *ee*) produced from kinetic resolution of racemic 1-phenylethylamine **1**b (10 mM) with the resting cells of *E. coli* (CepTA).

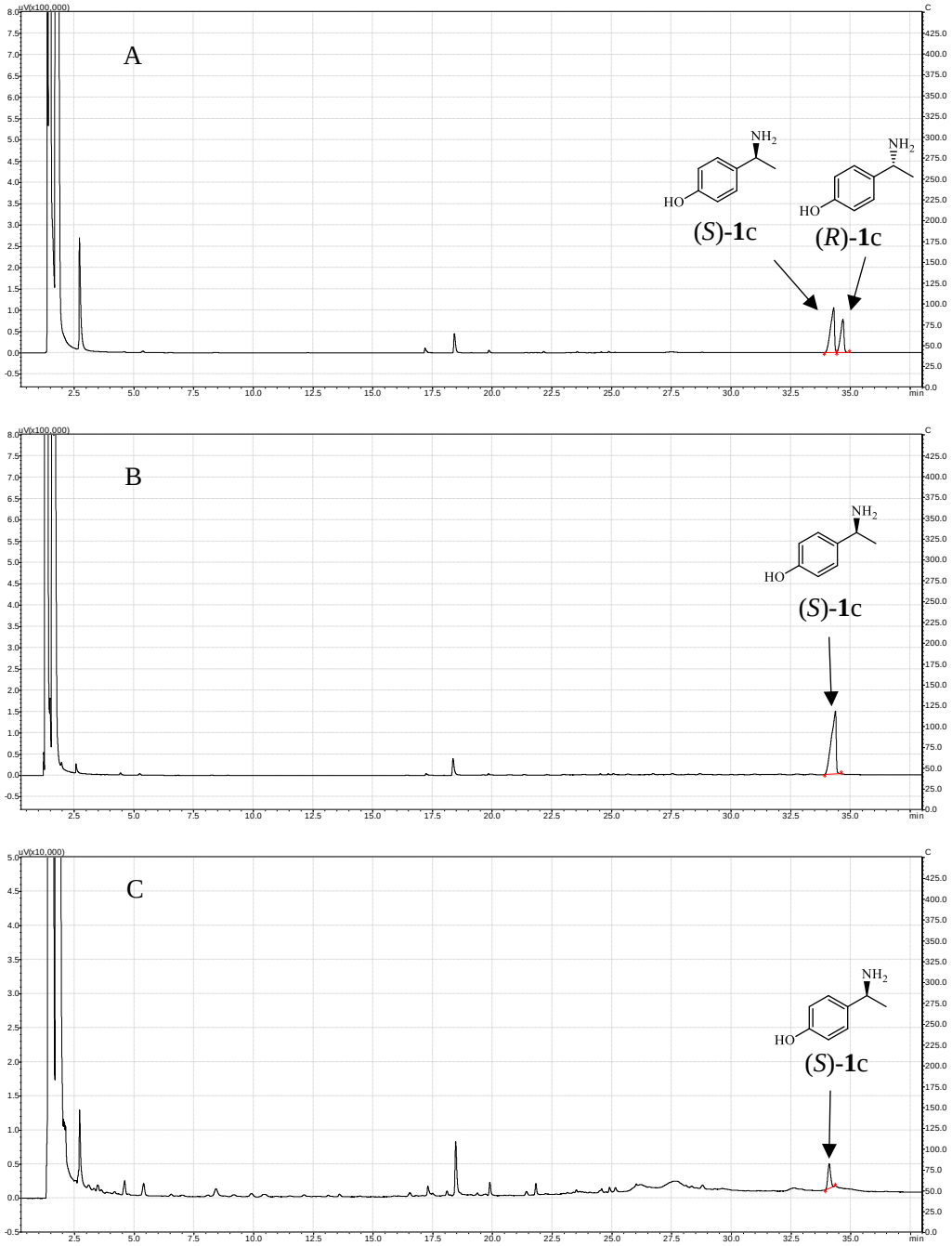

Fig. S9. Chiral GC analysis of 4-(1-aminoethyl)phenol **1**c. **A**: racemic 4-(1-aminoethyl)phenol (**1**c) standard; **B**: (*S*)-4-(1-aminoethyl)phenol (**1**c) standard; **C**: (*S*)-4-(1-aminoethyl)phenol (**1**c) (>99% *ee*) produced from kinetic resolution of racemic 4-(1-aminoethyl)phenol **1**c (10 mM) with the resting cells of *E. coli* (CepTA).

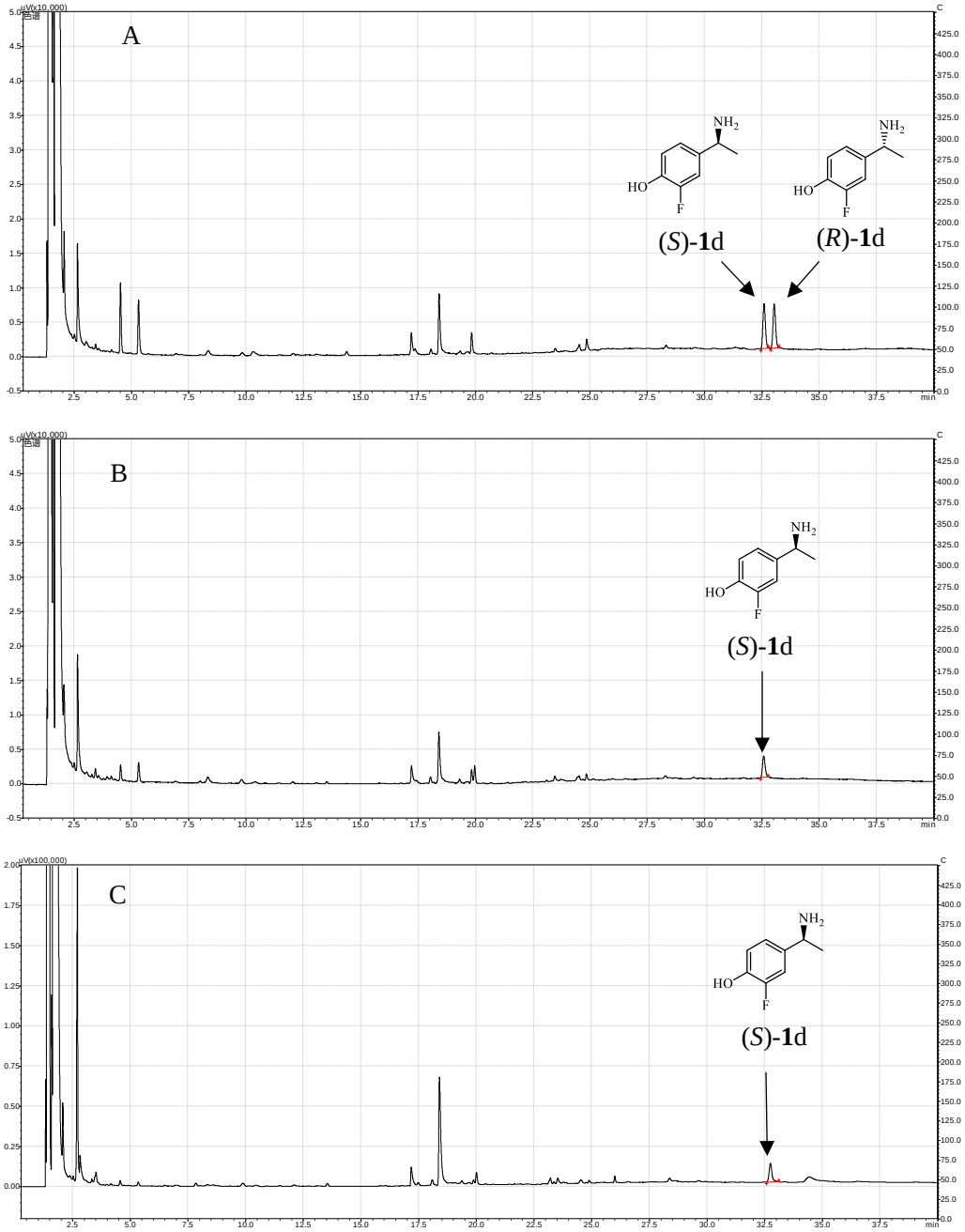

Fig. S10. Chiral GC analysis of 4-(1-aminoethyl)-2-fluorophenol **1**d. **A**: racemic 4-(1-aminoethyl)-2-fluorophenol (**1**d) standard; **B**: (*S*)-4-(1-aminoethyl)-2-fluorophenol (**1**d) standard; **C**: (*S*)-4-(1-aminoethyl)-2-fluorophenol (**1**d) (>99% *ee*) produced from kinetic resolution of racemic 4-(1-aminoethyl)-2-fluorophenol **1**d (10 mM) with the resting cells of *E. coli* (CepTA).

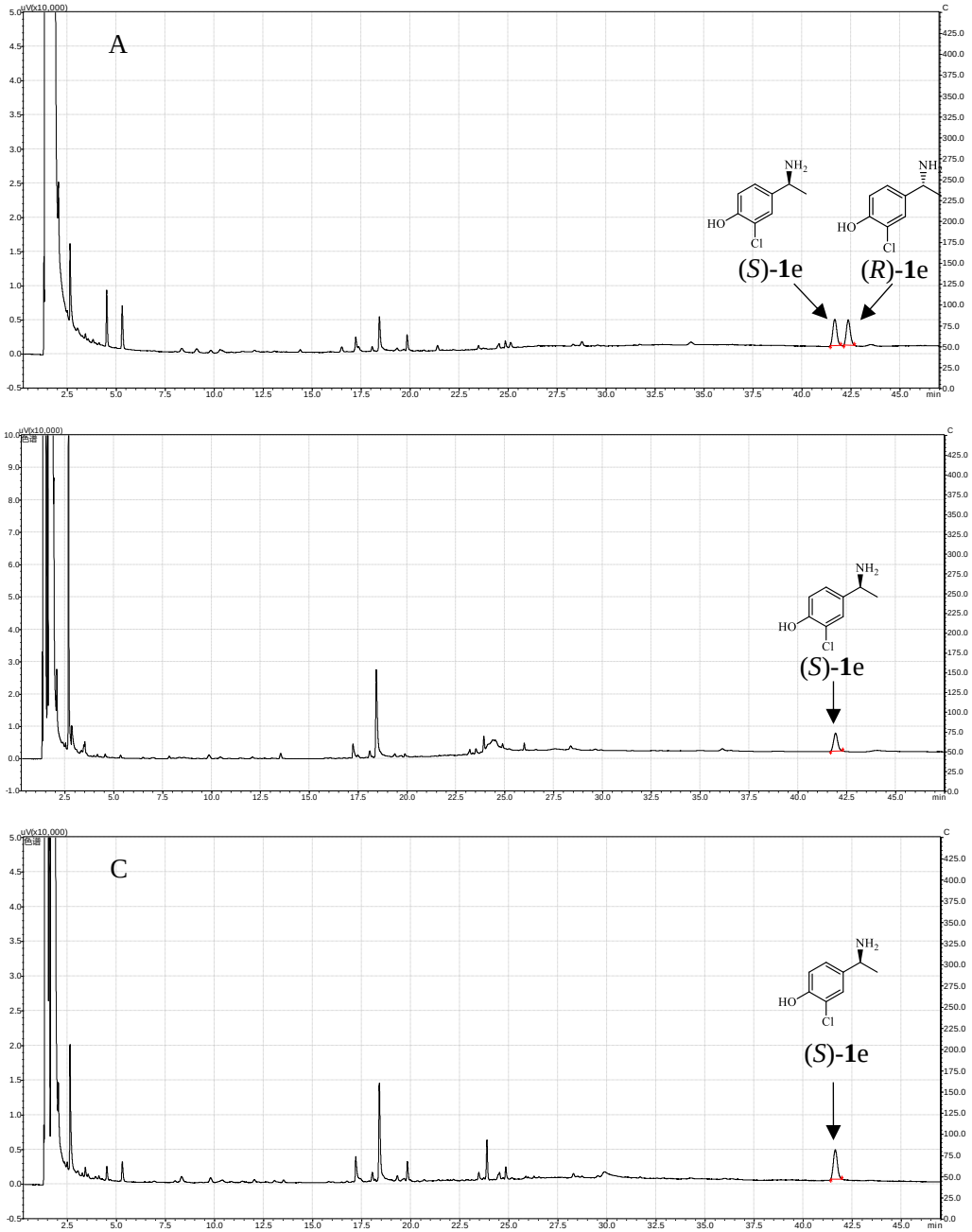

Fig. S11. Chiral GC analysis of 4-(1-aminoethyl)-2-chlorophenol **1**e. **A**: racemic 4-(1-aminoethyl)-2-chlorophenol (**1**e) standard; **B**: (*S*)-4-(1-aminoethyl)-2-chlorophenol (**1**e) standard; **C**: (*S*)-4-(1-aminoethyl)-2-chlorophenol (**1**e) (>99% *ee*) produced from kinetic resolution of racemic 4-(1-aminoethyl)-2-chlorophenol **1**e (10 mM) with the resting cells of *E. coli* (CepTA).

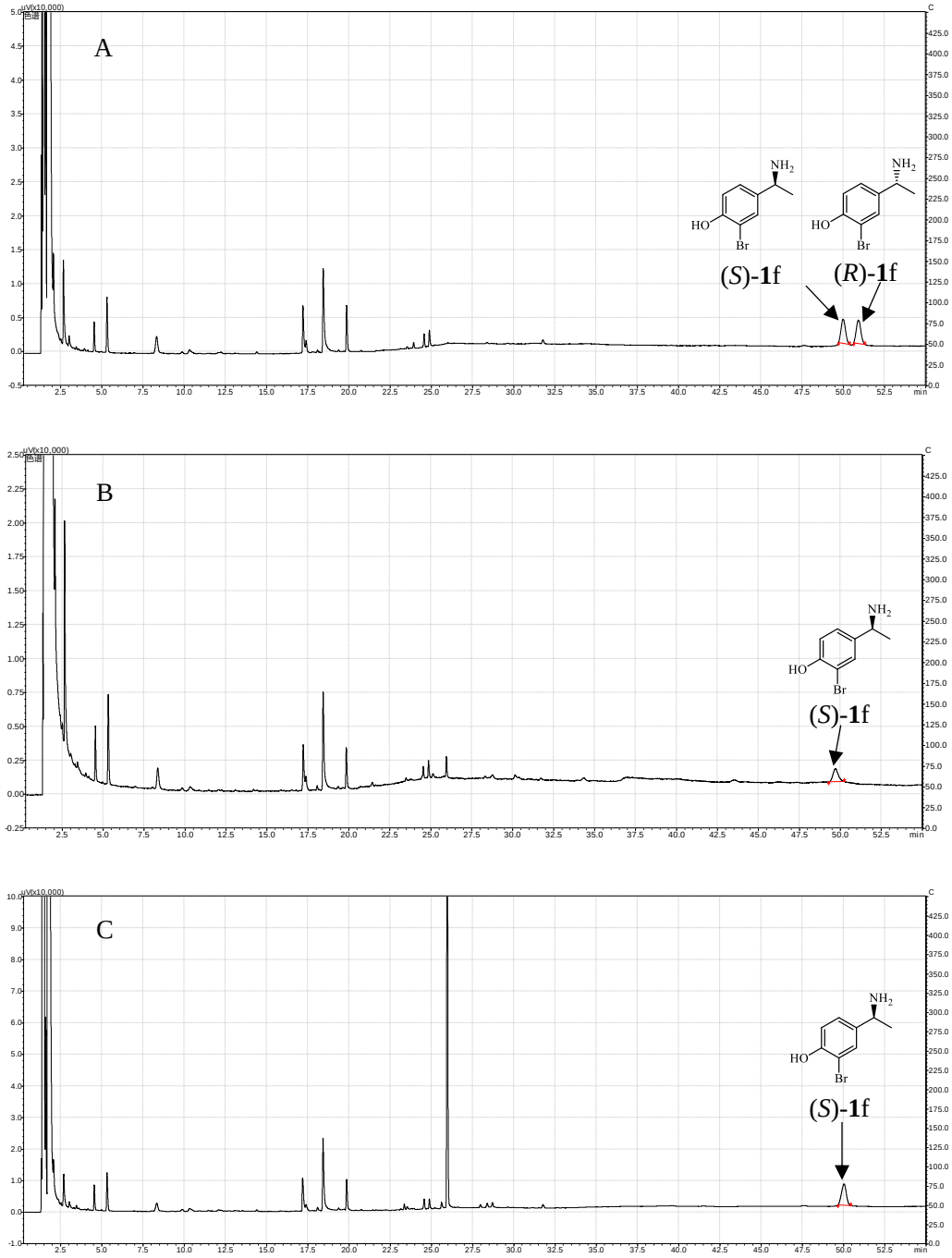

Fig. S12. Chiral GC analysis of 4-(1-aminoethyl)-2-bromophenol **1**f. **A**: racemic 4-(1-aminoethyl)-2-bromophenol (**1**f) standard; **B**: (*S*)-4-(1-aminoethyl)-2-bromophenol (**1**f) standard; **C**: (*S*)-4-(1-aminoethyl)-2-bromophenol (**1**f) (>99% *ee*) produced from kinetic resolution of racemic 4-(1-aminoethyl)-2-bromophenol **1**f (10 mM) with the resting cells of *E. coli* (CepTA).

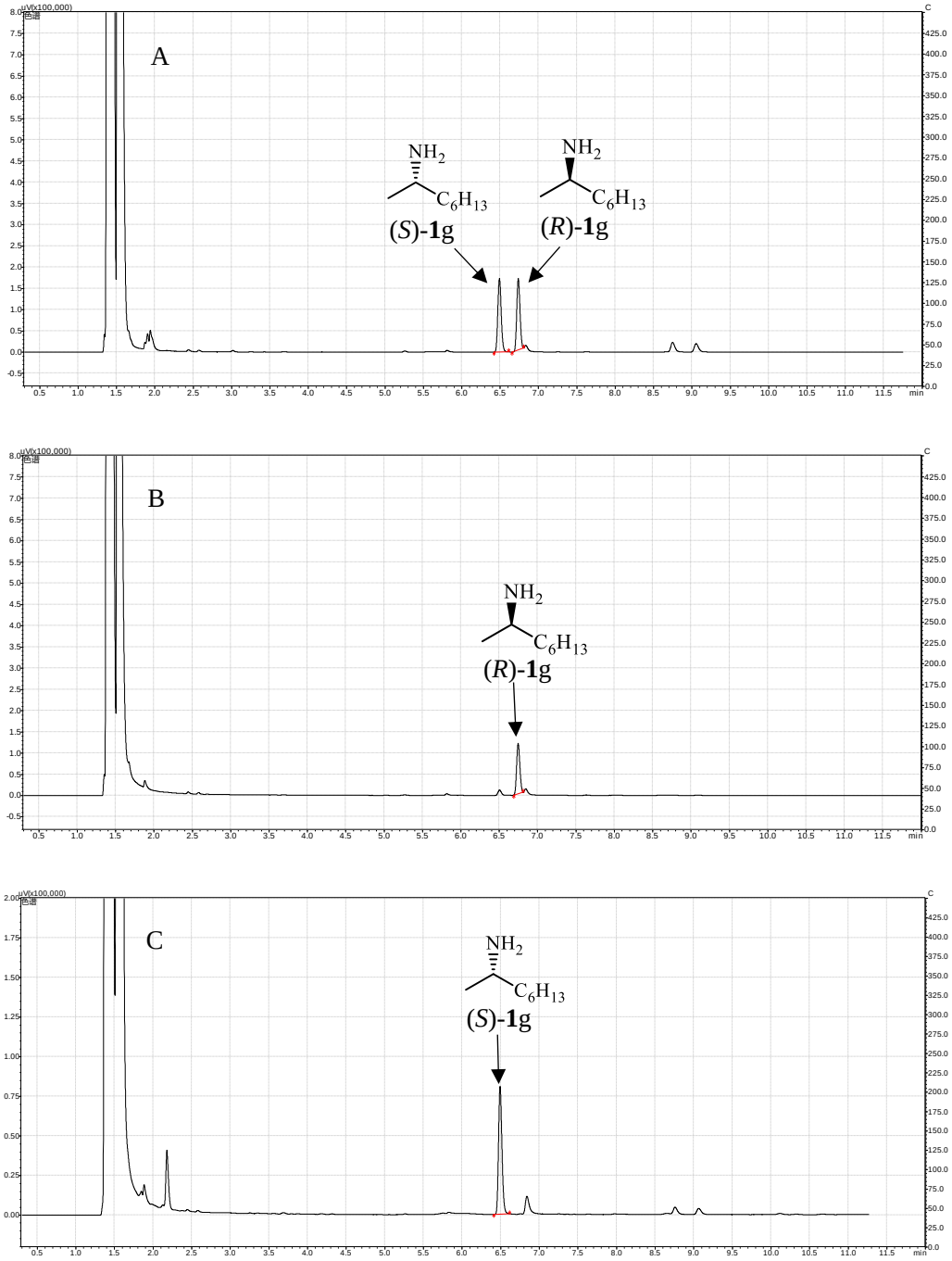

Fig. S13. Chiral GC analysis of 2-octanamine **1**g. **A**: racemic 2-octanamine (**1**g) standard; **B**: (*R*)-2-octanamine (**1**g) standard; **C**: (*S*)-2-octanamine (**1**g) (>99% *ee*) produced from kinetic resolution of racemic 2-octanamine **1**g (10 mM) with the resting cells of *E. coli* (CepTA).

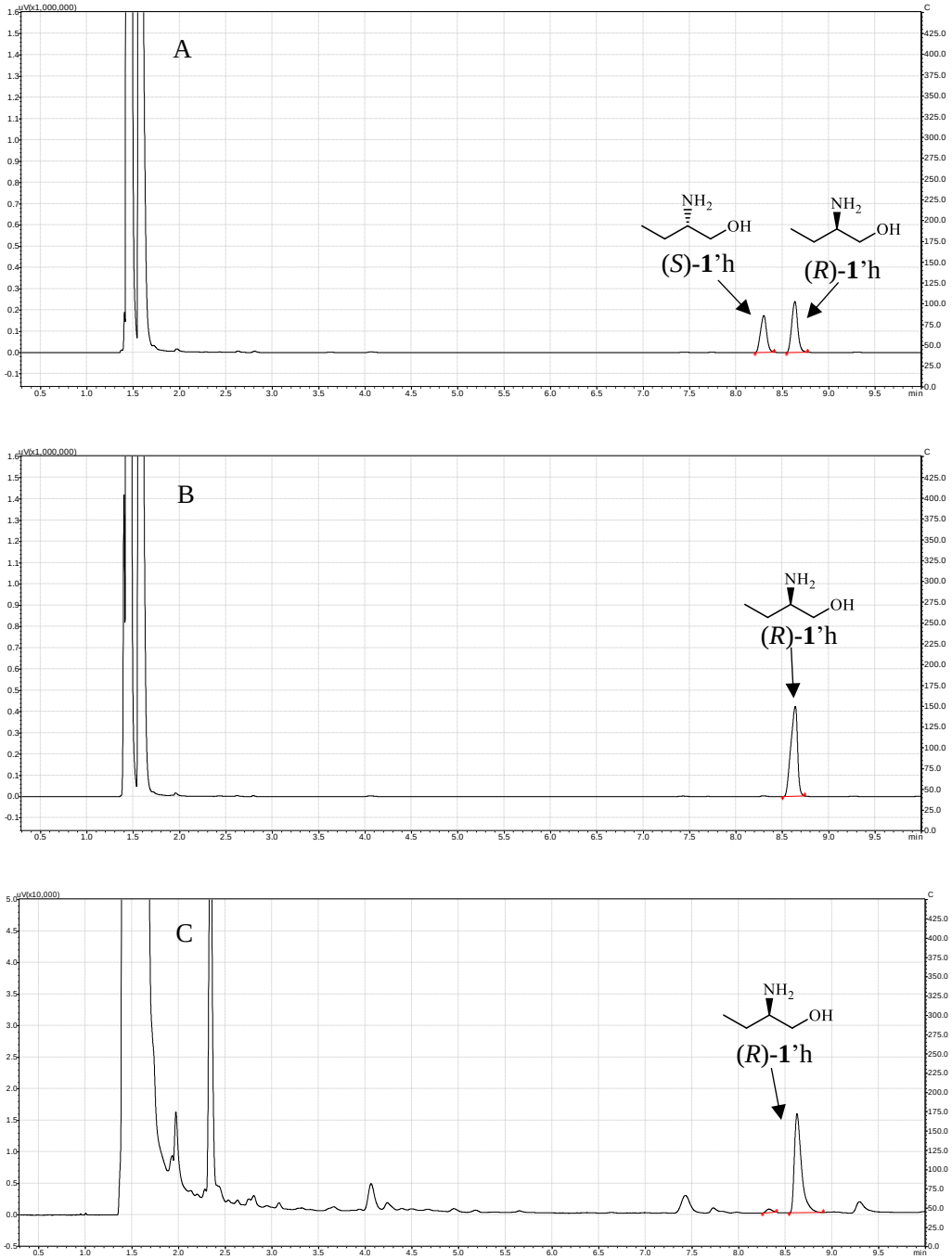

Fig. S14. Chiral GC analysis of 2-amino-1-butanol **1**'h. **A**: racemic 2-amino-1-butanol (**1**'h) standard; **B**: (*R*)-2-amino-1-butanol (**1**'h) standard; **C**: (*R*)-2-amino-1-butanol (**1**'h) (97% *ee*) produced from kinetic resolution of racemic 2-amino-1-butanol **1**'h (10 mM) with the resting cells of *E. coli* (CepTA).

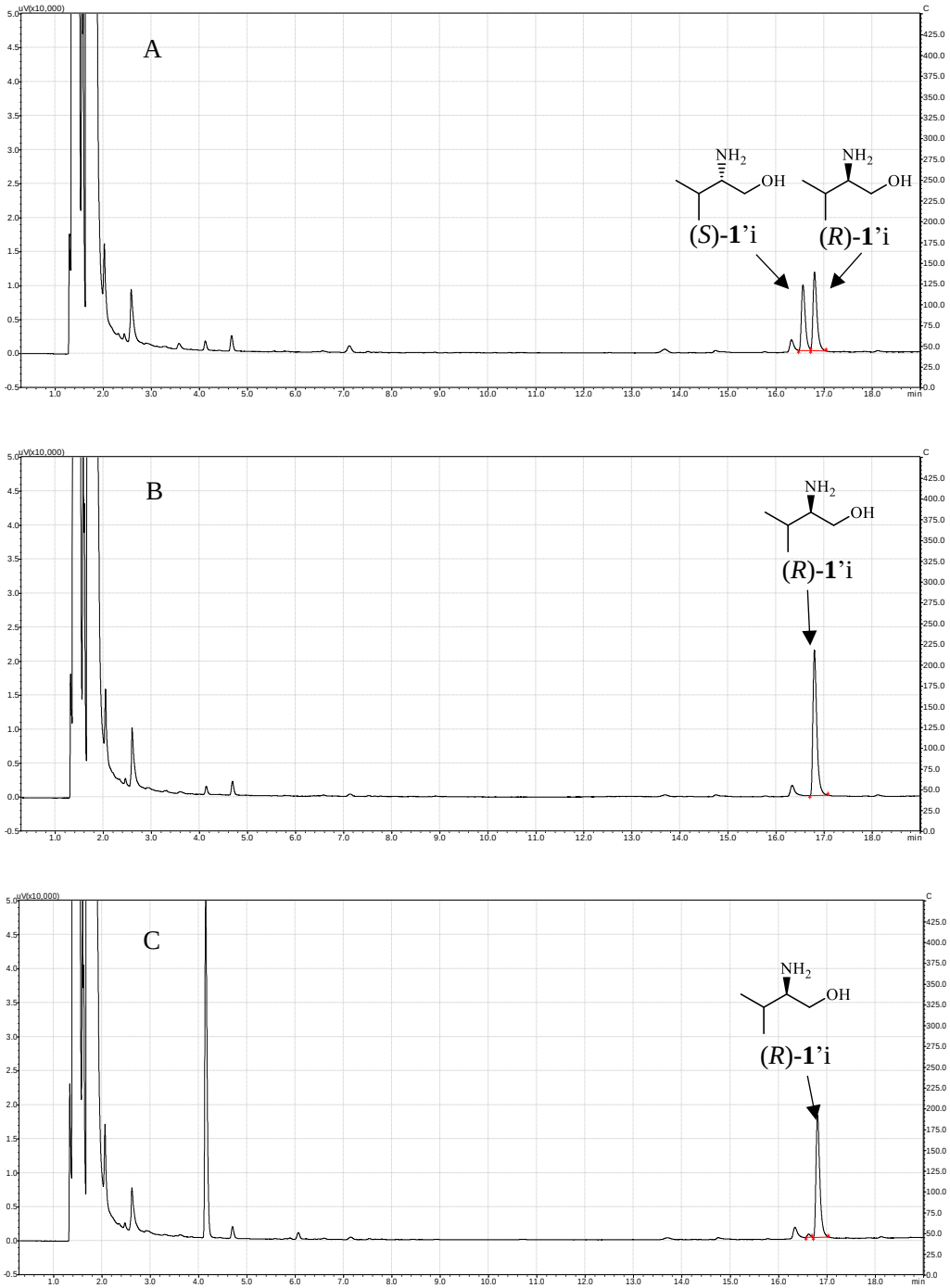

Fig. S15. Chiral GC analysis of valinol **1**'i. **A**: racemic valinol (**1**'i) standard; **B**: (*R*)-valinol (**1**'i) standard; **C**: (*R*)-valinol (**1**'i) (97% *ee*) produced from kinetic resolution of racemic valinol **1**'i (10 mM) with the resting cells of *E. coli* (CepTA).

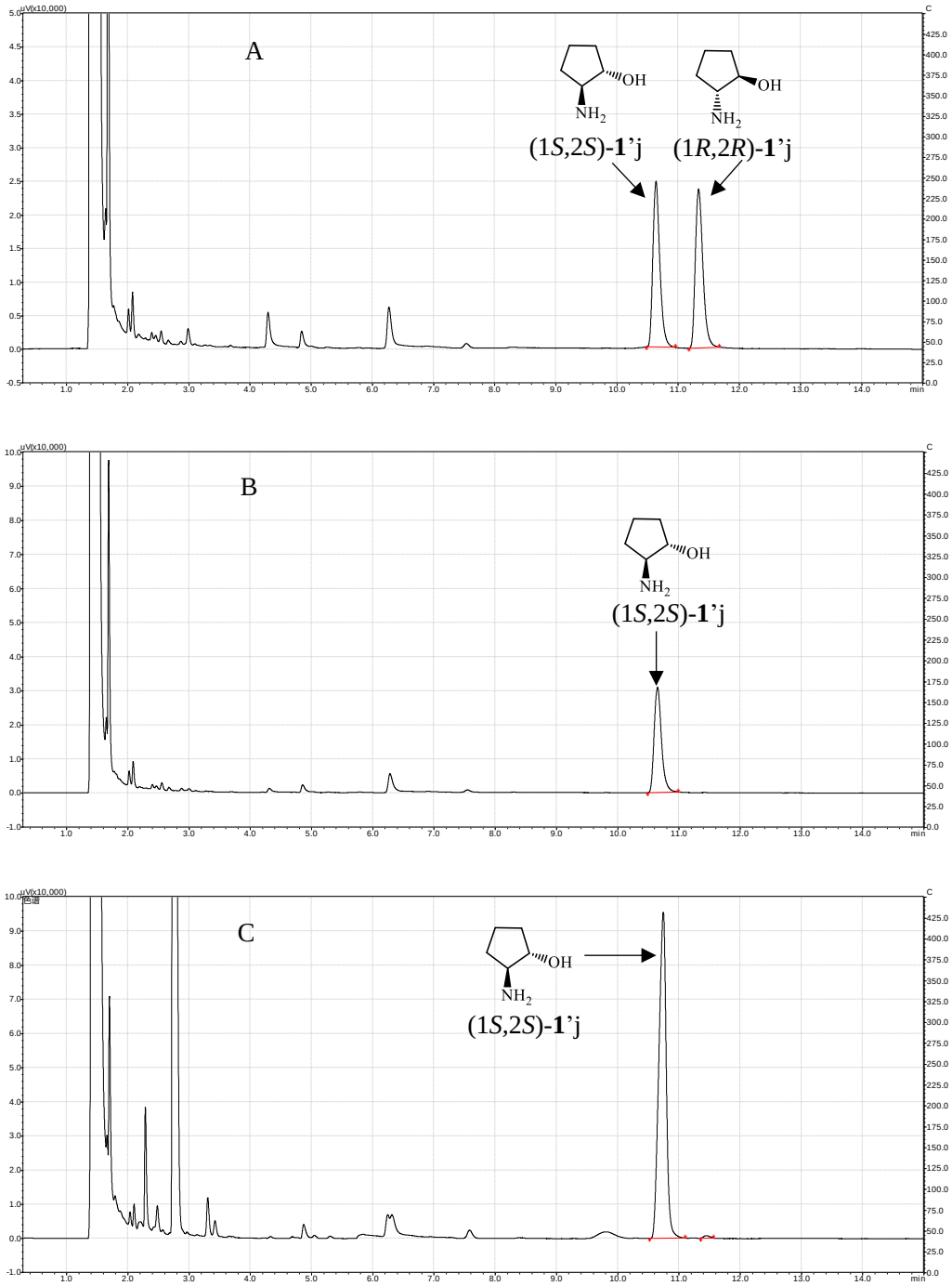

Fig. S16. Chiral GC analysis of 2-aminocyclopentanol **1**'j. **A**: *trans*-2-aminocyclopentanol (**1**'j) standard; **B**: (1*S*,2*S*)-2-aminocyclopentanol (**1**'j) standard; **C**: (1*S*,2*S*)-2-aminocyclopentanol (**1**'j) (>98% *ee*) produced from kinetic resolution of *trans*-2-aminocyclopentanol **1**'j (500 mM) with the resting cells of *E. coli* (CepTA).

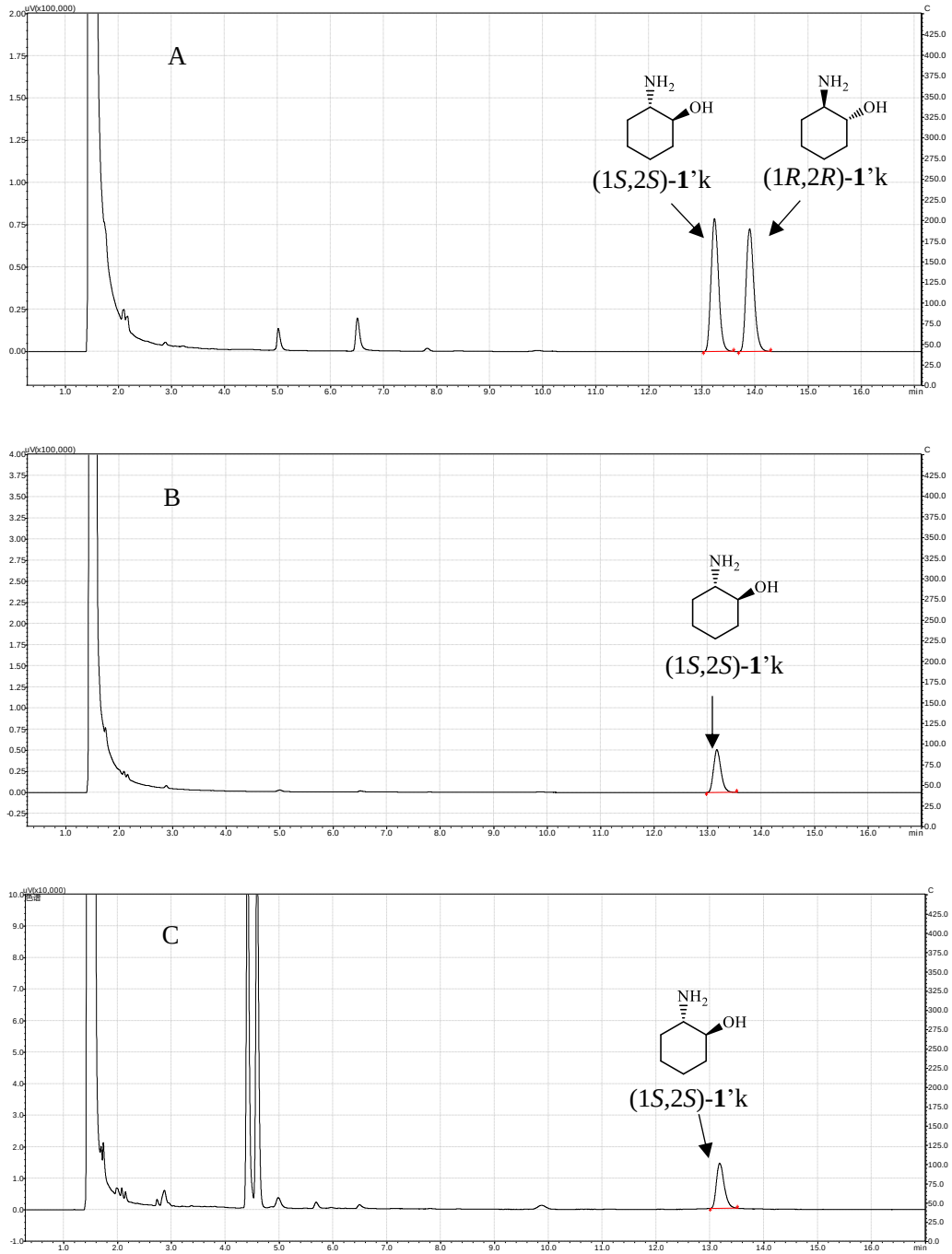

Fig. S17. Chiral GC analysis of 2-aminocyclohexanol **1**'k. **A**: *trans*-2-aminocyclohexanol (**1**'k) standard; **B**: (1*S*,2*S*)-2-aminocyclohexanol (**1**'k) standard; **C**: (1*S*,2*S*)- 2-aminocyclohexanol (**1**'k) (>99% *ee*) produced from kinetic resolution of *trans*-2-aminocyclohexanol **1**'k (10 mM) with the resting cells of *E. coli* (CepTA).

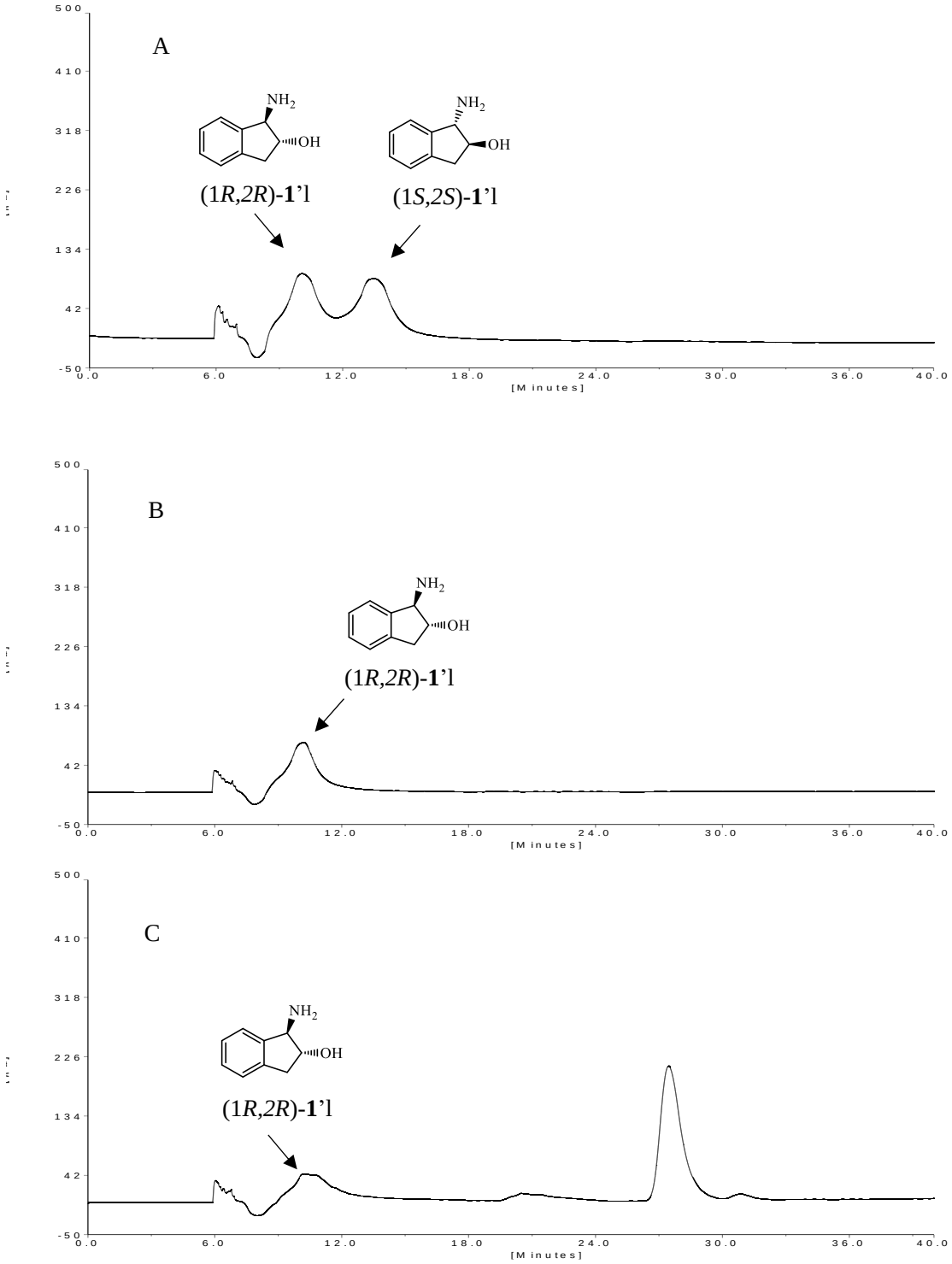

Fig. S18. Chiral HPLC analysis of *trans*-1-amino-2-indanol **1**'l. **A**: *trans*-1-amino-2-indanol (**1**'l) standard; **B**: (1*R*,2*R*)-1-amino-2-indanol (**1**'l) standard; **C**: (1*R*,2*R*)-1-amino-2-indanol (**1**'l) (>99% *ee*) produced from kinetic resolution of *trans*-1-amino-2-indanol **1**'l (20 mM) with the resting cells of *E. coli* (CepTA).

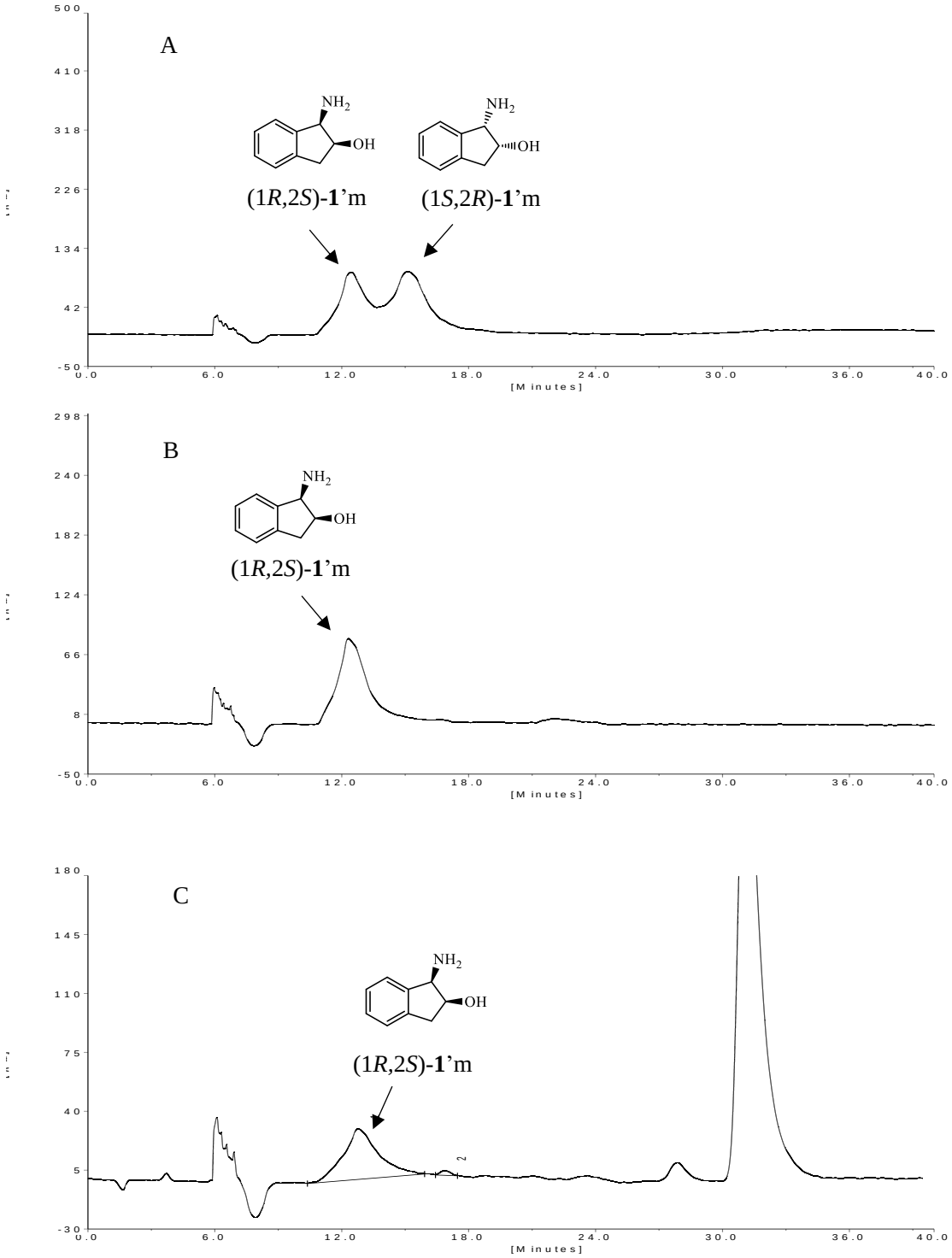

Fig. S19. Chiral HPLC analysis of *cis*-1-amino-2-indanol **1**'m. **A**: *cis*-1-amino-2-indanol (**1**'m) standard; **B**: (1*R*,2*S*)- 1-amino-2-indanol (**1**'m) standard; **C**: (1*R*,2*S*)- 1-amino-2-indanol (**1**'m) (96% *ee*) produced from kinetic resolution of *cis*-1-amino-2-indanol **1**'m (20 mM) with the resting cells of *E. coli* (CepTA).

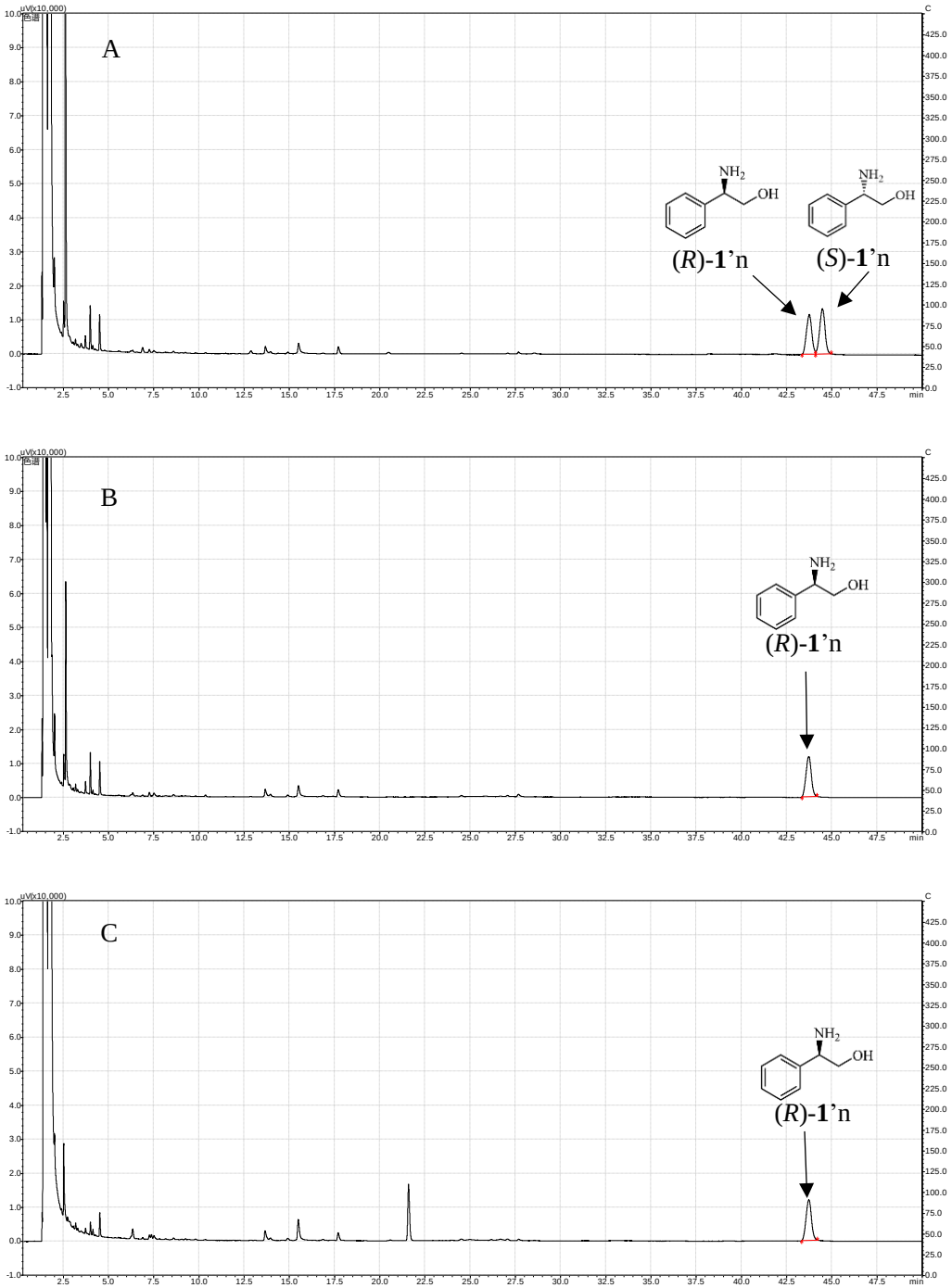

Fig. S20. Chiral GC analysis of phenylglycinol **1**'n. **A**: racemic phenylglycinol (**1**'n) standard; **B**: (*R*)-phenylglycinol (**1**'n) standard; **C**: (*R*)-phenylglycinol (**1**'n) (>99% *ee*) produced from kinetic resolution of racemic phenylglycinol **1**'n (10 mM) with the resting cells of *E. coli* (CepTA).

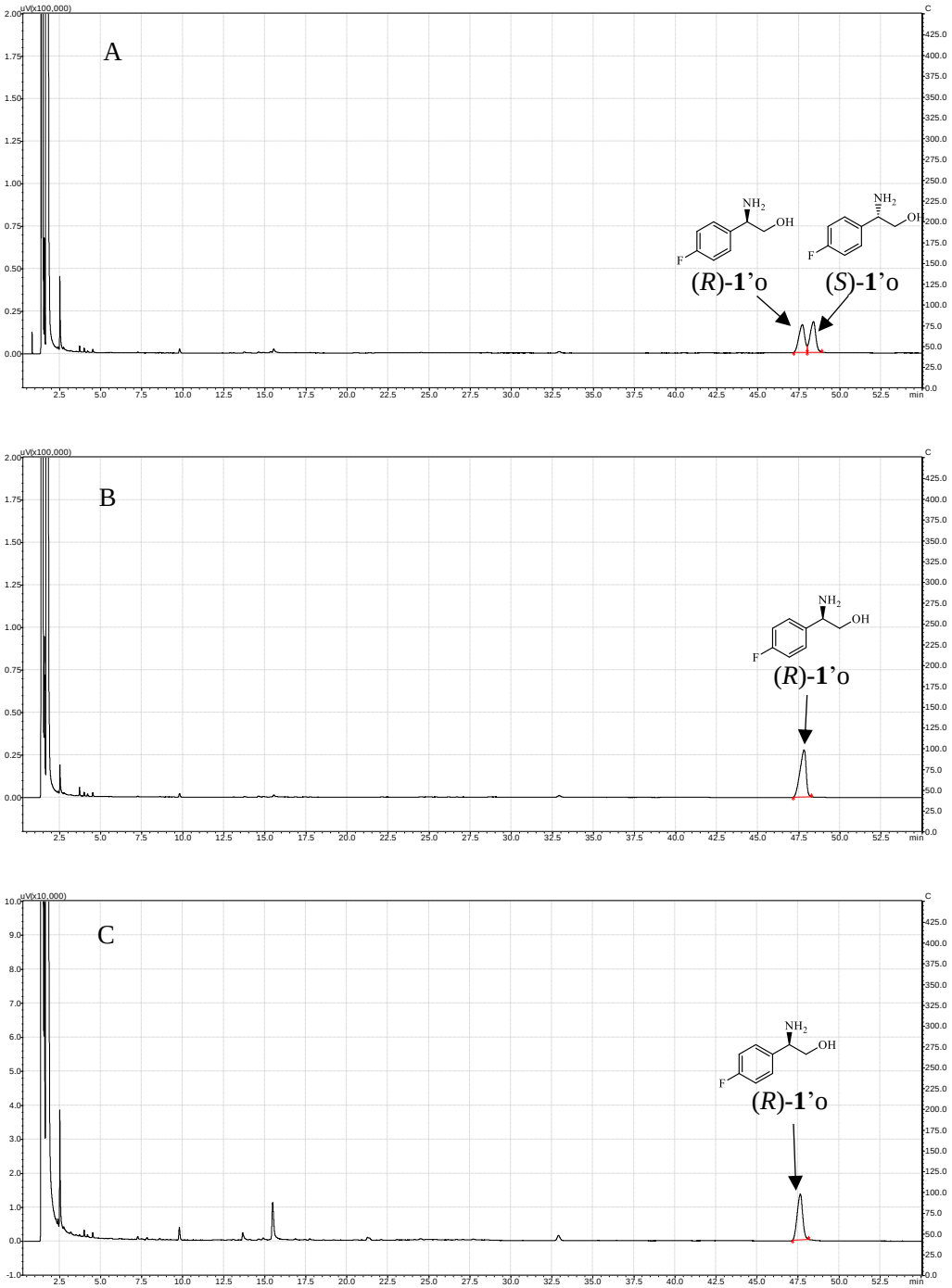

Fig. S21. Chiral GC analysis of 2-amino-2-(4-fluorophenyl)ethanol **1**'o. **A**: racemic 2-amino-2-(4-fluorophenyl)ethanol (**1**'o) standard; **B**: (*R*)-2-amino-2-(4-fluorophenyl)ethanol (**1**'o) standard; **C**: (*R*)-2-amino-2-(4-fluorophenyl)ethanol (**1**'o) (>99% *ee*) produced from kinetic resolution of racemic 2-amino-2-(4-fluorophenyl)ethanol **1**'o (10 mM) with the resting cells of *E. coli* (CepTA).

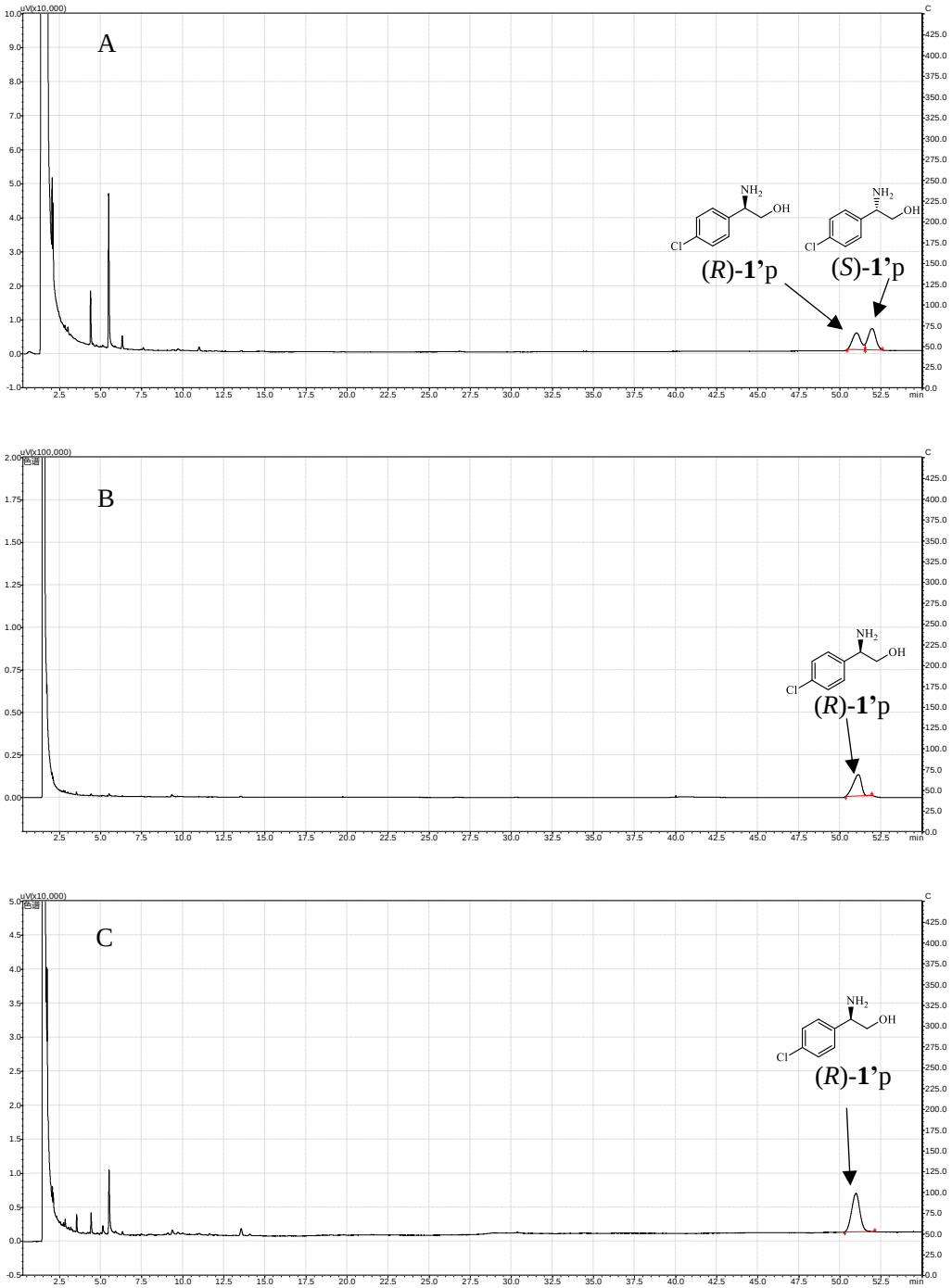

Fig. S22. Chiral GC analysis of 2-amino-2-(4-chlorophenyl)ethanol **1**'p. **A**: racemic 2-amino-2-(4-chlorophenyl)ethanol (**1**'p) standard; **B**: (*R*)-2-amino-2-(4-chlorophenyl)ethanol (**1**'p) standard; **C**: (*R*)-2-amino-2-(4-chlorophenyl)ethanol (**1**'p) (>99% ee) produced from kinetic resolution of racemic 2-amino-2-(4-chlorophenyl)ethanol **1**'p (10 mM) with the resting cells of *E. coli* (CepTA).

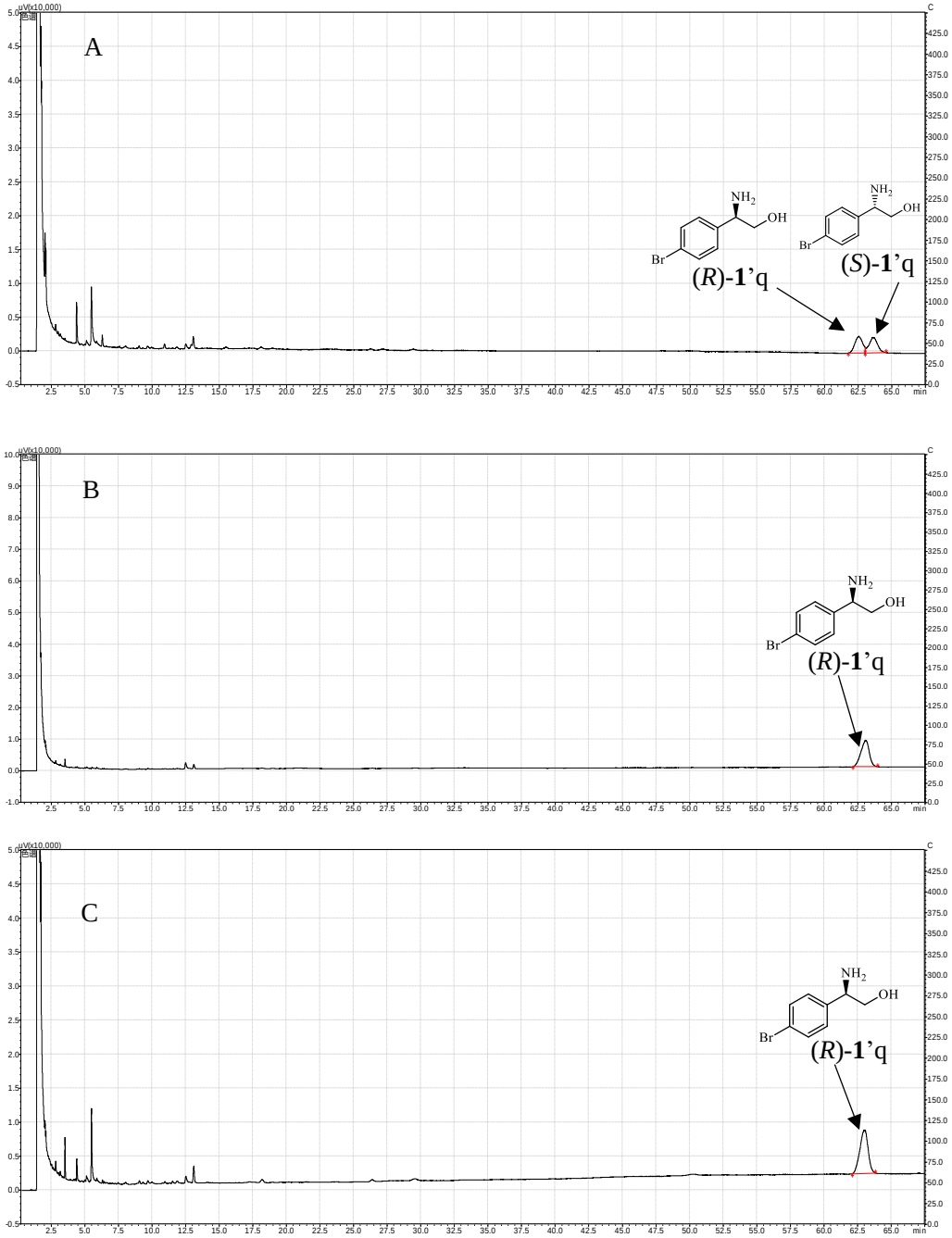

Fig. S23. Chiral GC analysis of 2-amino-2-(4-bromophenyl)ethanol **1**q. **A**: racemic 2-amino-2-(4-bromophenyl)ethanol (**1**q) standard; **B**: (*R*)- 2-amino-2-(4-bromophenyl)ethanol (**1**q) standard; **C**: (*R*)-2-amino-2-(4-bromophenyl)ethanol (**1**q) (>99% ee) produced from kinetic resolution of racemic 2-amino-2-(4-bromophenyl)ethanol **1**q (10 mM) with the resting cells of *E. coli* (CepTA).

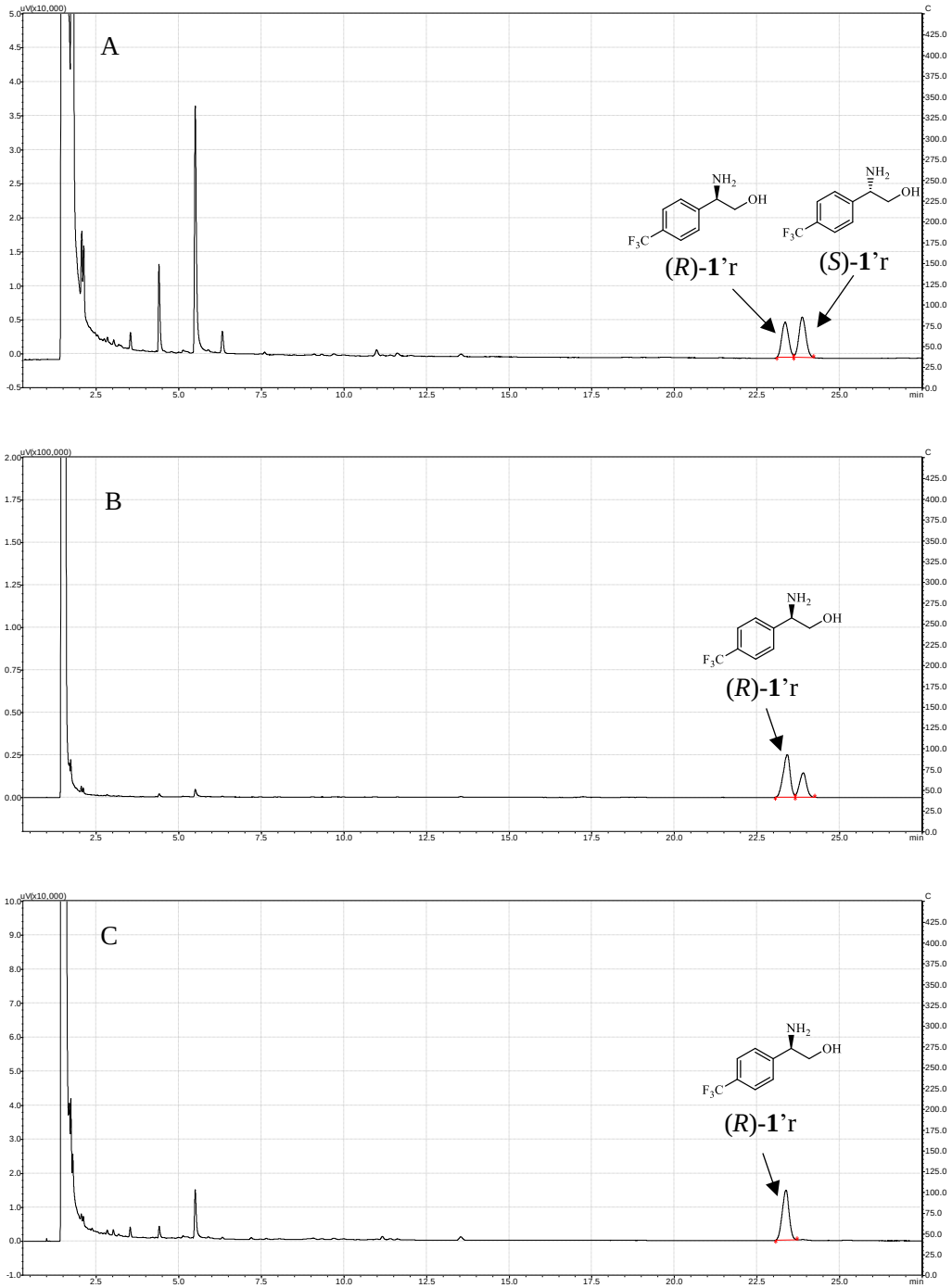

Fig. S24. Chiral GC analysis of 2-amino-2-[4-(trifluoromethyl)phenyl]ethanol **1**'r. **A**: racemic 2-amino-2-[4-(trifluoromethyl)phenyl]ethanol (**1**'r) standard; **B**: (*R*)-2-amino-2-[4-(trifluoromethyl)phenyl]ethanol (**1**'r) standard; **C**: (*R*)-2-amino-2-[4-(trifluoromethyl)phenyl]ethanol (**1**'r) (>99% ee) produced from kinetic resolution of racemic 2-amino-2-[4-(trifluoromethyl)phenyl]ethanol **1**'r (10 mM) with the resting cells of *E. coli* (CepTA).

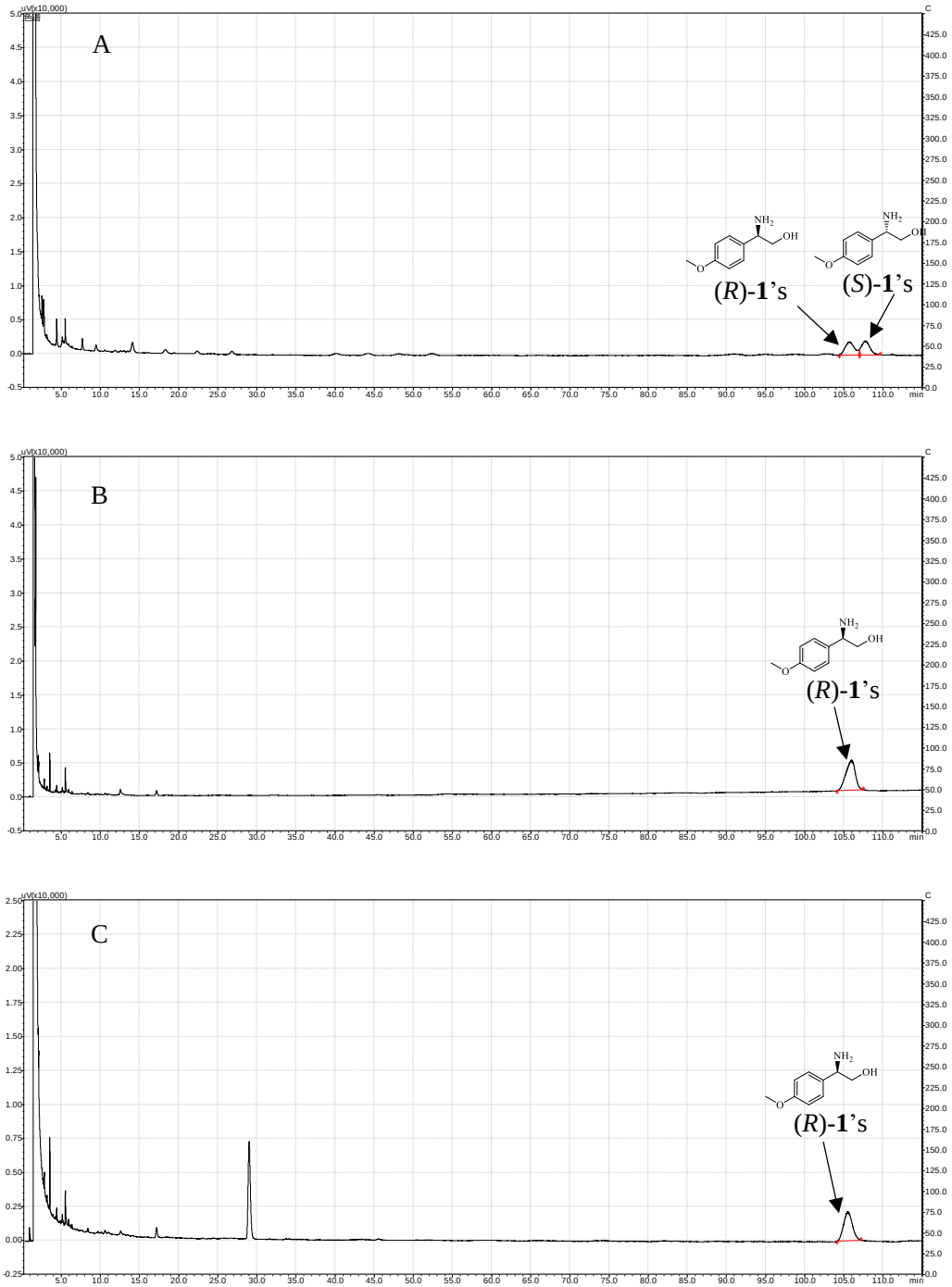

Fig. S25. Chiral GC analysis of 2-amino-2-(4-methoxyphenyl)ethanol **1**'s. **A**: racemic 2-amino-2-(4-methoxyphenyl)ethanol (**1**'s) standard; **B**: (*R*)- 2-amino-2-(4-methoxyphenyl)ethanol (**1**'s) standard; **C**: (*R*)- 2-amino-2-(4-methoxyphenyl)ethanol (**1**'s) (>99% ee) produced from kinetic resolution of racemic 2-amino-2-(4-methoxyphenyl)ethanol **1**'s (10 mM) with the resting cells of *E. coli* (CepTA).

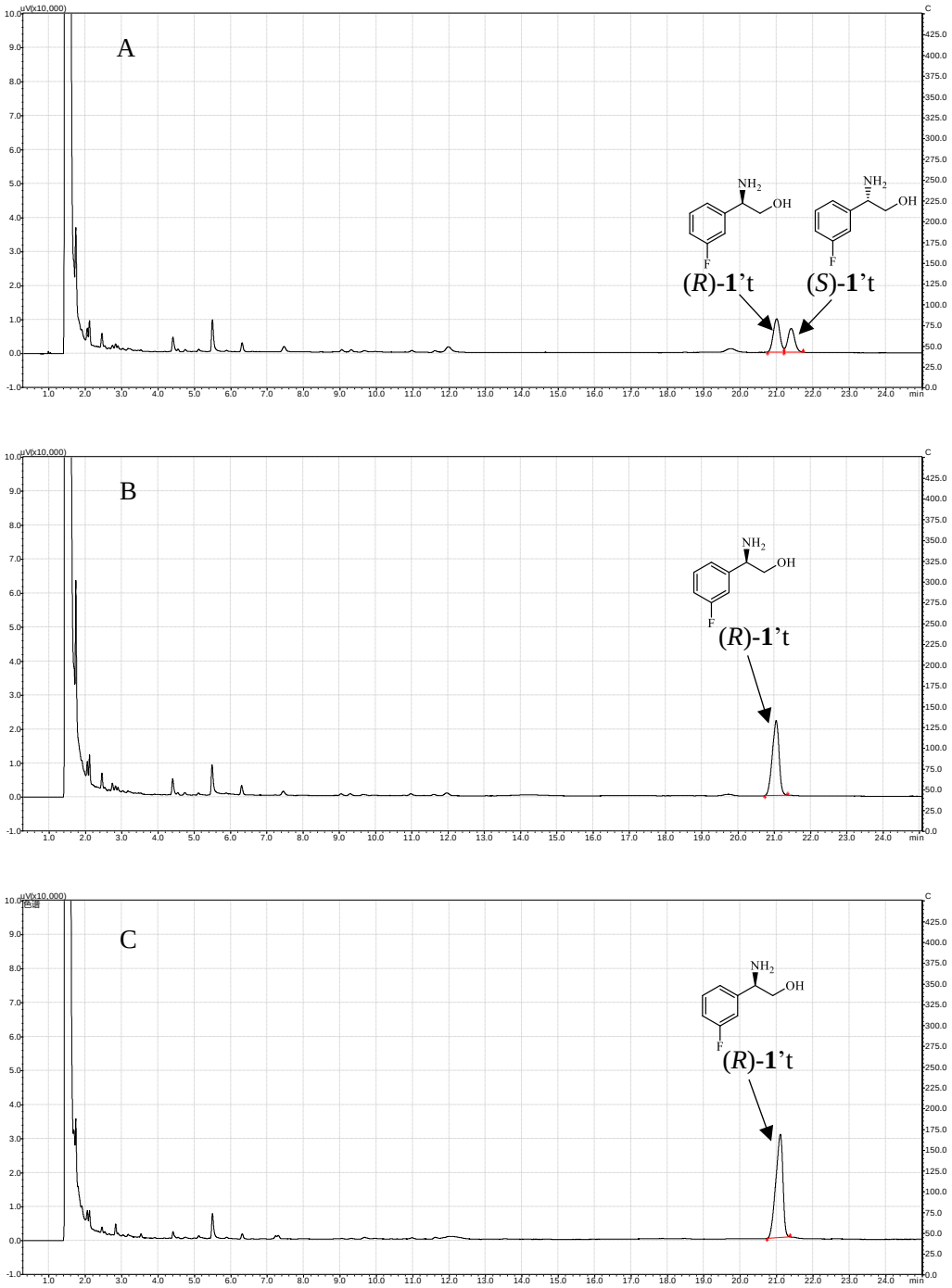

Fig. S26. Chiral GC analysis of 2-amino-2-(3-fluorophenyl)ethanol **1**'t. **A**: racemic 2-amino-2-(3-fluorophenyl)ethanol (**1**'t) standard; **B**: (*R*)- 2-amino-2-(3-fluorophenyl)ethanol (**1**'t) standard; **C**: (*R*)- 2-amino-2-(3-fluorophenyl)ethanol (**1**'t) (>99% ee) produced from kinetic resolution of racemic 2-amino-2-(3-fluorophenyl)ethanol **1**'t (10 mM) with the resting cells of *E. coli* (CepTA).

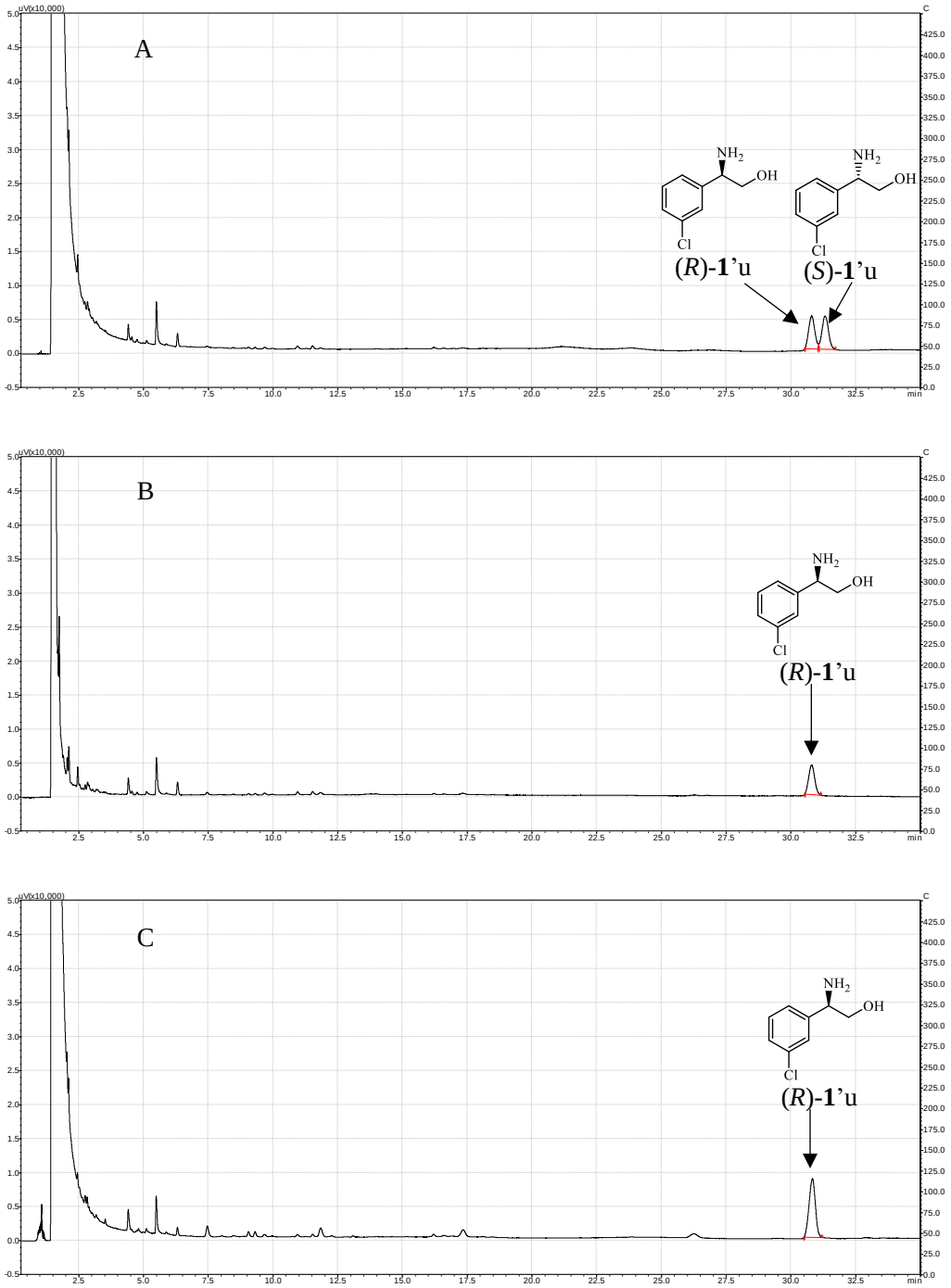

Fig. S27. Chiral GC analysis of 2-amino-2-(3-chlorophenyl)ethanol **1**'u. **A**: racemic 2-amino-2-(3-chlorophenyl)ethanol (**1**'u) standard; **B**: (*R*)-2-amino-2-(3-chlorophenyl)ethanol (**1**'u) standard; **C**: (*R*)-2-amino-2-(3-chlorophenyl)ethanol (**1**'u) (>99% ee) produced from kinetic resolution of racemic 2-amino-2-(3-chlorophenyl)ethanol **1**'u (10 mM) with the resting cells of *E. coli* (CepTA).

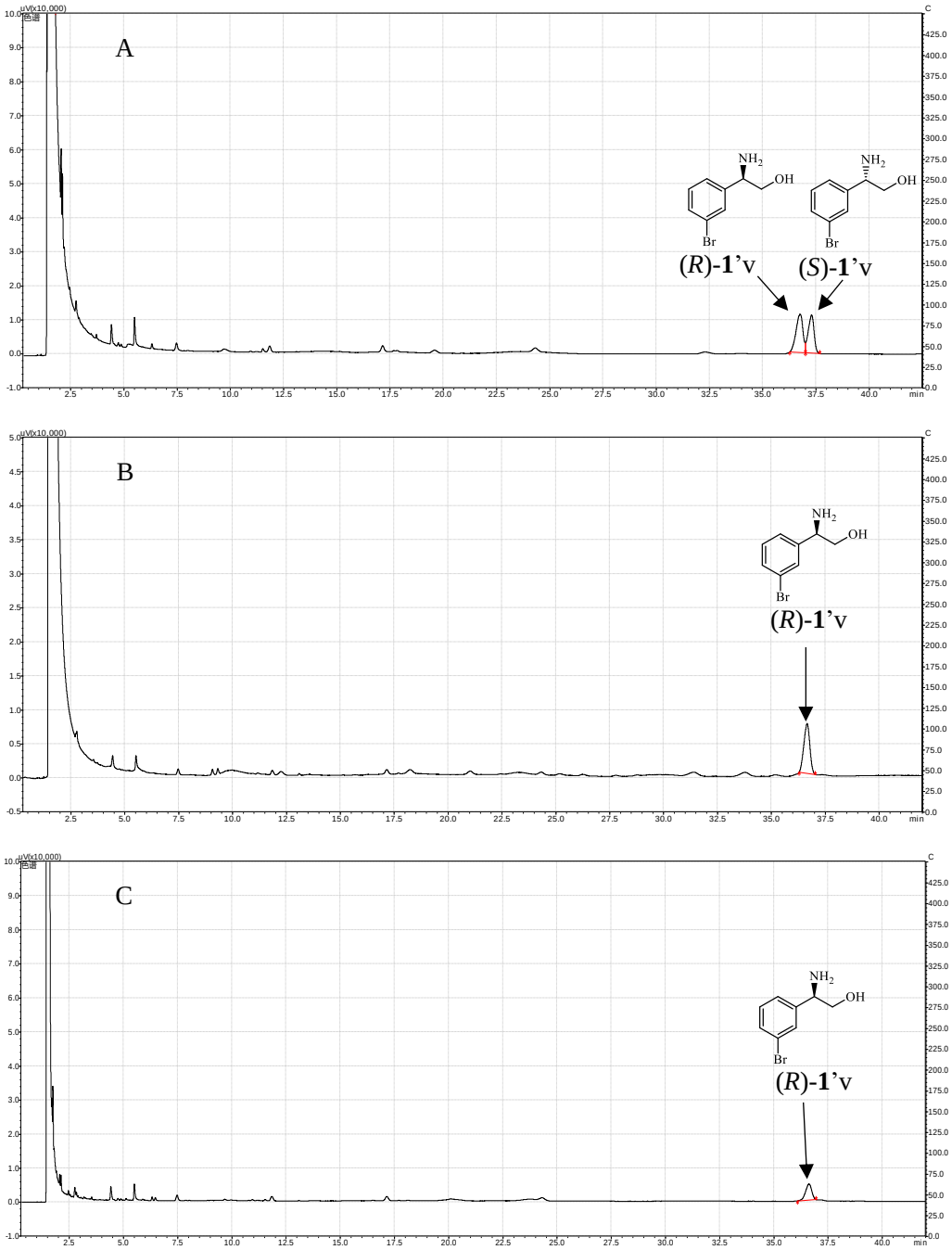

Fig. S28. Chiral GC analysis of 2-amino-2-(3-bromophenyl)ethanol **1**'v. **A**: racemic 2-amino-2-(3-bromophenyl)ethanol (**1**'v) standard; **B**: (*R*)-2-amino-2-(3-bromophenyl)ethanol (**1**'v) standard; **C**: (*R*)-2-amino-2-(3-bromophenyl)ethanol (**1**'v) (>99% *ee*) produced from kinetic resolution of racemic 2-amino-2-(3-bromophenyl)ethanol **1**'v (10 mM) with the resting cells of *E. coli* (CepTA).

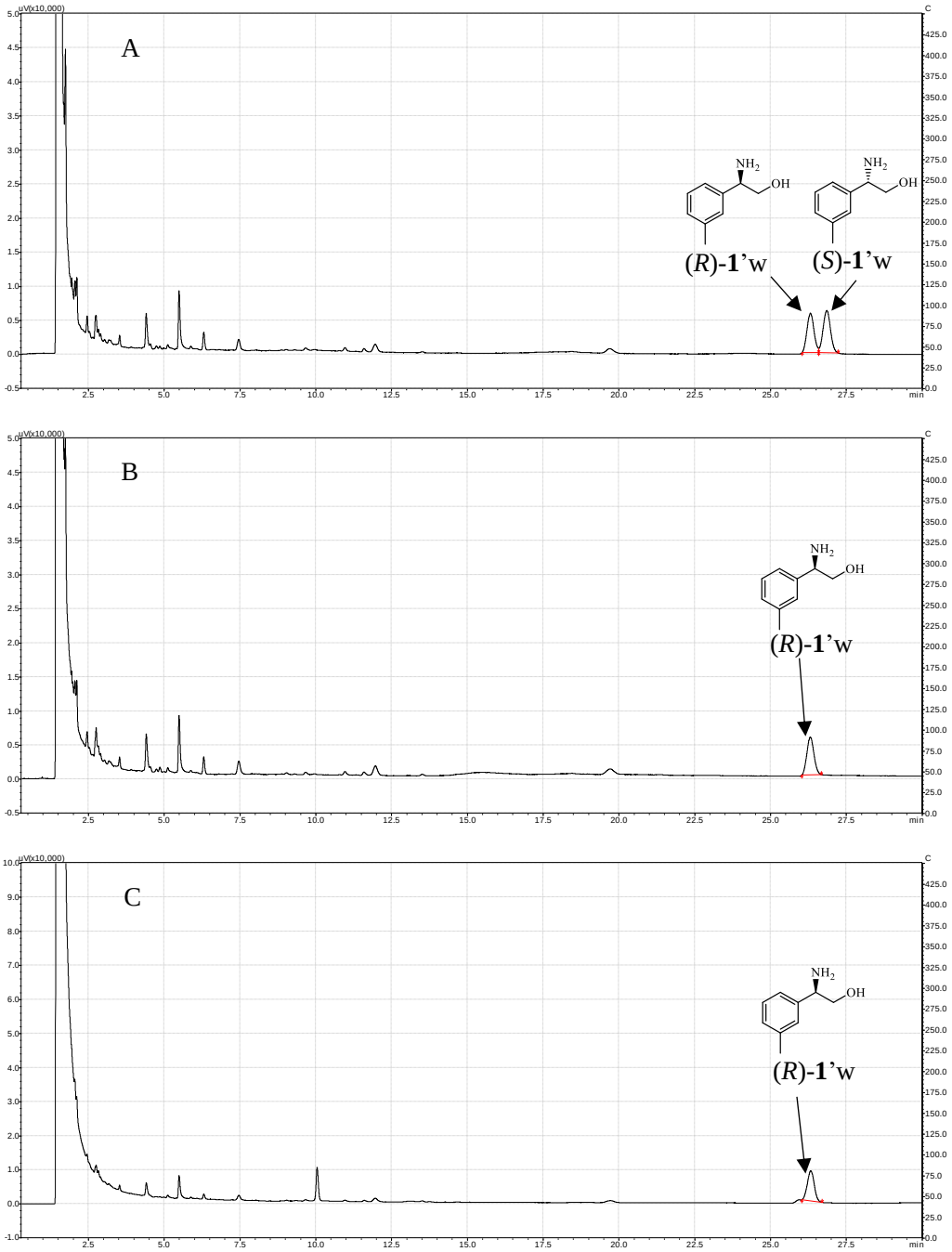

Fig. S29. Chiral GC analysis of 2-amino-2-(3-methylphenyl)ethanol **1**'w. **A**: racemic 2-amino-2-(3-methylphenyl)ethanol (**1**'w) standard; **B**: (*R*)- 2-amino-2-(3-methylphenyl)ethanol (**1**'w) standard; **C**: (*R*)- 2-amino-2-(3-methylphenyl)ethanol (**1**'w) (>99% *ee*) produced from kinetic resolution of racemic 2-amino-2-(3-methylphenyl)ethanol **1**'w (10 mM) with the resting cells of *E. coli* (CepTA).

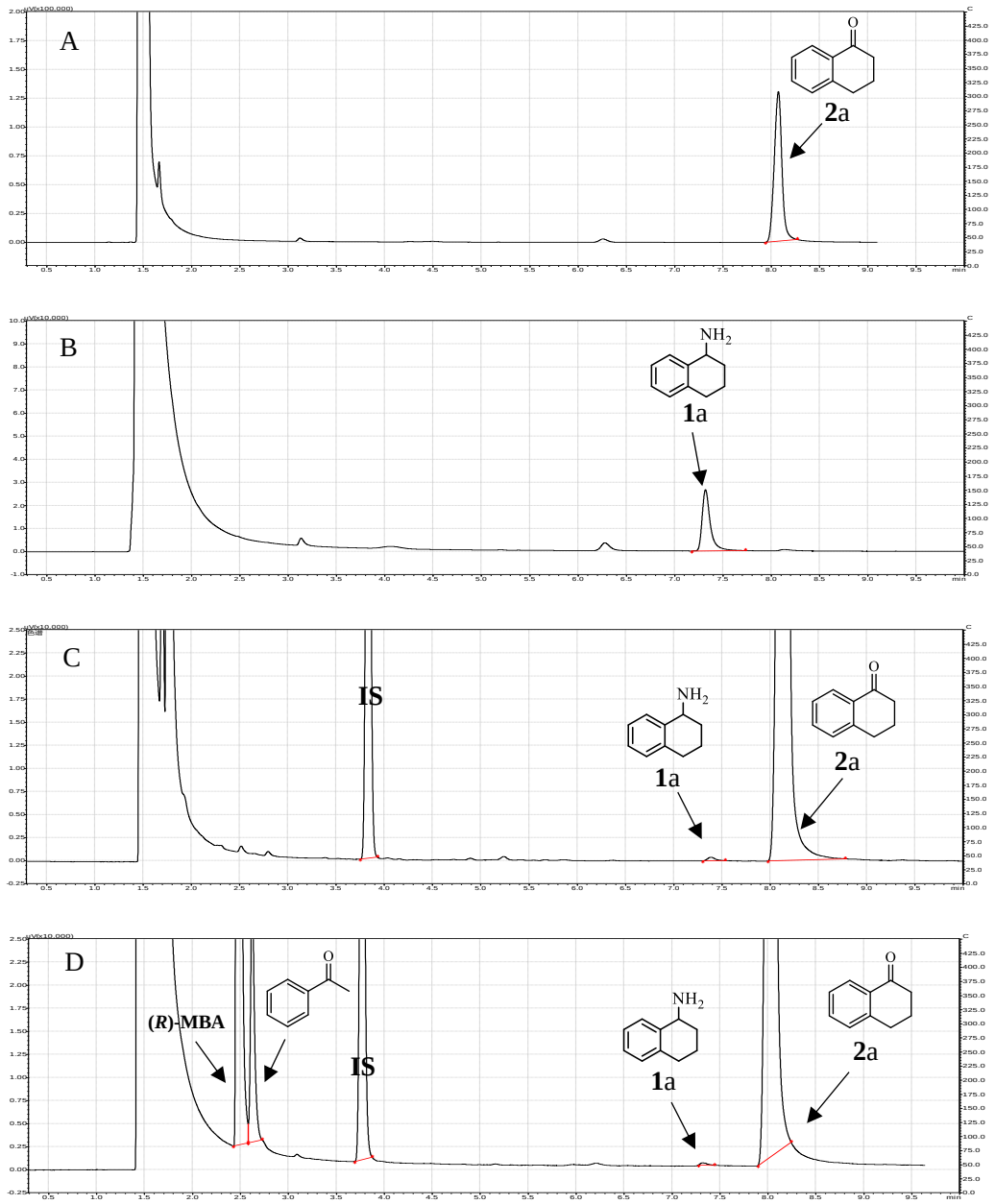

Fig. S30. Achiral GC analysis of 1,2,3,4-tetrahydro-1-naphthylamine **1**a. **A**: 1-tetralone (**2**a) standard; **B**: 1,2,3,4-tetrahydro-1-naphthylamine (**1**a) standard; **C**: 1,2,3,4-tetrahydro-1-naphthylamine (**1**a) produced from 1-tetralone (**2**a) (10 mM) with 200 mM D-Ala and 20 g CDW L^{-1} *E. coli*(CepTA) at 12 h. **D**: 1,2,3,4-tetrahydro-1-naphthylamine (**1**a) produced from 1-tetralone (**2**a) (10 mM) with 10 mM (*R*)-MBA and 20 g CDW L^{-1} *E. coli* (CepTA) at 12 h. IS: internal standard (dodecane).

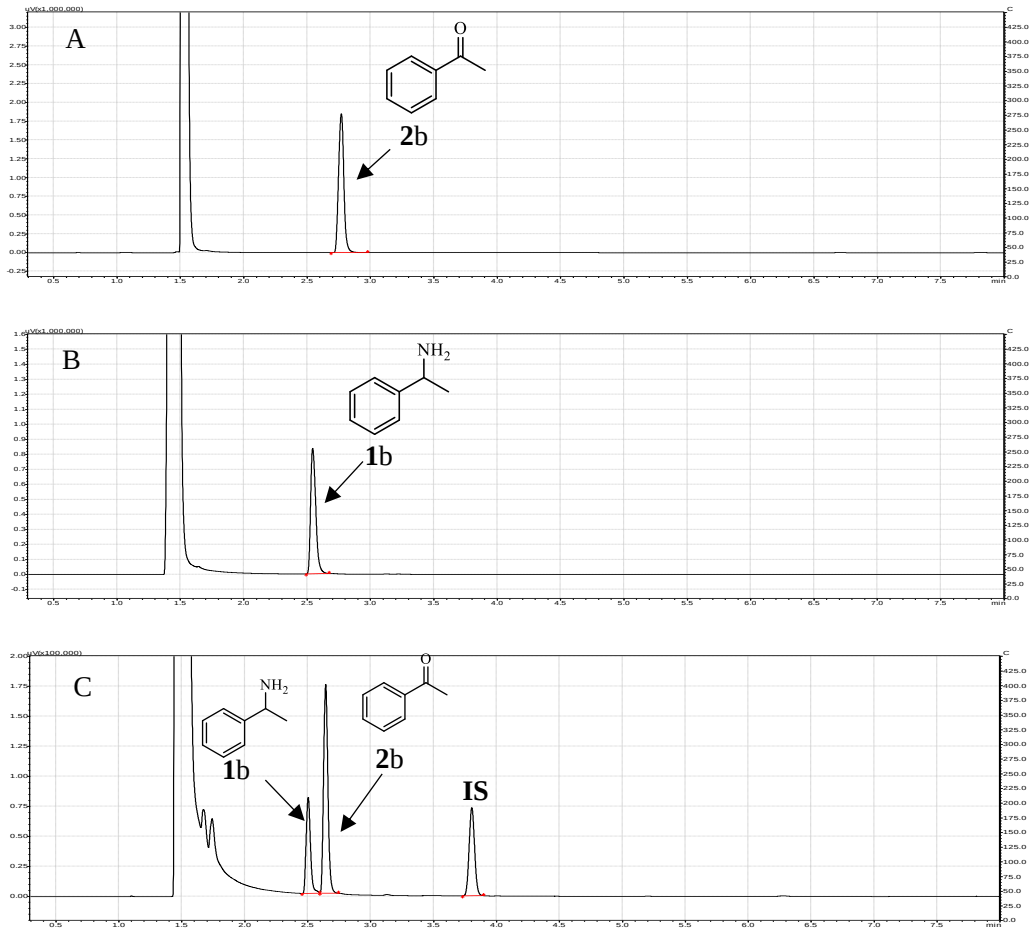

Fig. S31. Achiral GC analysis of 1-phenylethylamine **1**b. **A**: acetophenone (**2**b) standard; **B**: α-1-phenylethylamine (**1**b) standard; **C**: 1-phenylethylamine (**1**b) produced from acetophenone (**2**b) (10 mM) with 200 mM D-Ala and 20 g CDW L^{-1} *E. coli* (CepTA) at 12 h. IS: internal standard (dodecane).

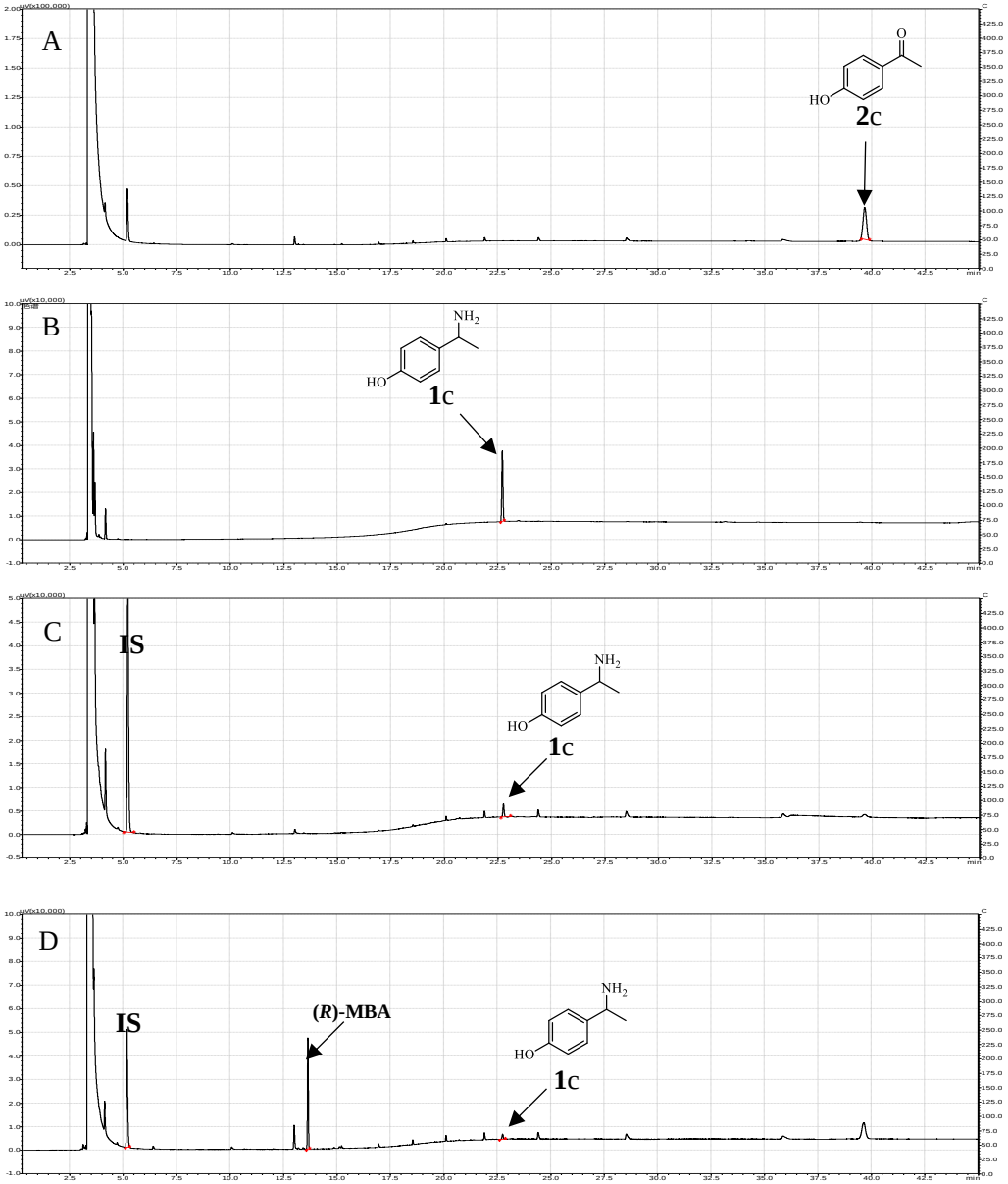

Fig. S32. Achiral GC analysis of 4-(1-aminoethyl)phenol **1**c. **A**: 4-hydroxyacetophenone (**2**c) standard ; **B**: 4-(1-aminoethyl)phenol (**1**c) standard; **C**: 4-(1-aminoethyl)phenol (**1**c) produced from 4-hydroxyacetophenone (**2**c) (10 mM) with 200 mM D-Ala and 20 g CDW L^{-1} *E. coli*(CepTA) at 12 h. **D**: 4-(1-aminoethyl)phenol (**1**c) produced from 4-hydroxyacetophenone (**2**c) (10 mM) with 10 mM (*R*)-MBA and 20 g CDW L^{-1} *E. coli* (CepTA) at 12 h. IS: internal standard (dodecane).

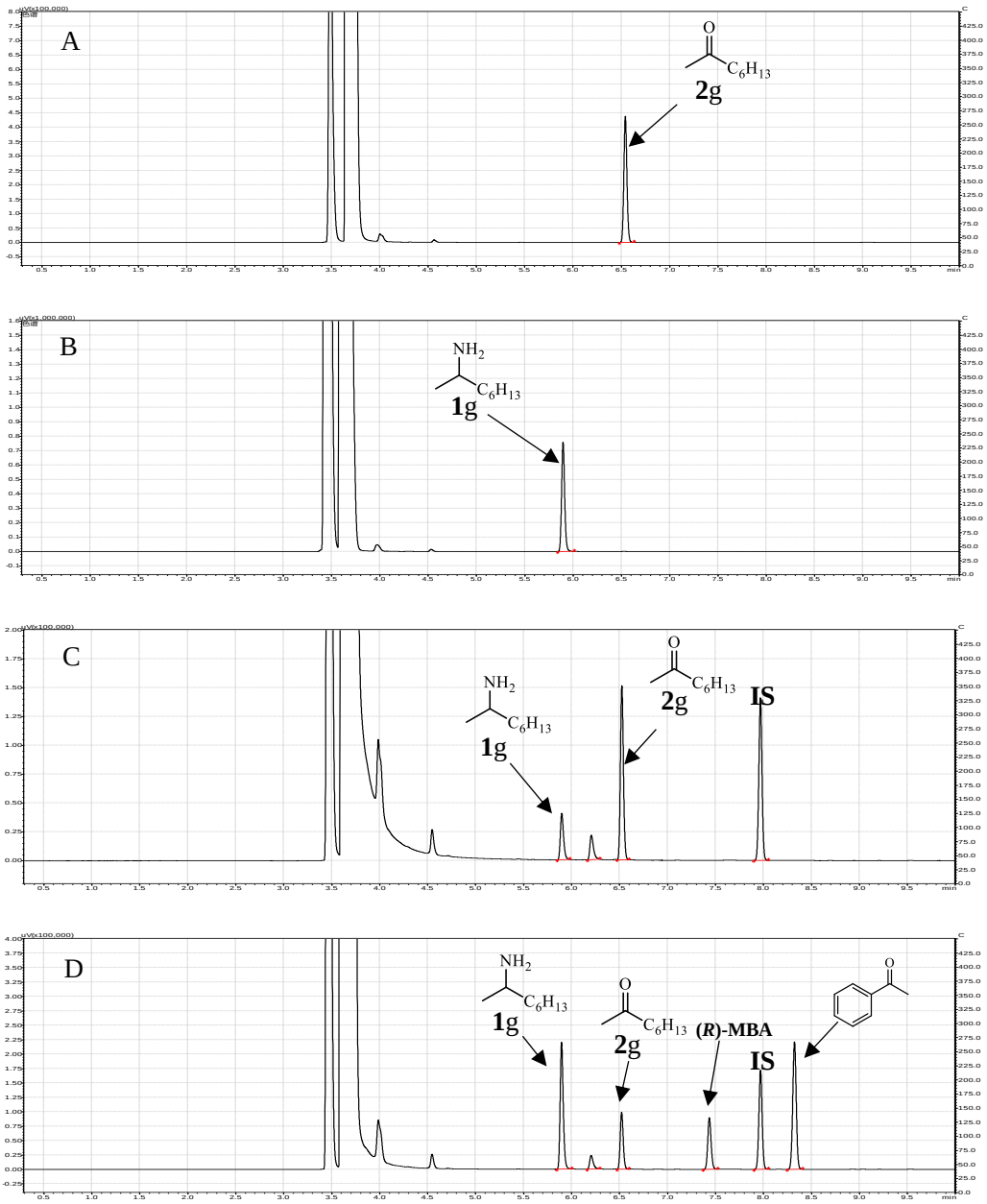

Fig. S33. Achiral GC analysis of 2-octanamine **1**g. **A**: 2-octanone (**2**g) standard; **B**: 2-octanamine (**1**g) standard; **C**: 2-octanamine (**1**g) produced from 2-octanone (**2**g) (10 mM) with 200 mM D-Ala and 20 g CDW L^{-1} *E. coli* (CepTA) at 12 h. **D**: 2-octanamine (**1**g) produced from 2-octanone (**2**g) (10 mM) with 10 mM (*R*)-MBA and 20 g CDW L^{-1} *E. coli* (CepTA) at 5 h. IS: internal standard (dodecane).

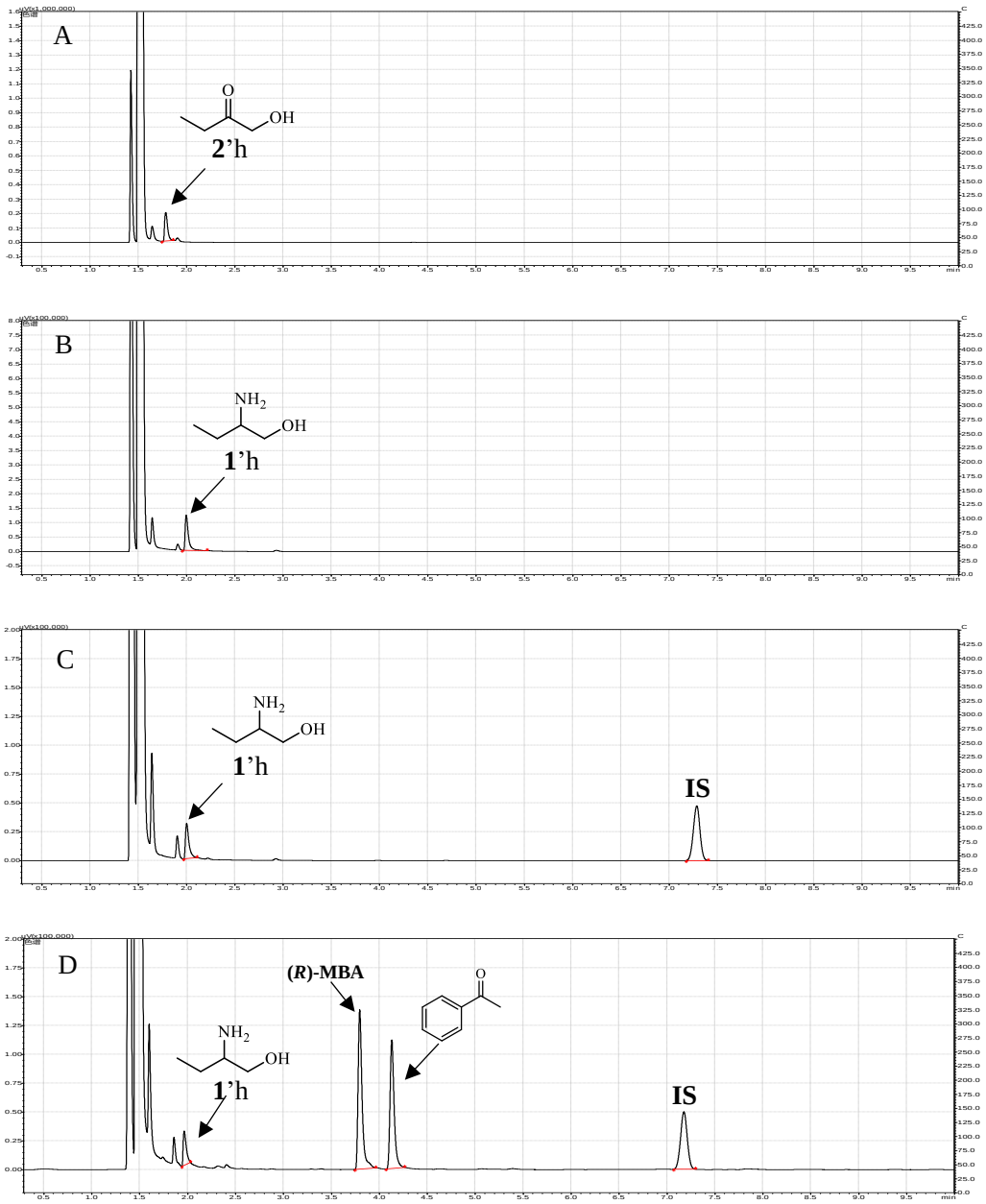

Fig. S34. Achiral GC analysis of 2-amino-1-butanol **1**'h. **A**: 1-hydroxy-2-butanone (**2**'h) standard ; **B**: 2-amino-1-butanol (**1**'h) standard; **C**: 2-amino-1-butanol (**1**'h) produced from 1-hydroxy-2-butanone (**2**'h) (50 mM) with 200 mM D-Ala and 20 g CDW L^{-1} *E. coli* (CepTA) at 24h. **D**: 2-amino-1-butanol (**1**'h) produced from 1-hydroxy-2-butanone (**2**'h) (50 mM) with 10 mM (*R*)-MBA and 20 g CDW L^{-1} *E. coli* (CepTA) at 6 h. IS: internal standard (dodecane).

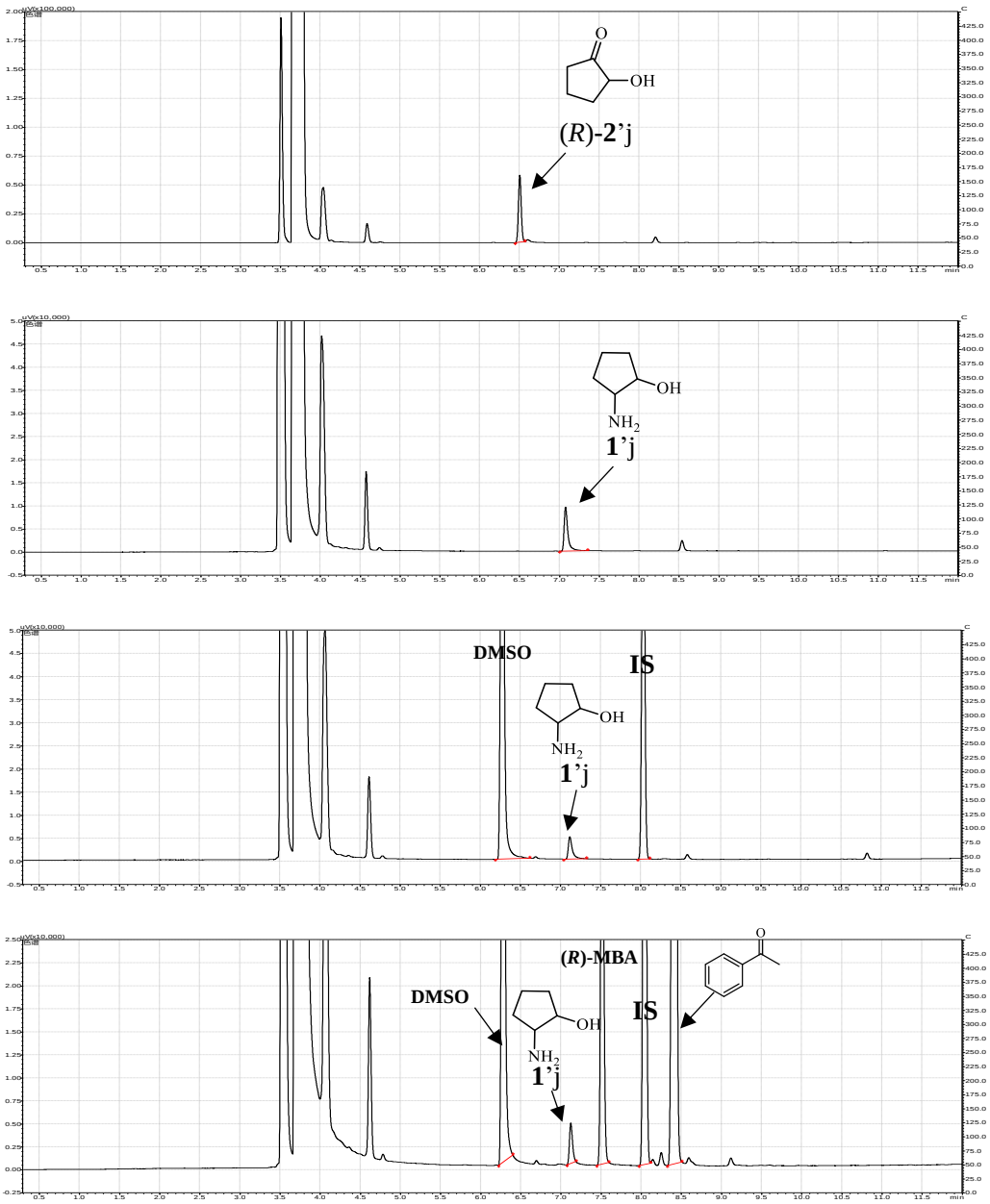

Fig. S35. Achiral GC analysis of 2-aminocyclopentanol **1**'j. **A**: (*R*)-α-hydroxycyclopentan-1-one (**2**'j) standard ; **B**: 2-aminocyclopentanol (**1**'j) standard; **C**: 2-aminocyclopentanol (**1**'j) produced from (*R*)-α-hydroxycyclopentan-1-one (**2**'j) (10 mM) with 200 mM D-Ala and 20 g CDW L^{-1} *E. coli* (CepTA) at 24h. **D**: 2-aminocyclopentanol (**1**'j) produced from (*R*)-α-hydroxycyclopentan-1-one (**2**'j) (10 mM) with 10 mM (*R*)-MBA and 20 g CDW L^{-1} *E. coli* (CepTA) at 6 h. IS: internal standard (dodecane).

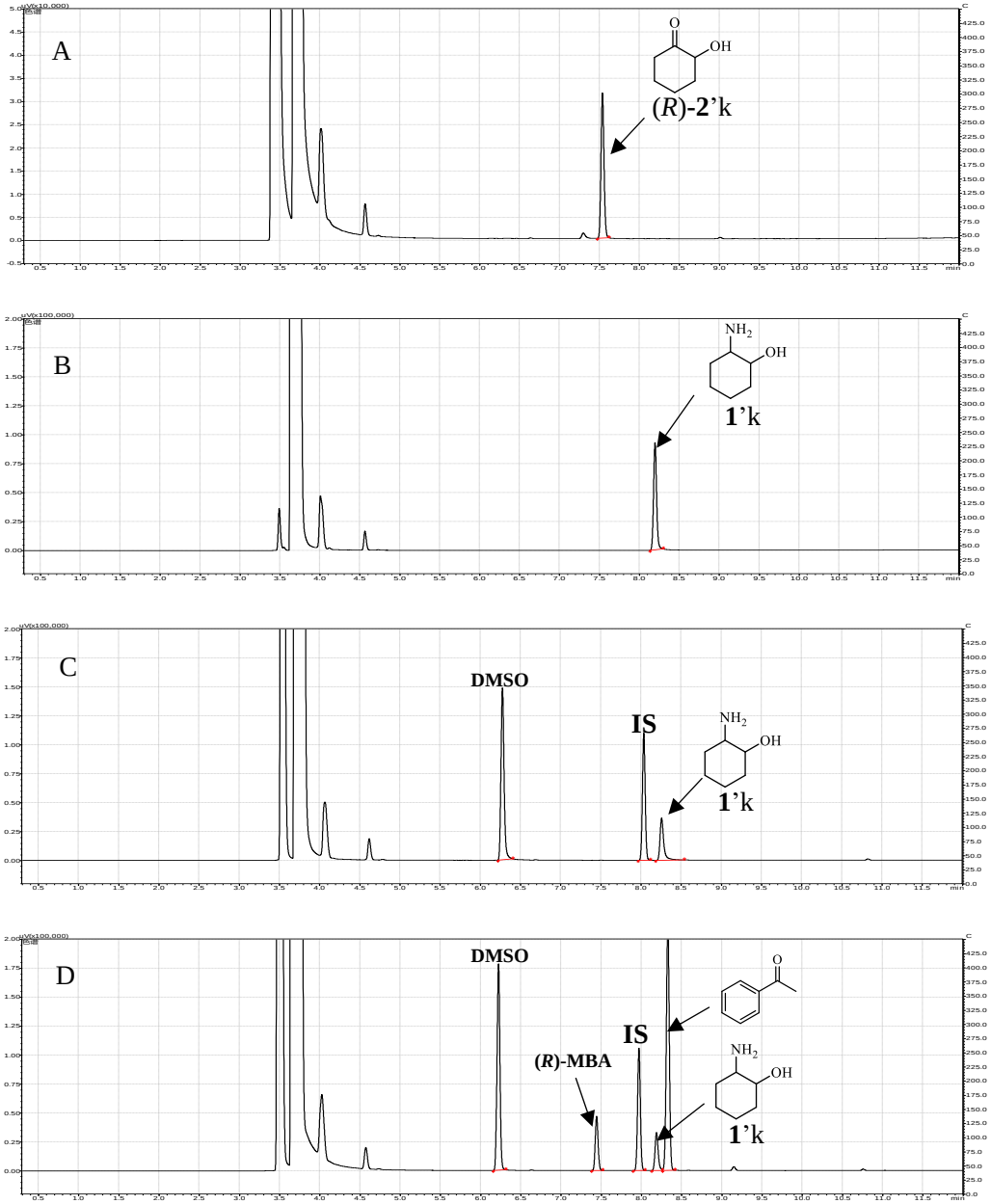

Fig. S36. Achiral GC analysis of 2-aminocyclohexanol **1**'k. **A**: (*R*)-α-hydroxycyclohexan-1-one (**2**'k) standard; **B**: 2-aminocyclohexanol (**1**'k) standard; **C**: 2-aminocyclohexanol (**1**'k) produced from (*R*)-α-hydroxycyclohexan-1-one (**2**'k) (10 mM) with 200 mM D-Ala and 20 g CDW L^{-1} *E. coli*(CepTA) at 12 h; **D**: 2-aminocyclohexanol (**1**'k) produced from (*R*)-α-hydroxycyclohexan-1-one (**2**'k) (10 mM) with 10 mM (*R*)-MBA and 20 g CDW L^{-1} *E. coli*(CepTA) at 12 h. IS: internal standard (dodecane).

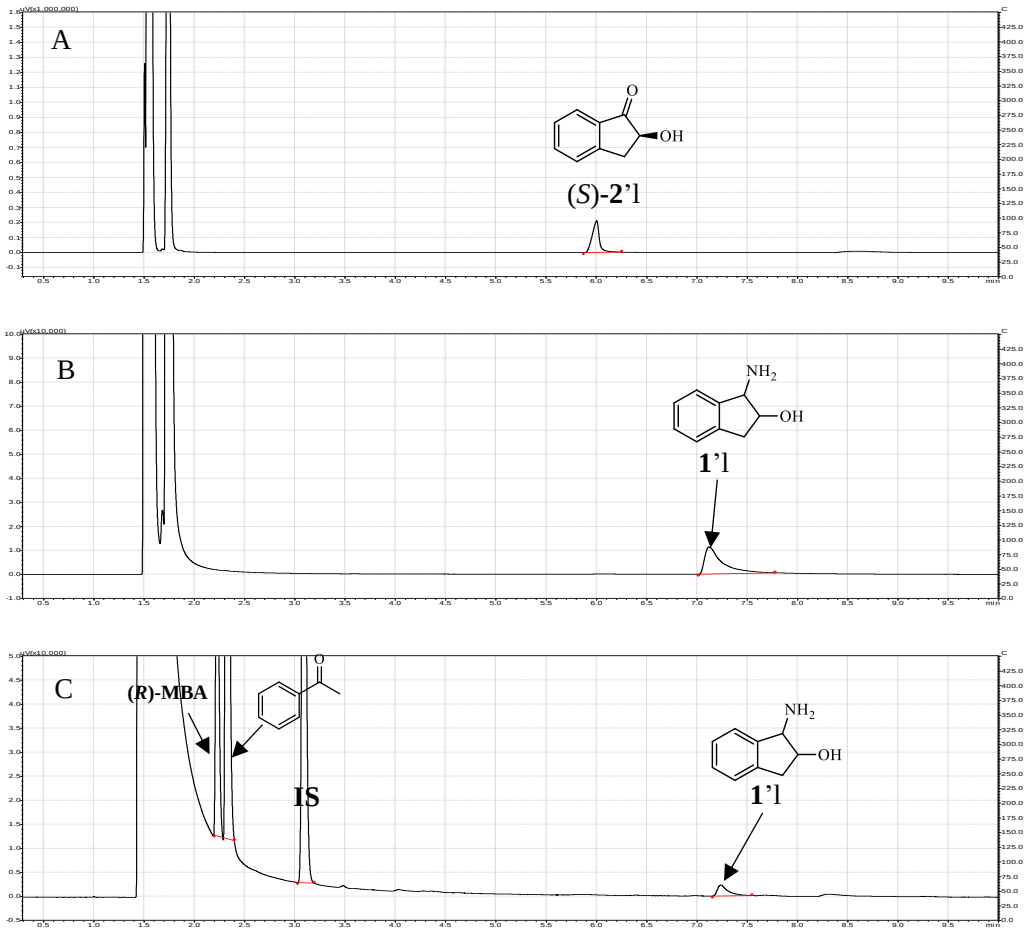

Fig. S37. GC analysis of 1-amino-2-indanol **1**'l. **A**: (*S*)-2-hydroxy-1-indanone (**2**'l) standard; **B**: 1-amino-2-indanol (**1**'l) standard; **C**: 1-amino-2-indanol (**1**'l) produced from 2-hydroxy-1-indanone (**2**'l) (10 mM) with 10 mM (*R*)-MBA and 20 g CDW L^{-1} *E. coli* (CepTA) at 12 h. IS: internal standard (dodecane).

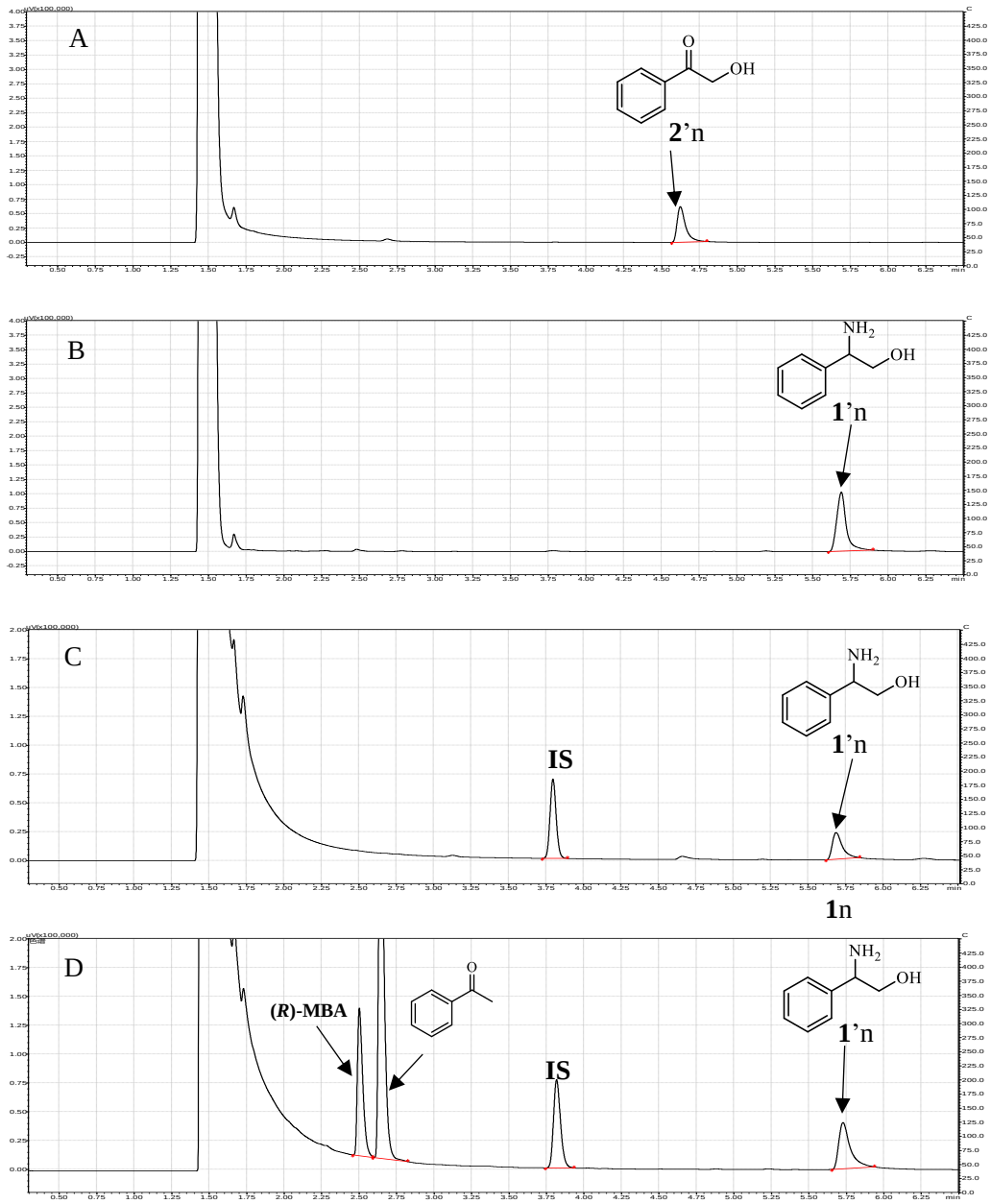

Fig. S38. Achiral GC analysis of phenylglycinol **1**'n. **A**: 2-hydroxyacetophenone (**2**'n) standard; **B**: phenylglycinol (**1**'n) standard; **C**: phenylglycinol (**1**'n) produced from 2-hydroxyacetophenone (**2**'n) (10 mM) with 200 mM D-Ala and 20 g CDW L^{-1} *E. coli* (CepTA) at 12 h. **D**: phenylglycinol (**1**'n) produced from 2-hydroxyacetophenone (**2**'n) (10 mM) with 10 mM (*R*)-MBA and 20 g CDW L^{-1} *E. coli* (CepTA) at 3 h. IS: internal standard (dodecane).

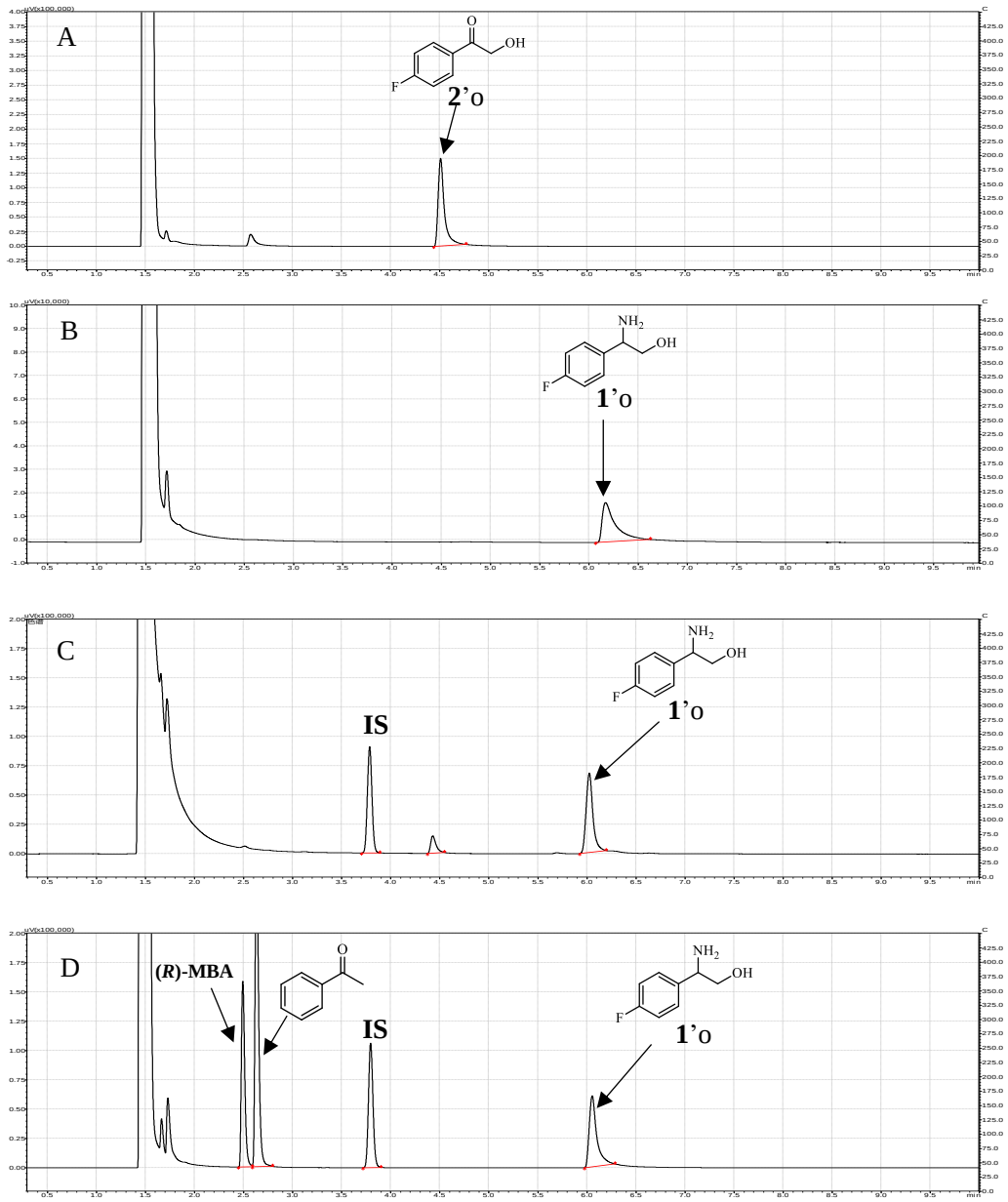

Fig. S39. Achiral GC analysis of 2-amino-2-(4-fluorophenyl)ethanol **1**'o. **A**: 1-(4-fluorophenyl)-2-hydroxyethanone (**2**'o) standard ; **B**: 2-amino-2-(4-fluorophenyl)ethanol (**1**'o) standard; **C**: 2-amino-2-(4-fluorophenyl)ethanol (**1**'o) produced from 1-(4-fluorophenyl)-2-hydroxyethanone (**2**'o) (10 mM) with 200 mM D-Ala and 20 g CDW L^{-1} *E. coli* (CepTA) at 12 h. **D**: 2-amino-2-(4-fluorophenyl)ethanol (**1**'o) produced from 1-(4-fluorophenyl)-2-hydroxyethanone (**2**'o) (10 mM) with 10 mM (*R*)-MBA and 20 g CDW L^{-1} *E. coli* (CepTA) at 1 h. IS: internal standard (dodecane).

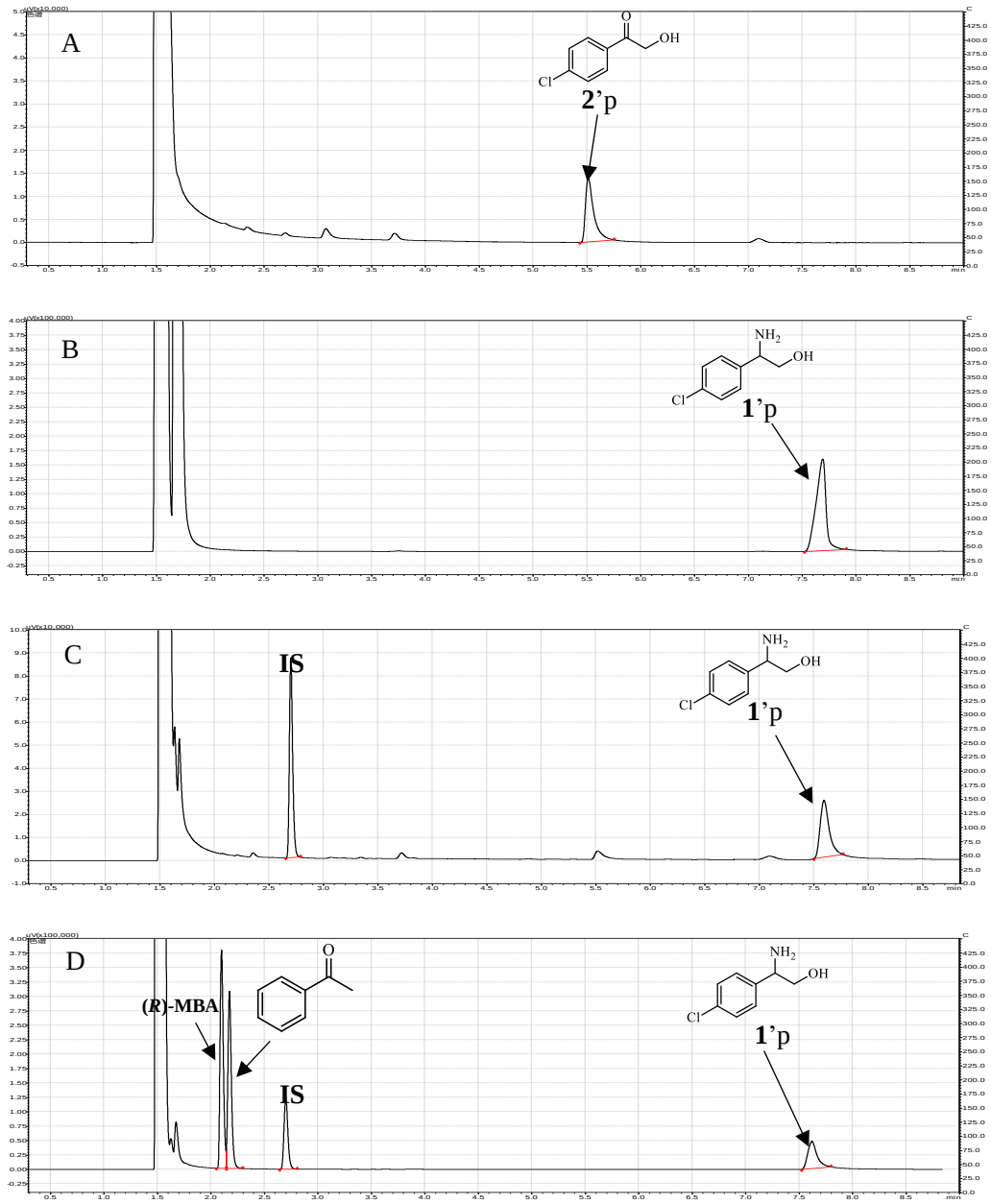

Fig. S40. Achiral GC analysis of 2-amino-2-(4-chlorophenyl)ethanol **1**'p. **A**: 1-(4-chlorophenyl)-2-hydroxyethanone (**2**'p) standard ; **B**: 2-amino-2-(4-chlorophenyl)ethanol (**1**'p) standard; **C**: 2-amino-2-(4-chlorophenyl)ethanol (**1**'o) produced from 1-(4-chlorophenyl)-2-hydroxyethanone (**2**'p) (10 mM) with 200 mM D-Ala and 20 g CDW L^{-1} *E. coli* (CepTA) at 12 h. **D**: 2-amino-2-(4-chlorophenyl)ethanol (**1**'p) produced from 1-(4-chlorophenyl)-2-hydroxyethanone (**2**'p) (10 mM) with 10 mM (*R*)-MBA and 20 g CDW L^{-1} *E. coli* (CepTA) at 1 h. IS: internal standard (dodecane).

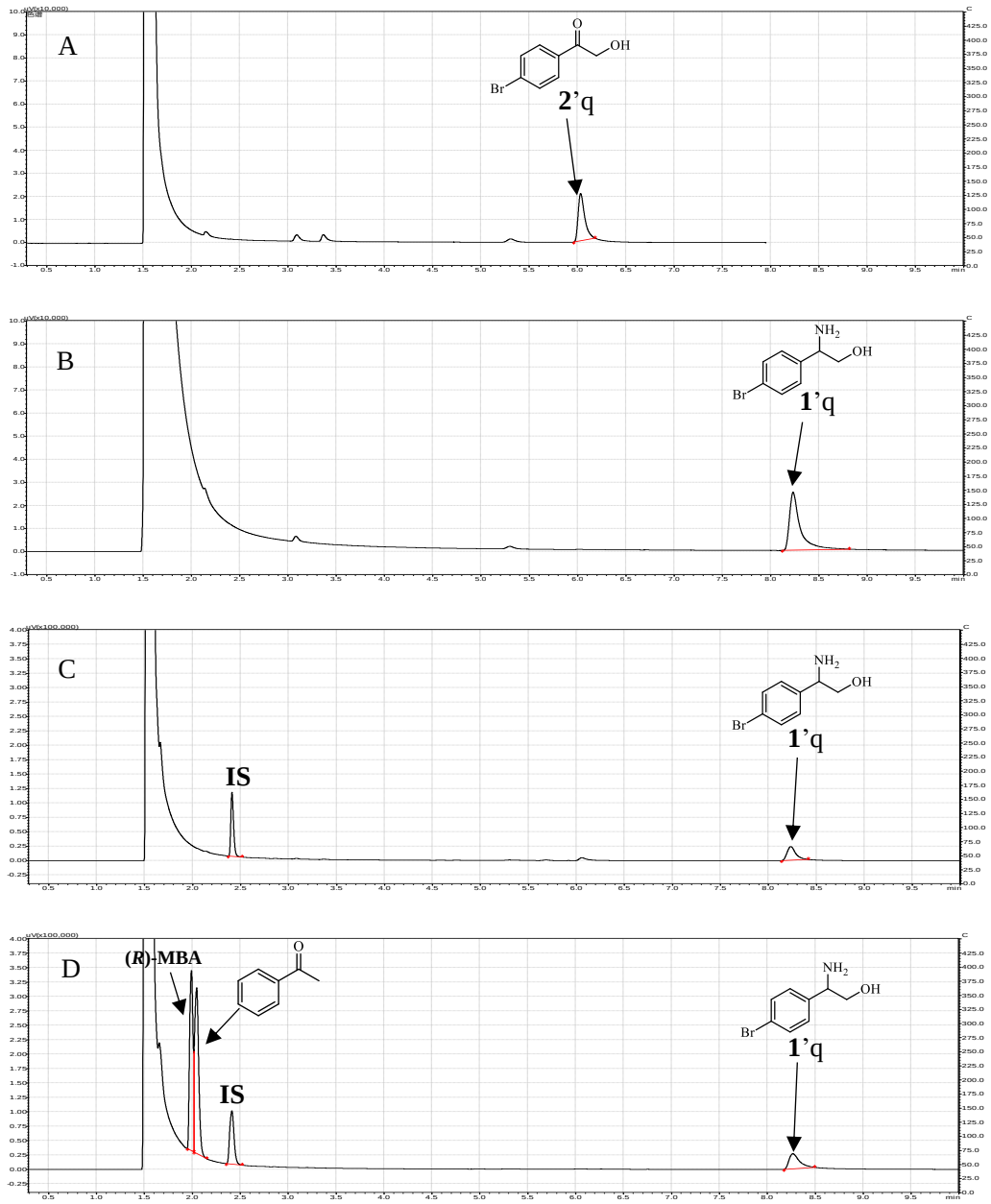

Fig. S41. Achiral GC analysis of 2-amino-2-(4-bromophenyl)ethanol **1**'q. **A**: 1-(4-bromophenyl)-2-hydroxyethanone (**2**'q) standard ; **B**: 2-amino-2-(4-bromophenyl)ethanol (**1**'q) standard; **C**: 2-amino-2-(4-bromophenyl)ethanol (**1**'q) produced from 1-(4-bromophenyl)-2-hydroxyethanone (**2**'q) (10 mM) with 200 mM D-Ala and 20 g CDW L^{-1} *E. coli* (CepTA) at 12 h. **D**: 2-amino-2-(4-bromophenyl)ethanol (**1**'q) produced from 1-(4-bromophenyl)-2-hydroxyethanone (**2**'q) (10 mM) with 10 mM (*R*)-MBA and 20 g CDW L^{-1} *E. coli* (CepTA) at 3 h. IS: internal standard (dodecane).

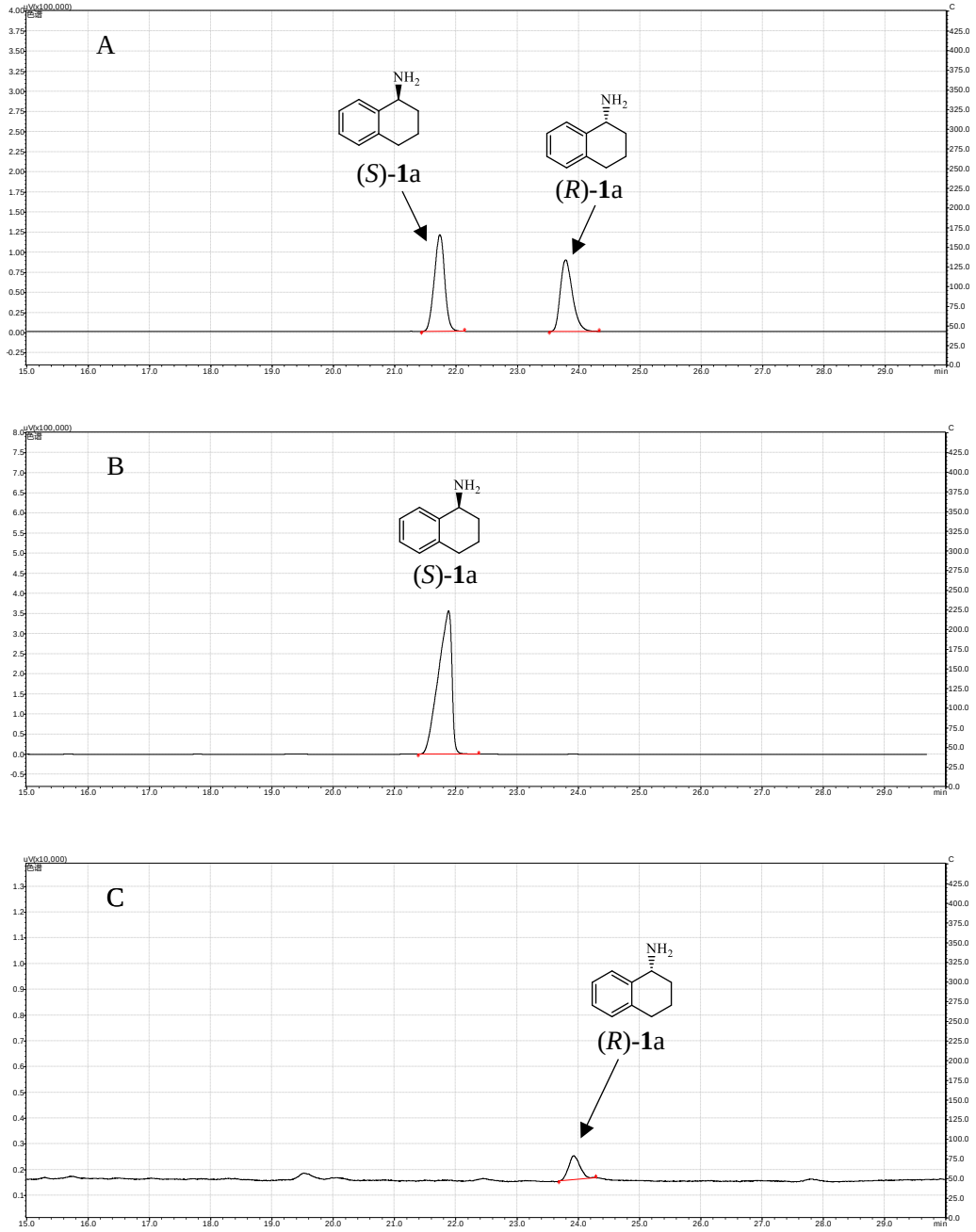

Fig. S42. Chiral GC analysis of 1,2,3,4-tetrahydro-1-naphthylamine **1**a produced from asymmetric reduction amination of 1-tetralone (**2**a). **A**: racemic 1,2,3,4-tetrahydro-1-naphthylamine (**1**a) standard; **B**: (*S*)-1,2,3,4-tetrahydro-1-naphthylamine (**1**a) standard; **C**: (*R*)-1,2,3,4-tetrahydro-1-naphthylamine (**1**a) (>99% *ee*) produced from asymmetric reduction amination of 1-tetralone (**2**a) (10 mM) with *E. coli* (CepTA).

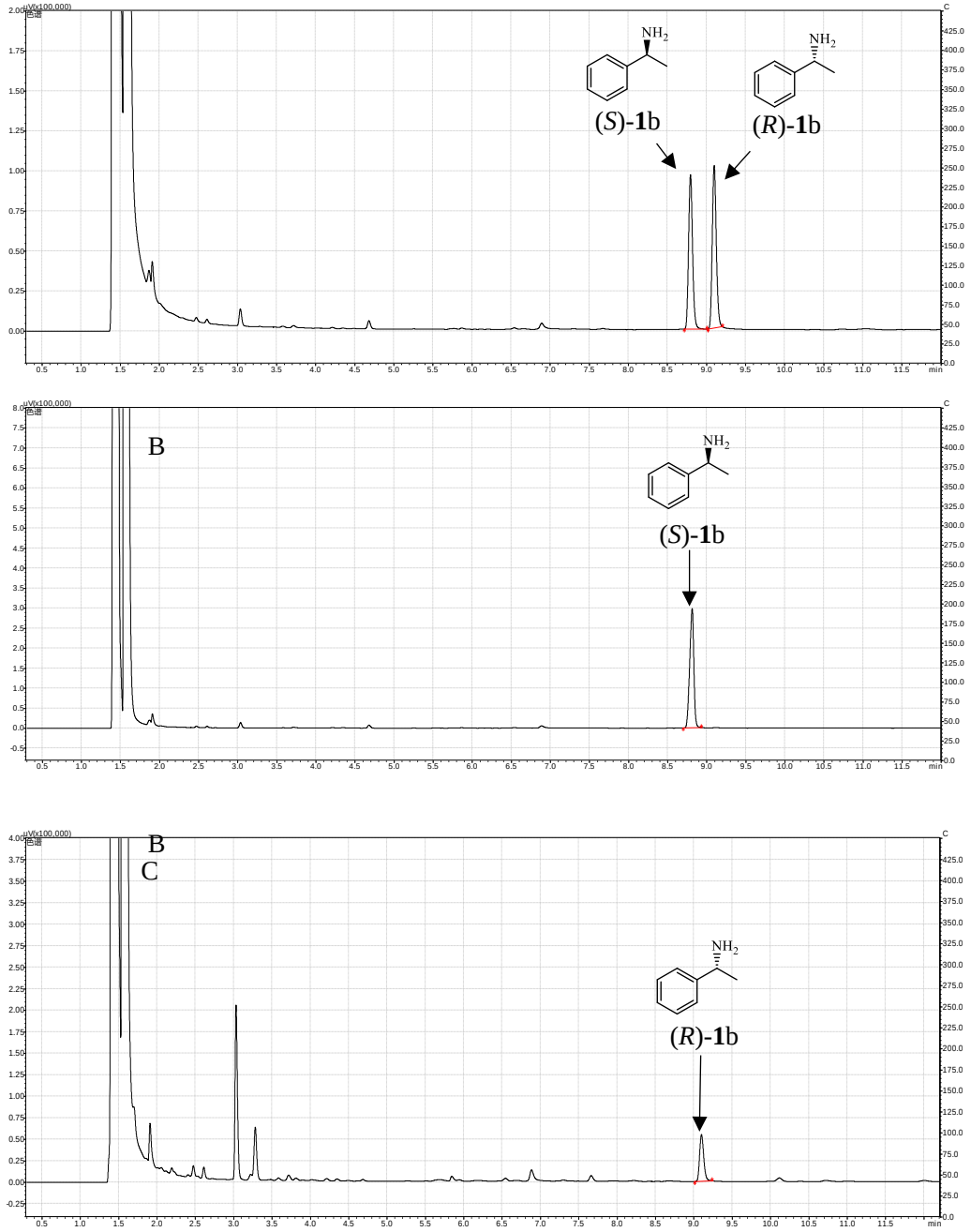

Fig. S43. Chiral GC analysis of 1-phenylethylamine **1**b produced from asymmetric reduction amination of acetophenone (**2**b). **A**: racemic 1-phenylethylamine (**1**b) standard; **B**: (*S*)-1-phenylethylamine (**1**b) standard; **C**: (*R*)- 1-phenylethylamine (**1**b) (>99% *ee*) produced from asymmetric reduction amination of acetophenone (**2**b) (10 mM) with *E. coli* (CepTA).

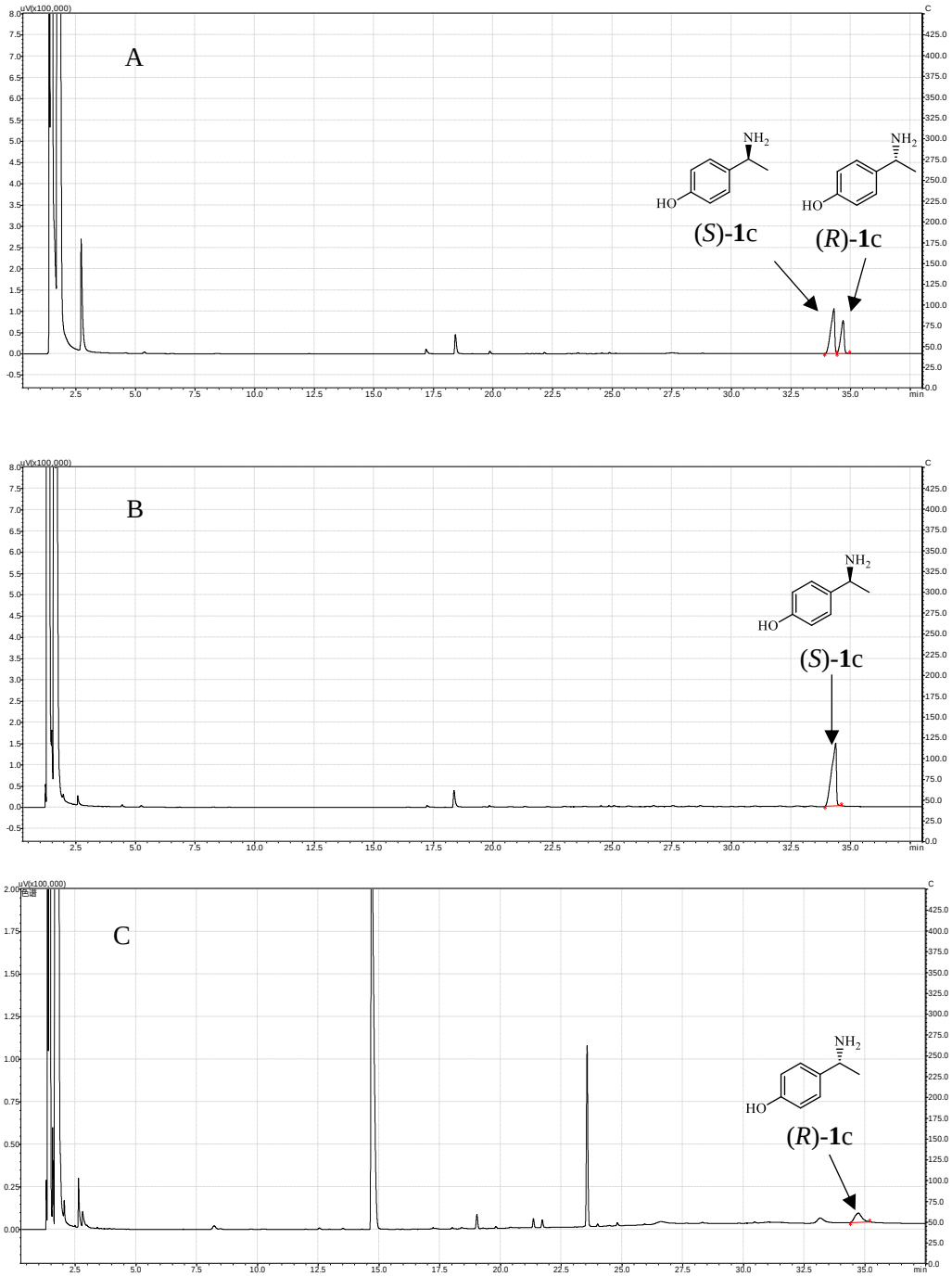

Fig. S44. Chiral GC analysis of 4-(1-aminoethyl)phenol **1**c produced from asymmetric reduction amination of 4-hydroxyacetophenone (**2**c). **A**: racemic 4-(1-aminoethyl)phenol (**1**c) standard; **B**: (*S*)- 4-(1-aminoethyl)phenol (**1**c) standard; **C**: (*R*)-4-(1-aminoethyl)phenol (**1**c) (>99% *ee*) produced from asymmetric reduction amination of 4-hydroxyacetophenone (**2**c) (10 mM) with *E. coli* (CepTA).

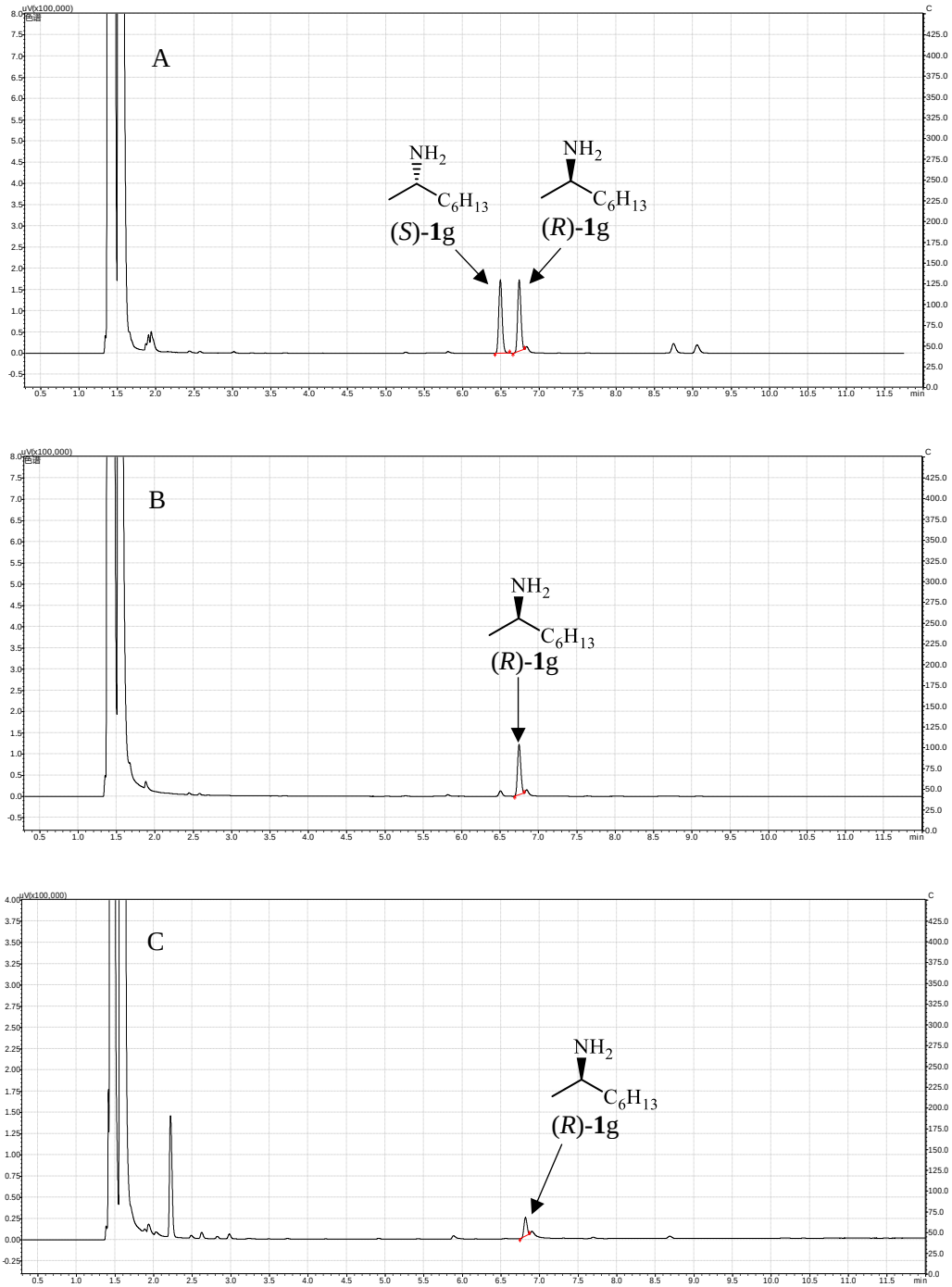

Fig. S45. Chiral GC analysis of 2-octanamine **1**g produced from asymmetric reduction amination of 2-octanone (**2**g). **A**: racemic 2-octanamine (**1**g) standard; **B**: (*R*)- 2-octanamine (**1**g) standard; **C**: (*R*)- 2-octanamine (**1**g) (>99% *ee*) produced from asymmetric reduction amination of 2-octanone (**2**g) (10 mM) with *E. coli* (CepTA).

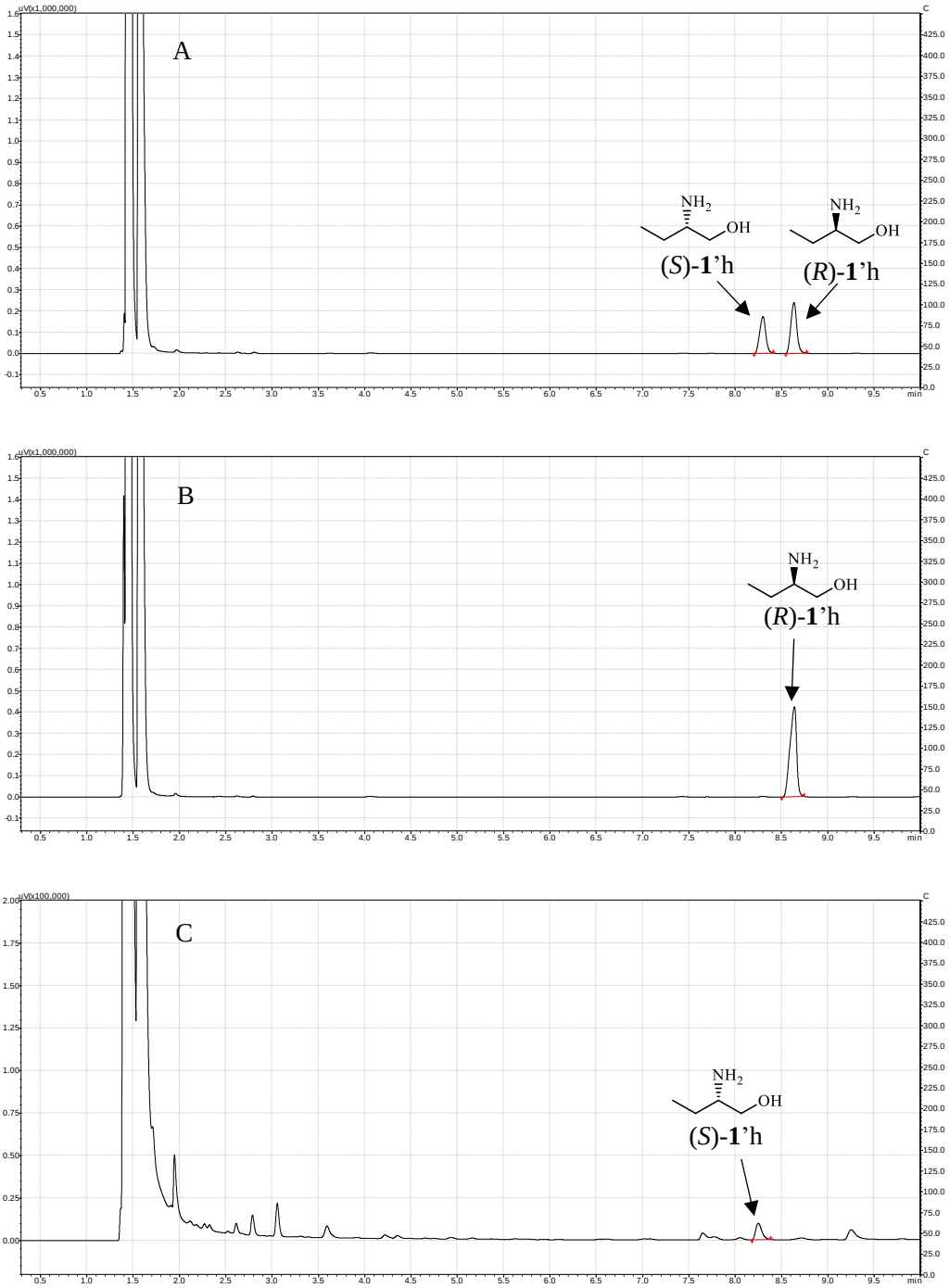

Fig. S46. Chiral GC analysis of 2-amino-1-butanol **1**'h produced from asymmetric reduction amination of 1-hydroxy-2-butanone (**2**'h). **A**: racemic 2-amino-1-butanol (**1**'h) standard; **B**: (*R*)-2-amino-1-butanol (**1**'h) standard; **C**: (*S*)-2-amino-1-butanol (**1**'h) (>99% *ee*) produced from asymmetric reduction amination of 1-hydroxy-2-butanone (**2**'h) (50 mM) with *E. coli* (CepTA).

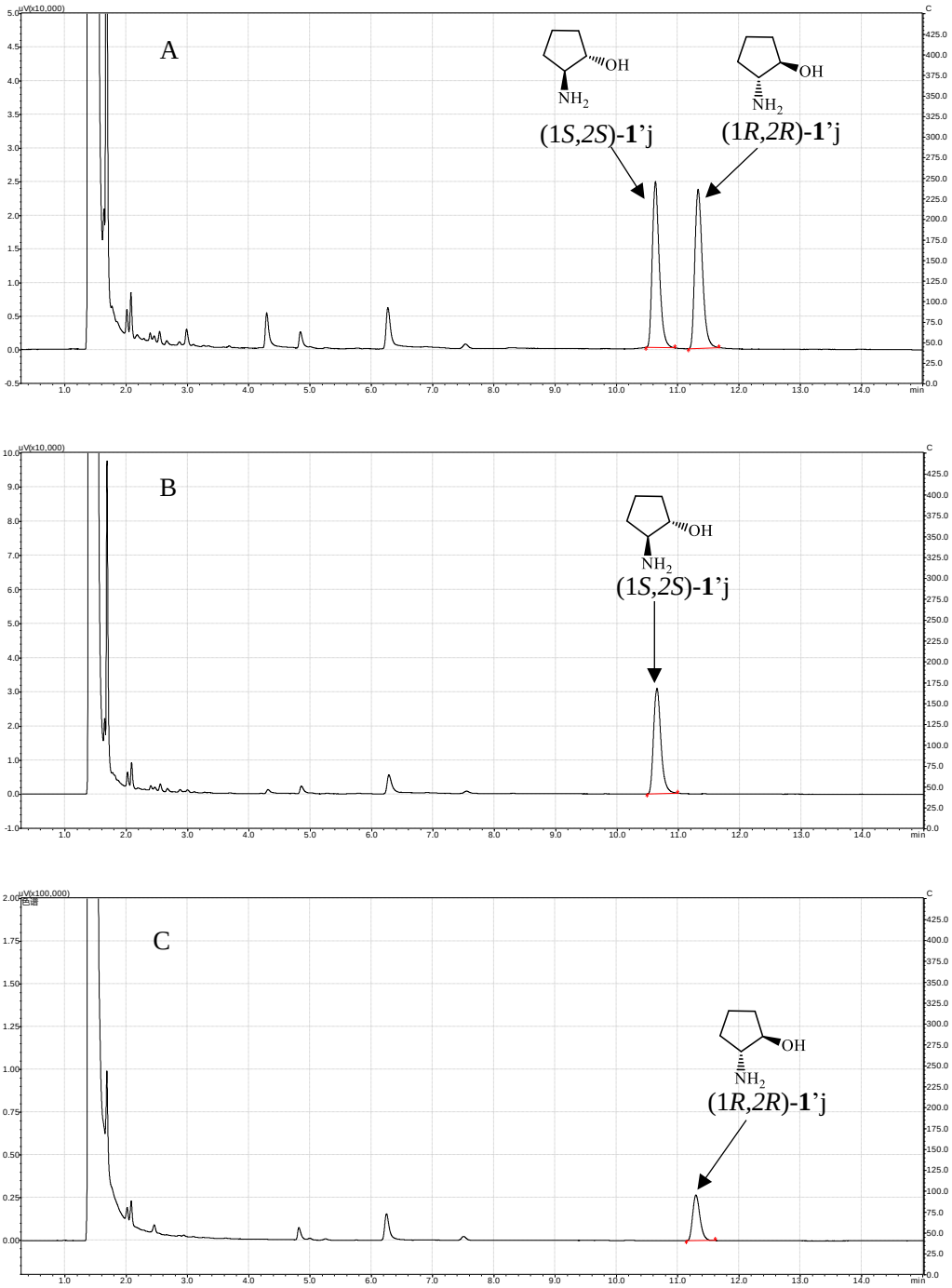

Fig. S47. Chiral GC analysis of 2-aminocyclopentanol **1**'j produced from asymmetric reduction amination of (*R*)-α-hydroxycyclopentan-1-one **2**'j. **A**: racemic *trans*-2-aminocyclopentanol (**1**'j) standard; **B**: (1*S*,2*S*)-*trans*-2-aminocyclopentanol (**1**'j) standard; **C**: (1*R*,2R)-*trans*-2-aminocyclopentanol (**1**'j) (>99% ee) produced from asymmetric reduction amination of (*R*)-α-hydroxycyclopentan-1-one **2**'j (10 mM) with CepTA.

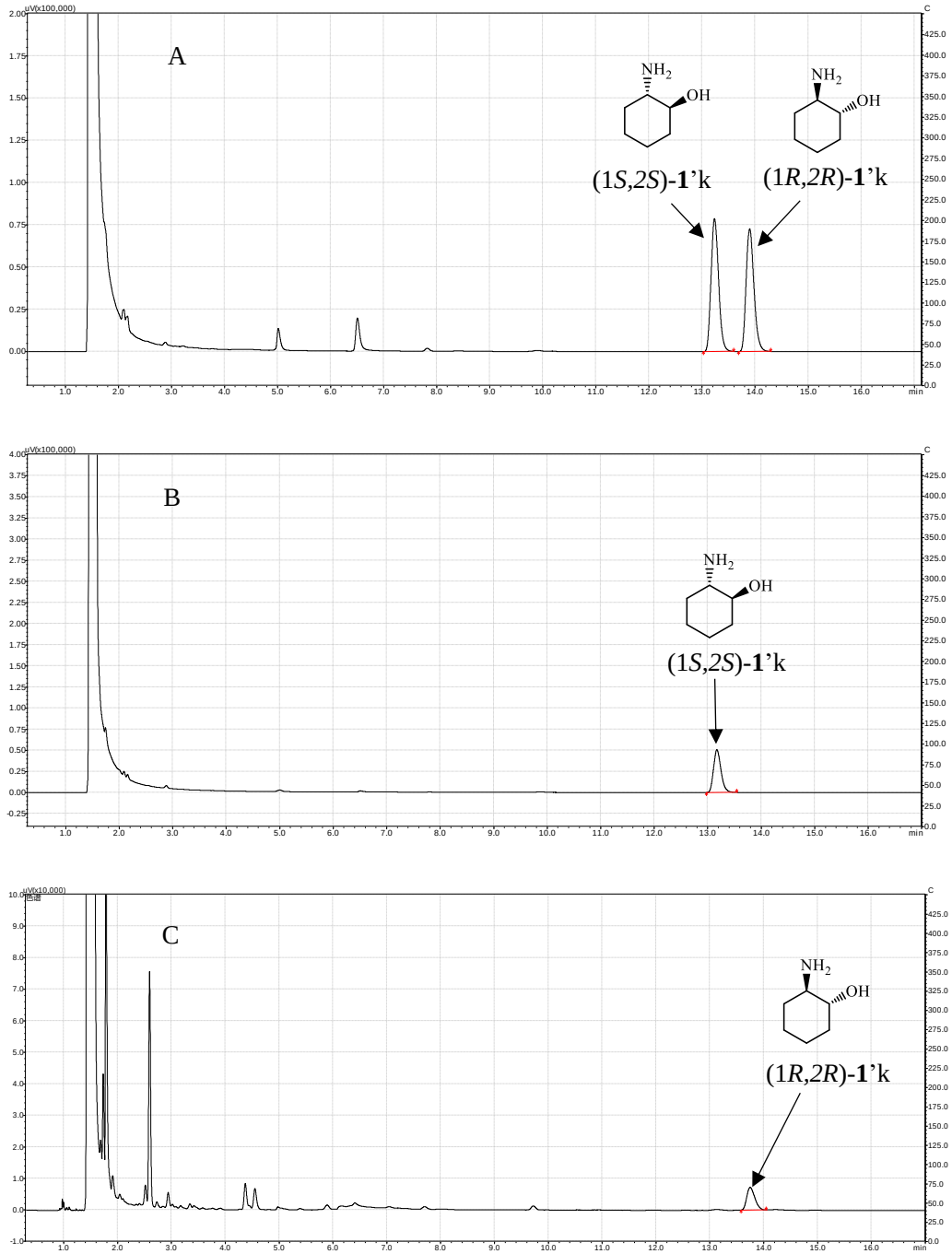

Fig. S48. Chiral GC analysis of 2-aminocyclohexanol **1**'k produced from asymmetric reduction amination of (*R*)-α-hydroxycyclohexan-1-one **2**'k. **A**: racemic *trans*-2-aminocyclohexanol (**1**'k) standard; **B**: (1*S*,2*S*)-*trans*-2-aminocyclohexanol (**1**'k) standard; **C**: (1*R*,2*R*)-*trans*-2-aminocyclohexanol (**1**'k) (>99% *ee*) produced from asymmetric reduction amination of (*R*)-α-hydroxycyclohexan-1-one **2**'k (10 mM) with *E. coli* (CepTA) resting cells.

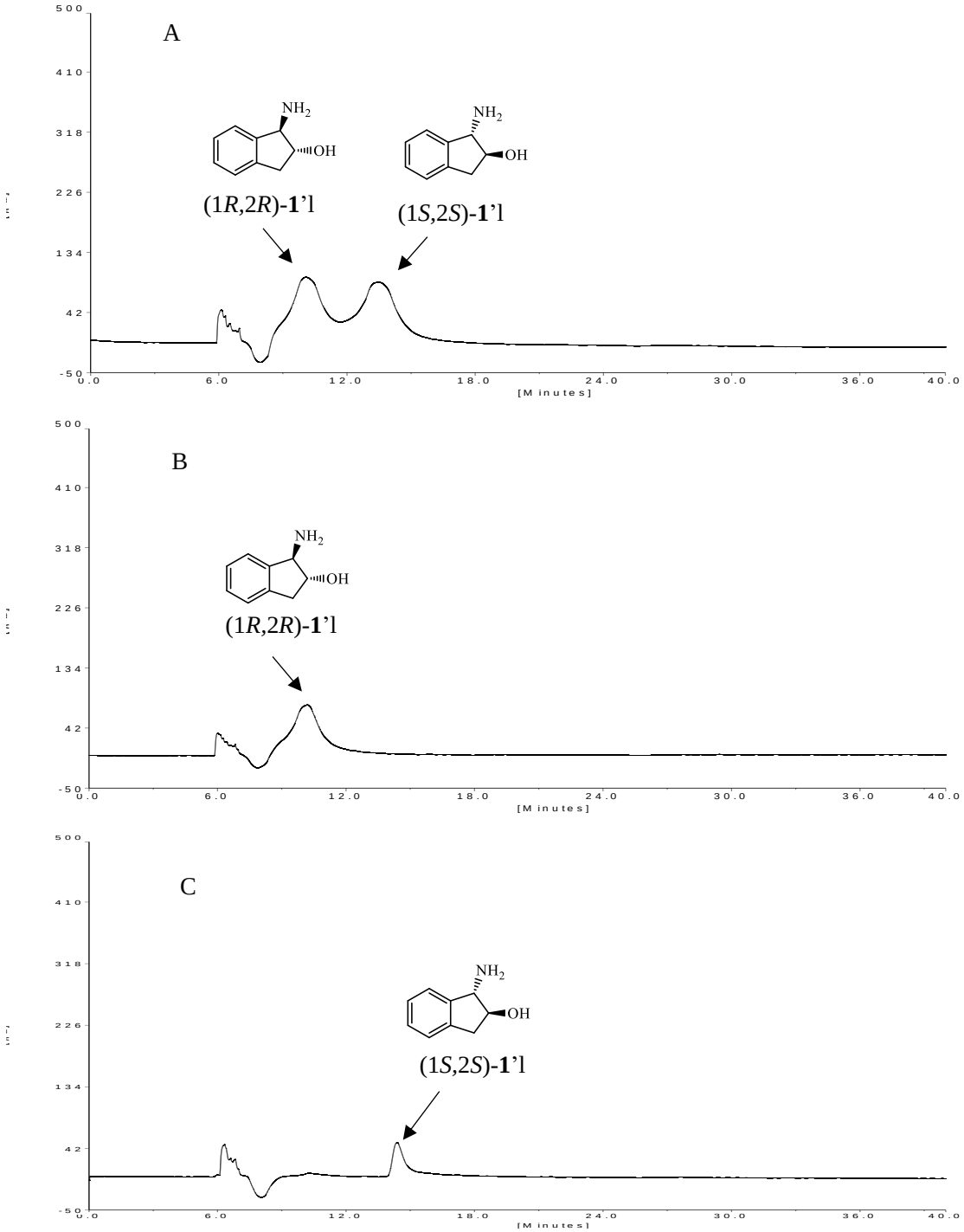

Fig. S49. Chiral HPLC analysis of *trans*-1-amino-2-indanol **1**'l produced from asymmetric reduction amination of (*S*)-2-hydroxy-1-indanone (**2**'l). **A**: racemic *trans*-1-amino-2-indanol (**1**'l) standard; **B**: (1*R*,2*R*)-*trans*-1-amino-2-indanol (**1**'l) standard; **C**: (1*S*,2*S*)-*trans*-1-amino-2-indanol (**1**'l) (>99% *ee*) produced from asymmetric reduction amination of (*S*)-2-hydroxy-1-indanone (**2**'l) (10 mM) with *E. coli* (CepTA) resting cells.

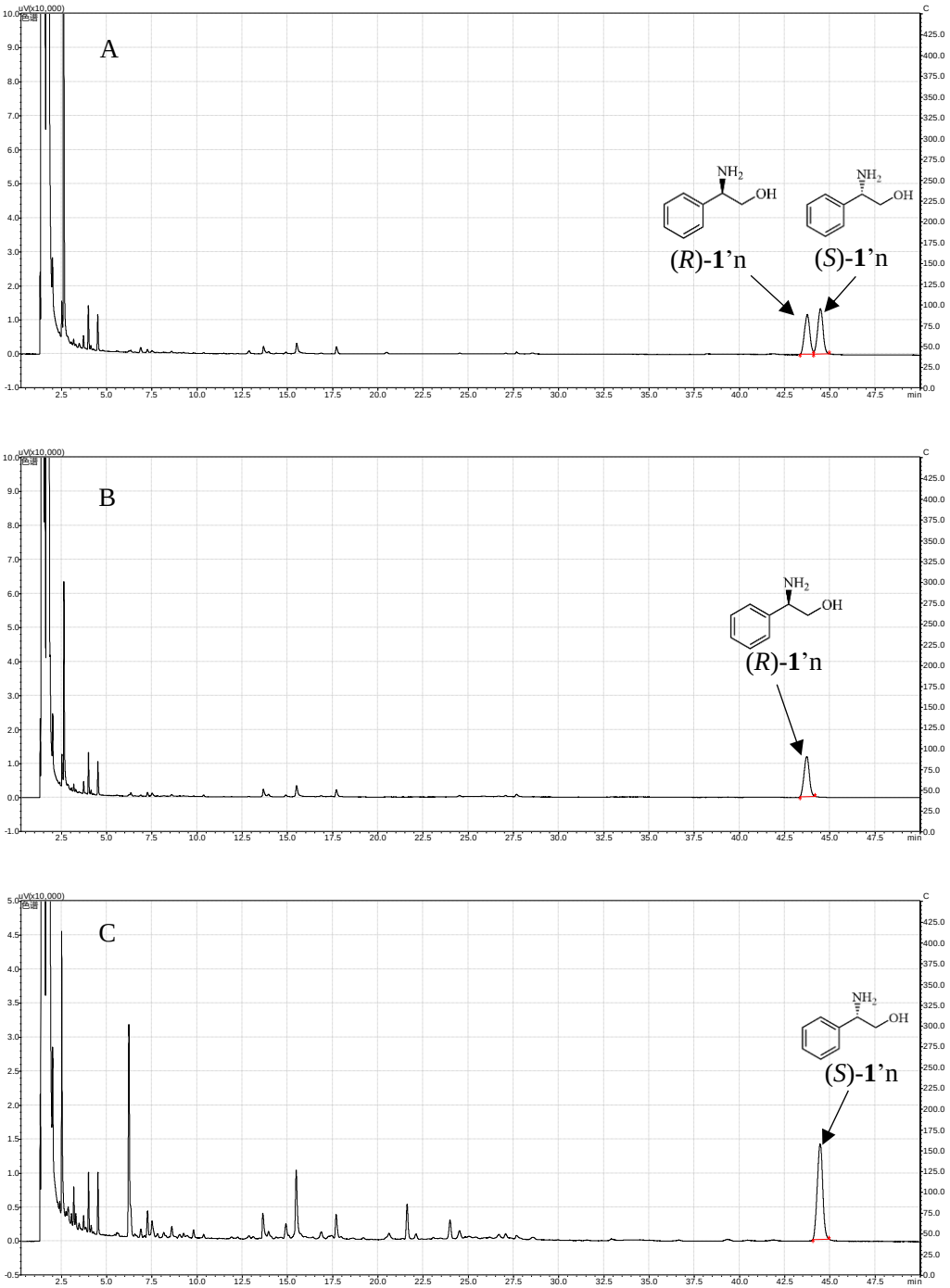

Fig. S50. Chiral GC analysis of phenylglycinol **1**'n produced from asymmetric reduction amination of 2-hydroxyacetophenone (**2**'n). **A**: racemic phenylglycinol (**1**'n) standard; **B**: (*R*)-phenylglycinol (**1**'n) standard; **C**: (*S*)-phenylglycinol (**1**'n) (>99% *ee*) produced from asymmetric reduction amination of 2-hydroxyacetophenone (**2**'n) (10 mM) with *E. coli* (CepTA).

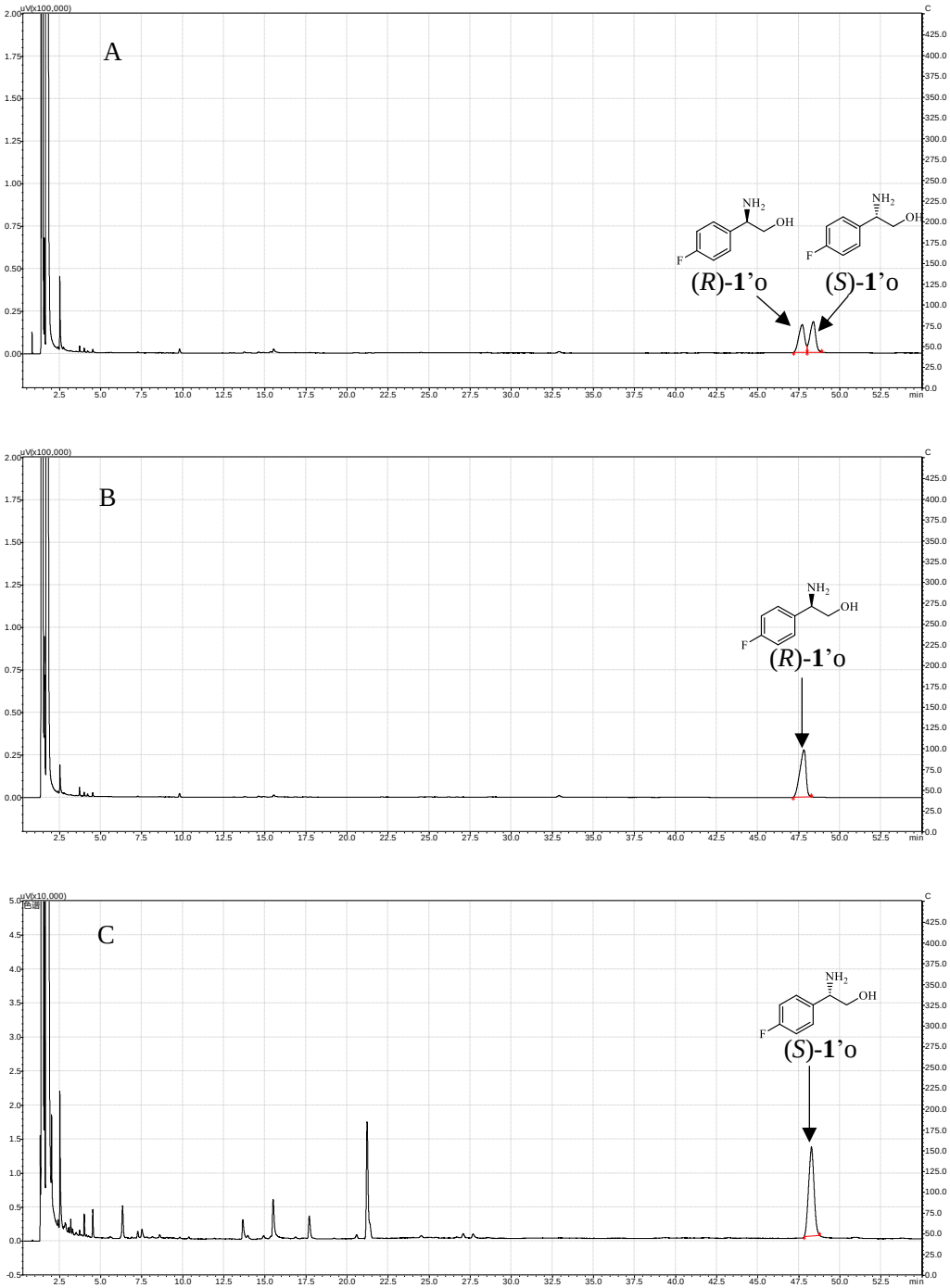

Fig. S51. Chiral GC analysis of 2-amino-2-(4-fluorophenyl)ethanol **1**'o produced from asymmetric reduction amination of 1-(4-fluorophenyl)-2-hydroxyethanone (**2**'o). **A**: racemic 2-amino-2-(4-fluorophenyl)ethanol (**1**'o) standard; **B**: (*R*)-2-amino-2-(4-fluorophenyl)ethanol (**1**'o) standard; **C**: (*S*)-2-amino-2-(4-fluorophenyl)ethanol (**1**'o) (>99% ee) produced from asymmetric reduction amination of 1-(4-fluorophenyl)-2-hydroxyethanone (**2**'o) (10 mM) with *E. coli* (CepTA).

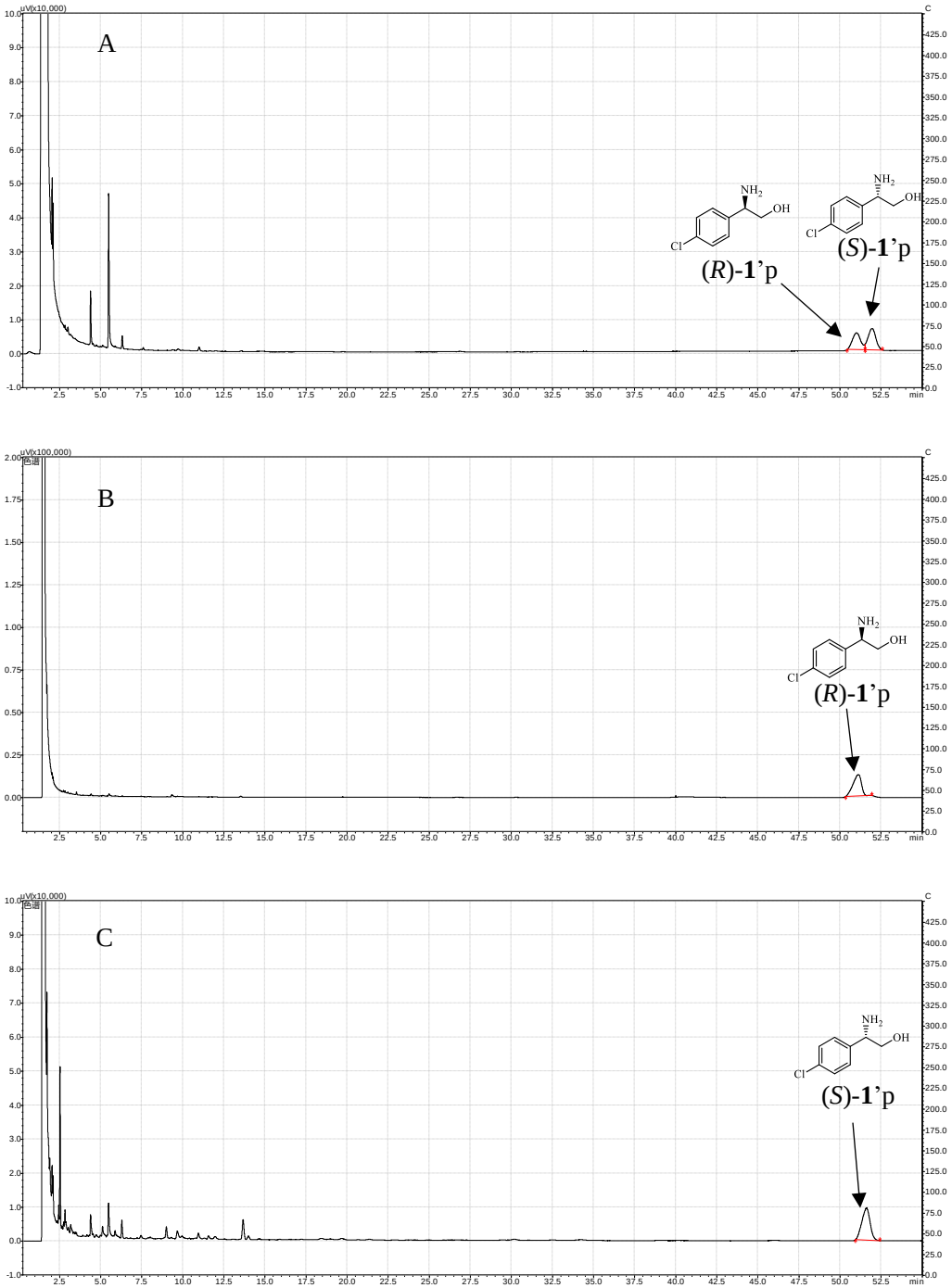

Fig. S52. Chiral GC analysis of 2-amino-2-(4-chlorophenyl)ethanol **1**'p produced from asymmetric reduction amination of 1-(4-chlorophenyl)-2-hydroxyethanone (**2**'p). **A**: racemic 2-amino-2-(4-chlorophenyl)ethanol (**1**'p) standard; **B**: (*R*)-1-2-amino-2-(4-chlorophenyl)ethanol (**1**'p) standard; **C**: (*S*)-1-2-amino-2-(4-chlorophenyl)ethanol (**1**'p) (>99% *ee*) produced from asymmetric reduction amination of 1-(4-chlorophenyl)-2-hydroxyethanone (**2**'p) (10 mM) with *E. coli* (CepTA).

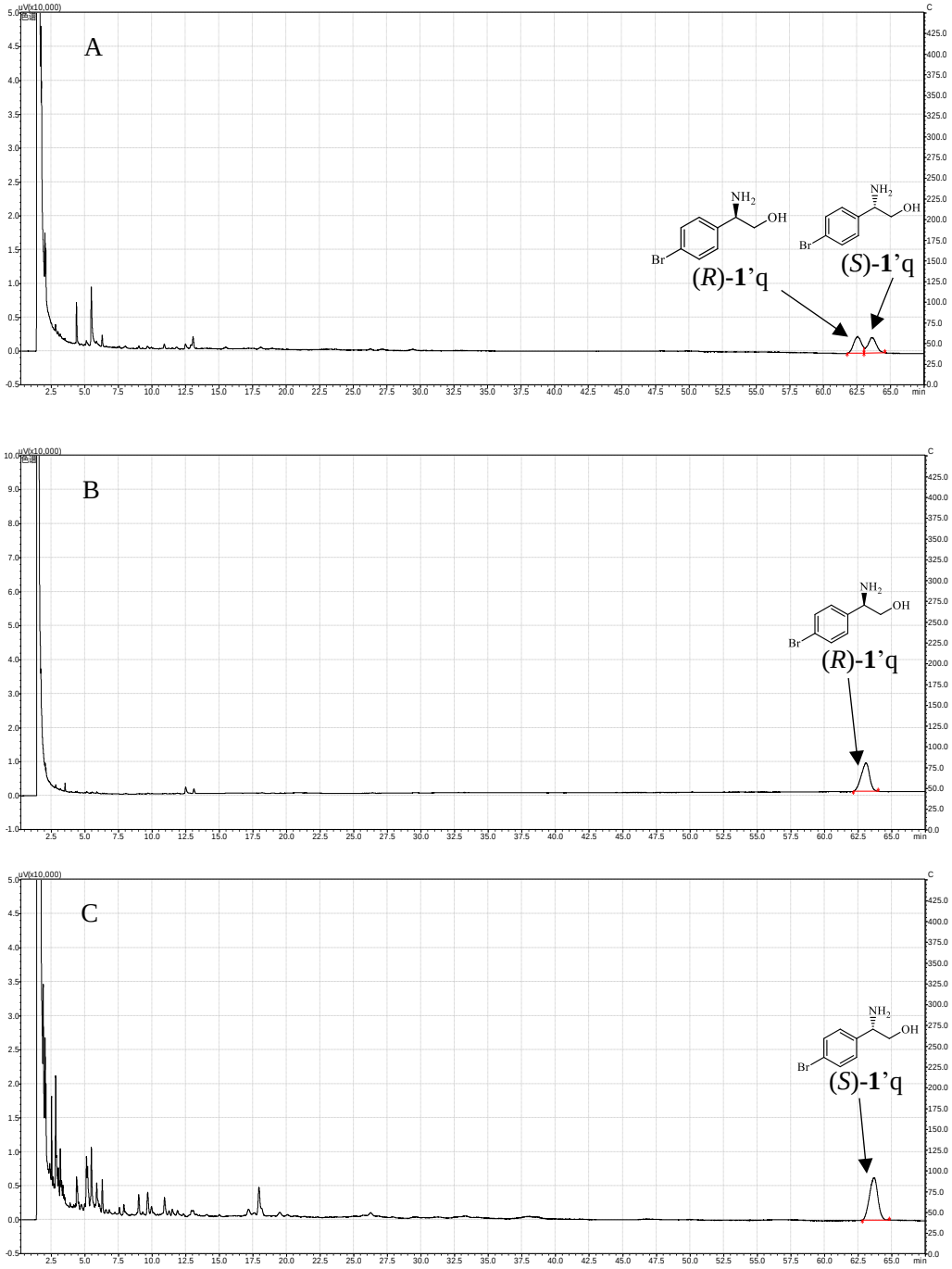

Fig. S53. Chiral GC analysis of 2-amino-2-(4-bromophenyl)ethanol **1**'q produced from asymmetric reduction amination of 1-(4-bromophenyl)-2-hydroxyethanone (**2**'q). **A**: racemic 2-amino-2-(4-bromophenyl)ethanol (**1**'q) standard; **B**: (*R*)-2-amino-2-(4-bromophenyl)ethanol (**1**'q) standard; **C**: (*S*)-2-amino-2-(4-bromophenyl)ethanol (**1**'q) (>99% *ee*) produced from asymmetric reduction amination of 1-(4-bromophenyl)-2-hydroxyethanone (**2**'q) (10 mM) with *E. coli* (CepTA).

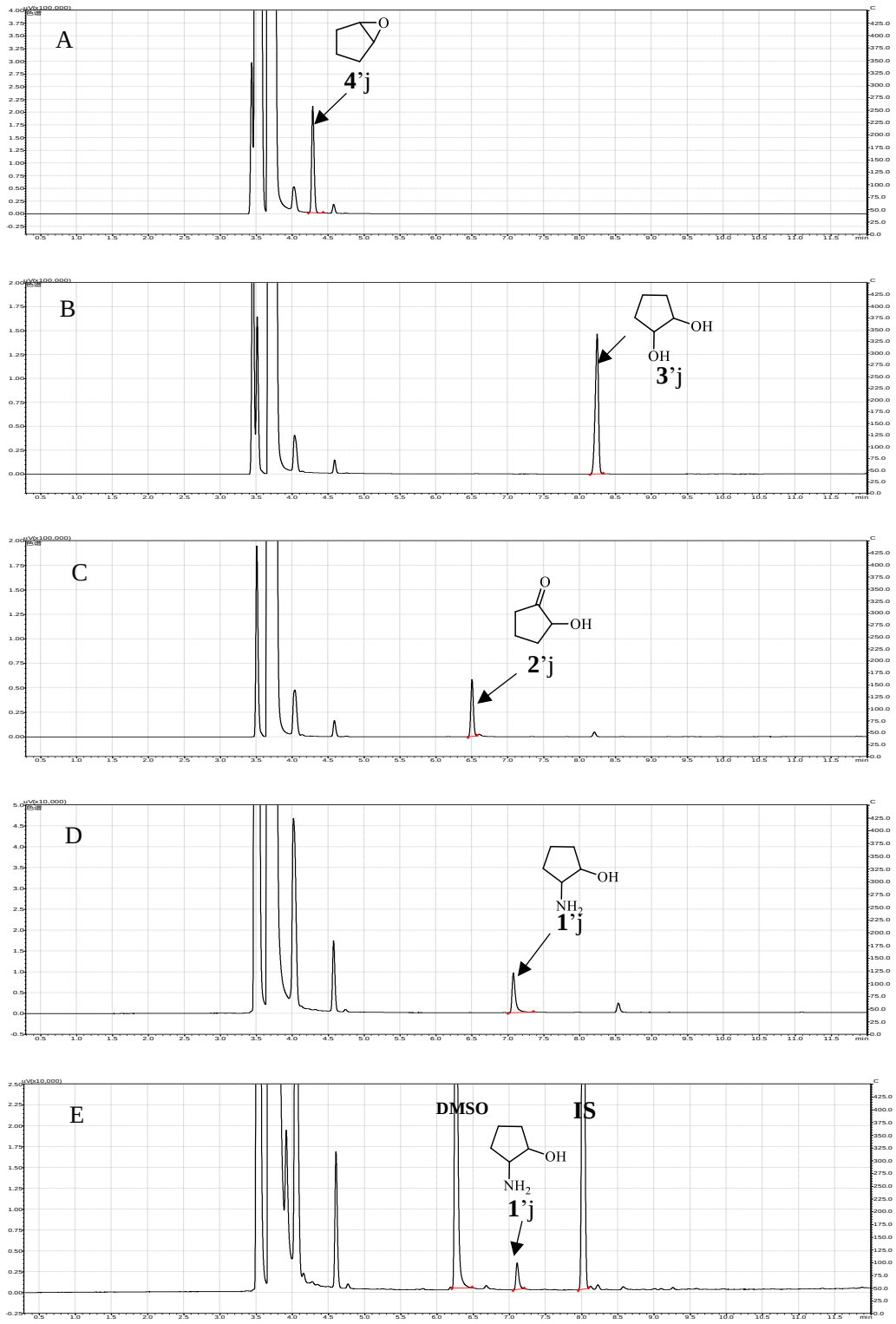

Figure S54. Achiral GC chromatograms of (1*R*,2*R*)-*trans*-2-aminocyclopentanol **1**'j produced from cyclopentene oxide **4**'j. **A**: cyclopentene oxide (**4**'j) standard. **B**: (1*R*,2*R*)-1, 2-cyclopentanediol (**3**'j) standard. **C:** (*R*)-α-hydroxycyclopentan-1-one **2**'j standard. **D**: *trans*-2-aminocyclopentanol (**1**'j) standard. **E**: (1*R*,2*R*)-*trans*-**1**'j produced from cyclopentene oxide (**4**'j) (10 mM) with the mixture of recombinant *E. coli* (SpEH-AnDDH-BsLDH) and *E. coli* (CepTA) resting cells.

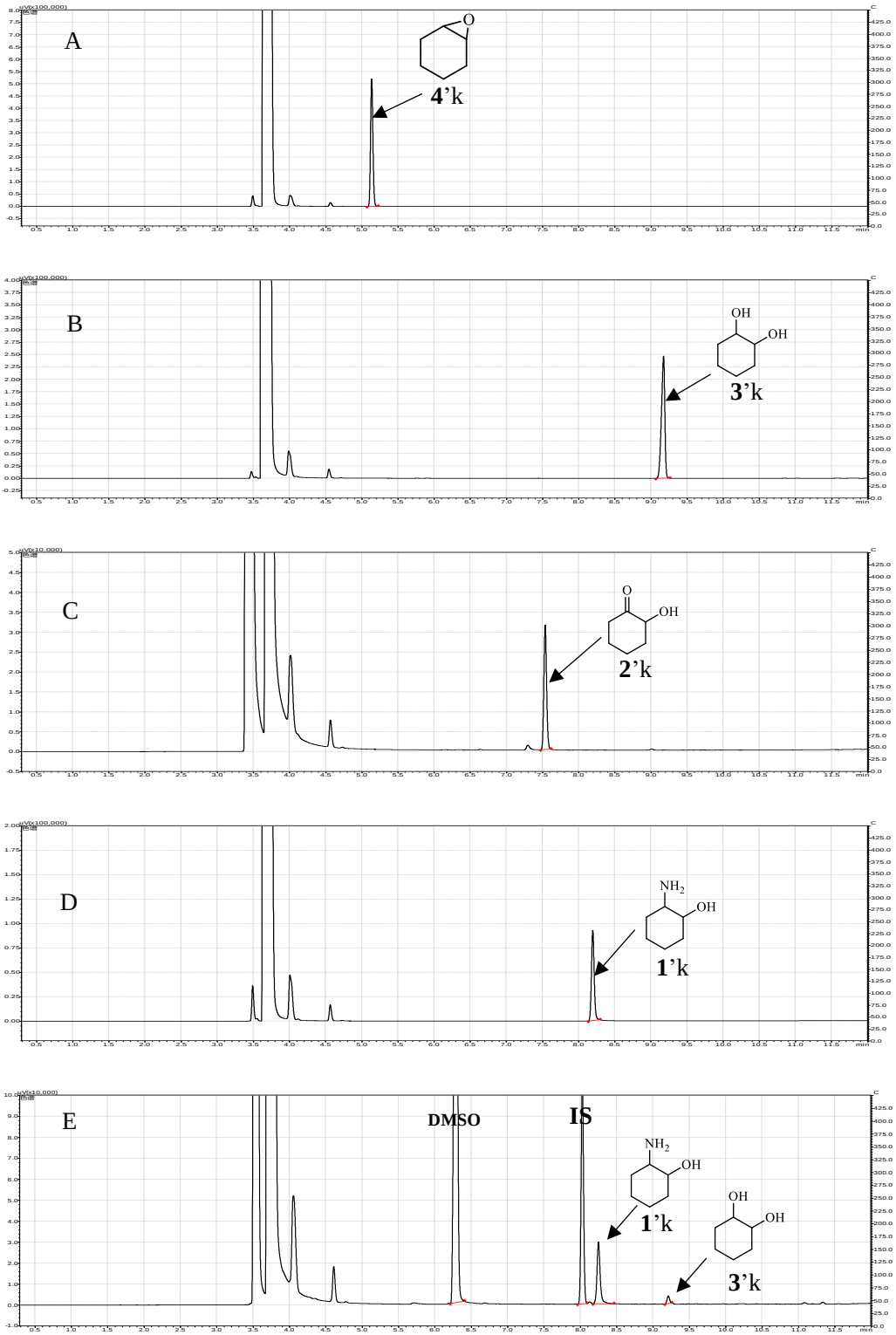

Figure S55. Achiral GC chromatograms of (1*R*,2*R*)-*trans*-2-aminocyclohexanol **1**'k produced from cyclohexene oxide **4**'k. **A**: cyclohexene oxide (**4**'k) standard. **B**: (1*R*,2*R*)-1, 2-cyclohexanediol (**3**'**k**) standard. **C**: (*R*)-α-hydroxycyclohexan-1-one **2**'k standard. **D**: 2-aminocyclohexanol (**1**'k) standard. **E**: (1*R*,2*R*)-*trans*-**1**'k produced from **4**'k (10 mM) with the mixture of recombinant *E. coli* (SpEH-AnDDH-BsLDH) and *E. coli* (CepTA) resting cells.

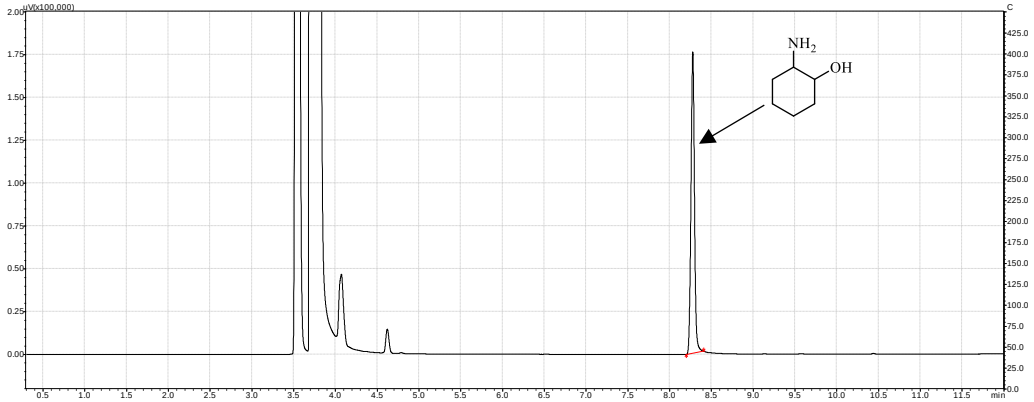

Figure S56. Achiral GC chromatograms of (1*R*,2*R*)-*trans*-2-aminocyclohexanol **1**'k prepared from **4**'k.

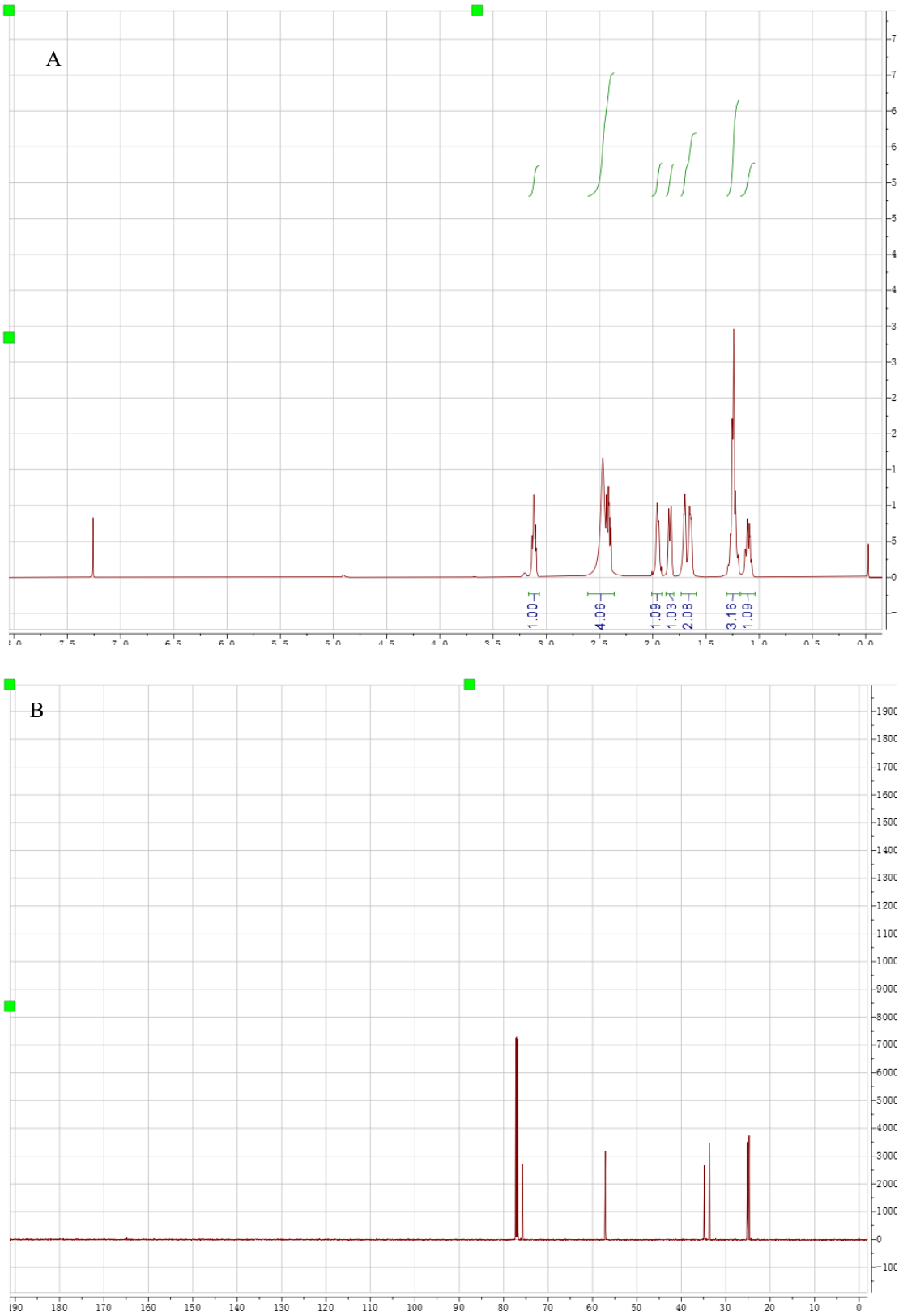

Figure S57. ^{1}H NMR (A) and ^{13}C-NMR (B) spectra analysis of (1*R*,2*R*)-*trans*-2-aminocyclohexanol **1**'k prepared from **4**'k. (1*R*,2*R*)-*trans*-**1**'k: White solid.

References:

[1] J. D. Zhang, S. Wu, J. Wu, Z. Li, Enantioselective cascade biocatalysis via epoxide hydrolysis and alcohol oxidation: One-pot synthesis of (*R*)-α-hydroxy ketones from meso- or racemic Epoxides. *ACS Catal*. 2015, **5**, 51–58.

[2] J. D. Zhang, X. X. Yang, Q. Jia, J. W. Zhao, L. L. Gao, W. C. Gao, H. H. Chang, W. L. Wei, J. H. Xu, *Catal. Sci. Technol*. 2019, **9**, 70–74.

[3] J. D. Zhang, R. Dong, X. X. Yang, L. L. Gao, C. F. Zhang, F. Ren, J. Li, H. H. Chang, *Chinese J. Chem. Eng*. 2022, **47**, 145–154.

[4] Q. Jin, J. Q. Zhang, S. P. Huang, L. L. Gao, H. H. Chang, J. D. Zhang, *Green Chem*. 2023, **25**, 4840–4848.

[5] S. Schätzle, M. Höhne, E. Redestad, K. Robins, U. T. Bornscheuer, *Anal. Chem*. 2009, **81**, 8244–8248.

[6] J. D. Zhang, H. L. Wu, T. Meng, C. F. Zhang, X. J. Fan, H. H. Chang, W. L. Wei. A high-throughput microtiter plate assay for the discovery of active and enantioselective amino alcohol-specific transaminases. *Anal. Biochem*. 2017, **518**, 94–101.

[7] M. M. Bradford, A rapid and sensitive for the quantitation of microgram quantitites of protein utilizing the principle of protein-dye binding. *Anal. Biochem*. 1976, **72**, 248–254.

[8] E. S. Park, J. S. Shin, Free energy analysis of ω-transaminase reactions to dissect how the enzyme controls the substrate selectivity. *Enzyme Microb. Technol*. 2011, **49**, 380 –387.

[9] J. D. Zhang, J. W. Zhao, L. L. Gao, H. H. Chang, W. L. Wei, J. H. Xu, *J. Biotechnol.* 2019, **290**, 24–32.

[10]. A. Waterhouse, M. Bertoni, S. Bienert, G. Studer, G. Tauriello, R. Gumienny, F. T. Heer, T.A.P. de Beer, C. Rempfer, L. Bordoli, R. Lepore, T. Schwede, *Nucleic Acids Res*. 2018, **46**, W296–W303.

[11]. (a) C. R. Søndergaard, M. H. M. Olsson, M. Rostkowski, J. H. Jensen. *J. Chem. Theory Comput*. 2011, **7**, 2284–2295; (b) M. H. M. Olsson, C. R. Søndergaard, M. Rostkowski, J. H. Jensen, *J. Chem. Theory Comput.* 2011, **7**, 525–537.

[12]. (a) C. T. Lee, W. T. Yang, R. G. Parr, *Phys. Rev. B*. 1988, **37**, 785-789; (b) A. D. Becke, *J. Chem. Phys*. 1993, **98**, 5648–5652.

[13]. C. I. Bayly, P. Cieplak, W. D. Cornell, P. A. Kollman, *J. Phys. Chem*. 1993, **97**, 10269–10280.

[14]. (a) J. Eberhardt, D. Santos-Martins, A. F. Tillack, S. Forli, *J. Chem. Inf. Model.* 2021, **61**, 3891–

3898; (b) O. Trott, A. J. Olson, *J. Comput. Chem.* 2010, **31**, 455-461.

[15]. (a) M. Parrinello, A. Rahman, *J. Appl. Phys.* 1981, **52**, 7182–7190; (b) G. Bussi, D. Donadio, M. Parrinello, *J. Chem. Phys*. 2007, **126**, 014101.

[16]. (a) D. Van Der Spoel, E. Lindahl, B. Hess, G. Groenhof, A. E. Mark, H. J. C. Berendsen, *J. Comput. Chem*. 2005, **26**, 1701–1718; (b) J. A.Maier, C. Martinez, K. Kasavajhala, L. Wickstrom, K. E. Hauser, C. Simmerling, *J. Chem. Theory Comput.* 2015, **11**, 3696–3713.

[17] F. G. Mutti, C. S.Fuche, D. Pressnitz, N. G.Turrini, J. H.Sattler, A. Lerchner, A. Skerra, W. Kroutil, *Eur. J. Org. Chem.* 2012, **2012**, 1003–1007.

[18] A. Iwasaki, Y. Yamada, N. Kizaki, Y. Ikenaka, J. Hasegawa, *Appl. Microbiol. Biotechnol.* 2006, **69**, 499–505.

[19] F. Li, Y. Liang, Y. Wei, Y. Zheng, Y. Du, H. Yu, *Adv. Synth. Catal*. 2021, **363**, 4582–4589.

[20] U. Kaulmann, K. Smithies, M. E. B. Smith, H. C. Hailes, J. M. Ward, *Enz. Microb. Tech*., 2007, **41**, 628–637.

[21] R. L. Hanson, B. L. Davis, Y. Chen, S. L. Goldberg, W. L. Parker, T. P. Tully, M. A. Montana, R. N. Patel, *Adv. Synth. Catal.*, 2008, **350**, 1367–1375.

[22] H. L. Wu, J. D. Zhang, C. F. Zhang, X. J. Fan, H. H. Chang, W. L. Wei. *Appl. Biochem. Biotechnol.*, 2017, **181**, 972–985.

[23] Y. W. Chang, J. D. Zhang, X. X. Yang, J. Li, L. L. Gao, S. P. Huang, X. M. Guo, C. F. Zhang, H. H. Chang, J. H. Xu. *Biotechnol. Lett.*, 2020, **42**, 1501–1511.

[24] J. A. Birrell and E. N. Jacobsen, *Org. lett.*, 2013, **15**, 2895–2897.